A UNITED STATES
DEPARTMENT OF
COMMERCE
PUBLICATION

NBS SPECIAL PUBLICATION 338

Status of Thermal Analysis

U.S.
DEPARTMENT
OF
COMMERCE

National
Bureau
of
Standards

Status of Thermal Analysis

Proceedings of a Symposium on the Current Status of Thermal Analysis Held at Gaithersburg, Maryland, April 21-22, 1970

Oscar Menis, Editor

Analytical Chemistry Division
Institute for Materials Research
National Bureau of Standards
Washington, D.C.   20234

FOREWORD

This series of papers was presented at a Symposium on the
Current Status of Thermal Analysis as part of a joint NBS-ASTM
effort to focus attention on the recent trends and needs in the
field of thermal analysis. The selected papers cover discussions
of the importance of experimental parameters for obtaining infor-
mation from differential thermal analysis and the evaluation of
errors of classical calorimetric measurements. They also include
a review of the progress on the development of Standards for tem-
perature calibration based on dynamic measurements. Other papers
sampled a representative cross section of thermal analysis appli-
cations. They encompass areas of high temperature measurements,
biochemical, polymer, and explosive materials. In addition, they
provide an evaluation of errors in differential scanning calor-
imetry and modifications of thermogravimetric apparatus for kinetic
studies. Many facets of this rapidly expanding technique for re-
searchers and students were revealed. It is hoped that this publi-
cation may be useful as an overall review for updating textbook
information.

In order to describe adequately experimental procedures, it is
occasionally necessary to identify commercial products and equip-
ment by the manufacturer's name or label. In no instance does such
identification imply recommendation or endorsement by the National
Bureau of Standards, nor does it imply that the particular product
or equipment is necessarily the best available for that purpose.

The assistance of Mrs. Rosemary Maddock and Mr. J. I. Shultz
in the preparation of this publication is gratefully acknowledged.
The assistance of Dr. Frank E. Karash of Massachusetts University
in organizing the scientific program is greatly appreciated.

Oscar Menis

CONTENTS

The isolation of the specimen reaches an extreme in adiabatic calorimetry wherein the interchange, by intent at least, is reduced to zero. That approach cannot very well be used in differential thermal analysis, but we can and do isolate to varying degrees for different purposes.

Then, too, maximizing the signal is not necessarily the best solution -- that is, the desired information may be in the shape of the peak rather than in the magnitude. Our electronics coworkers have developed amplifiers far better than we can use effectively, so we can turn up the gain so much that it becomes virtually a pulse of great magnitude, structureless except for length, truly a single byte of information. Or, if we choose, we can heat the specimen so fast that the thermal event takes place in a very short time; since some quantity of energy must be taken in or given out, the rate of heat transfer must be high and hence the differential temperature is high.

Either way, the result is a peak with little character. So the question may be asked -- Is there any unique feature which may be hidden?

Let us look at silver sulfate. There is no particular evidence in Figure 1a that anything is awry. Here the temperature is also being plotted so we can get a really good look at the behavior. We see only one unique feature in the heating curve, and that is the lack of a really clear thermal arrest in the temperature plot. These curves were obtained using a block (Fig. 2) containing a few hundred milligrams. Slowing the heating somewhat without increasing the gain correspondingly, it becomes clear that the peak (Fig. 1b) is very obviously skewed. Some poorly-defined rate effect is operating. We may not know what it is yet, but at least we know it's there.

Naturally if we were measuring on the outside of the sample we would see less structure, but if we choose to use very small samples, we have no choice but to measure on the outside. A
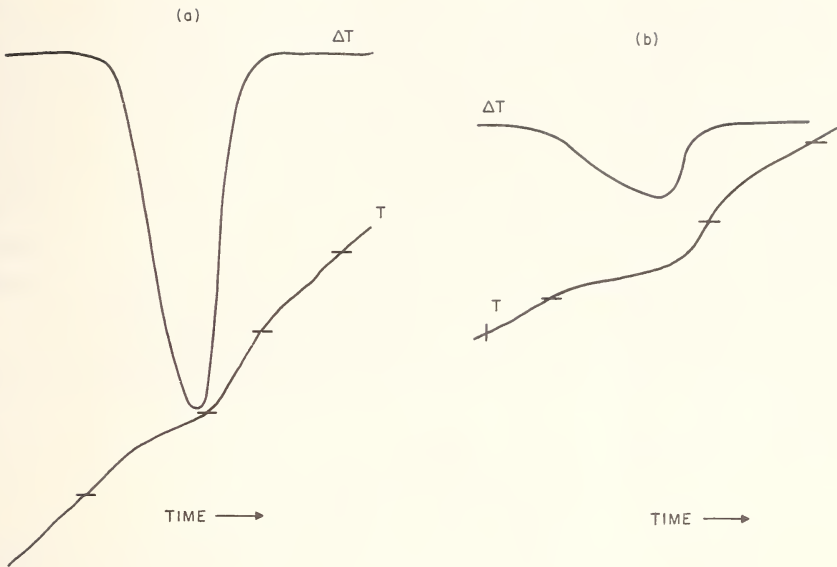
Figure 1.   Thermal curve of silver sulfate.   (a) 8 °C/min.
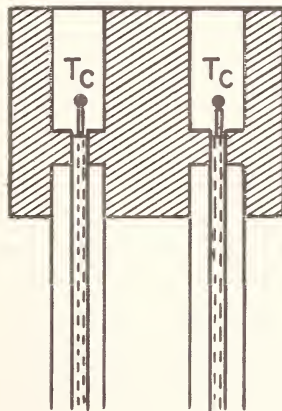(b) 2.8 °C/min.

Figure 2.   Sample block with axially located thermocouples.

thermocouple bead would be a substantial part of the sample-thermo-
couple assembly. Using small samples is, of course, no very diffi-
cult task. Even with a relatively low gain, heavily stabilized
amplifier, and with a very simple holding device, (Fig. 3) use of
sub-milligram quantities of materials was not at all difficult [1].
The sample cavity was just a dimple in the gold sheet, to which was
welded a thermocouple wire. Relative to the sample, the gold sheet
provides a very satisfactory heat sink so that very rapid reactions
can dissipate or absorb heat quickly. So a fraction of a milligram
of potassium sulfate (Fig. 4) is plenty to obtain a good peak.
The new transistor amplifiers could possibly extend the peak a
thousand fold and still maintain good stability, but we would learn
no more.
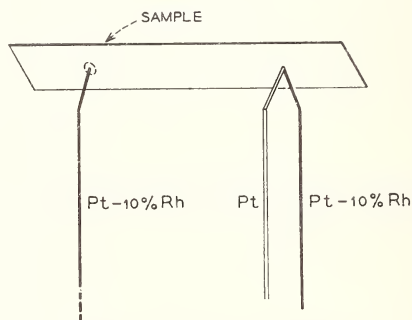
Figure 3. Micro free-diffusion sample holder (Garn [1]). The
           gold sheet acts as the joining wire of the differen-
           tial thermocouple. The sample is placed directly
           over the junction with the fine wire.

    Diffusion of gases into or out of a small sample is very rapid
so dehydrations (Fig. 5) may give small peaks but oxidation reac-
tions proceed very rapidly for the same reason.

    We can control the atmosphere in several ways including the
self-generated atmosphere technique, (Fig. 6) so that by using a
different sample holder and even a lesser amount of material the
dehydration is seen clearly (Fig. 7). The second reaction is now
the loss of carbon dioxide because oxygen cannot diffuse into the
reaction chamber.

Figure 4. Thermal curve of potassium
sulfate (0.1 mg) (Garn [1]).
The local cooling permits
ready detection of phase
transformations.
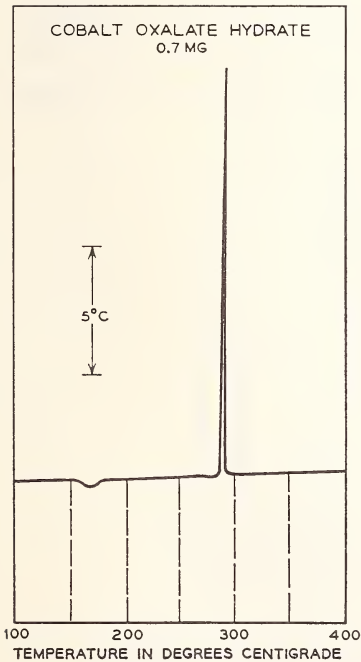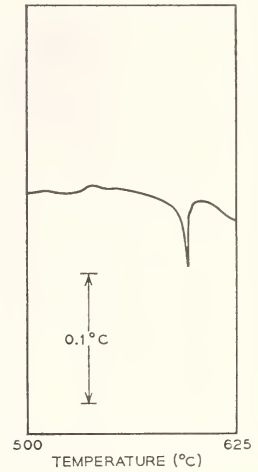
Figure 5. Thermal curve of 0.7 mg cobalt
oxalate hydrate (Garn [1]).
The ease of entry of oxygen
permits rapid enough oxidation
to cause a 15 °C exothermic
deflection.

SAMPLE
0.1 – 4.0 MG

SHIELDED
THERMOCOUPLE

CERAMIC
TUBE
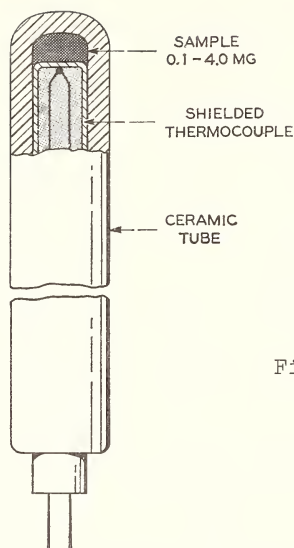
Figure 6. Inhibited-diffusion sample
holder for small samples
(Garn [1]). Even with
shielded thermocouples
very small effects can be
detected.

0.25°C

100   200   300   400   500
TEMPERATURE (°C)
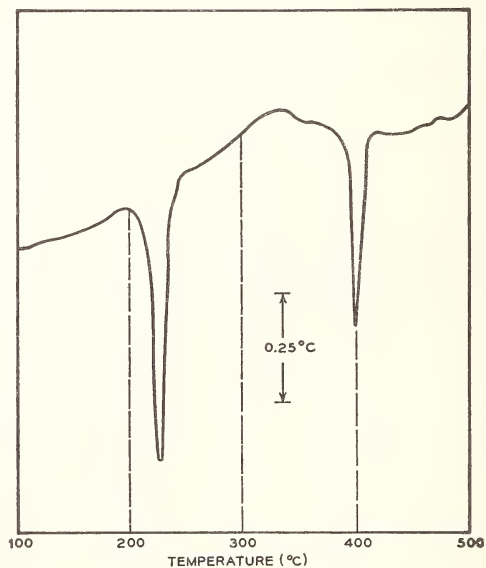
Figure 7. Thermal curve of 0.3 mg cobalt oxalate hydrate
(Garn [1]). The inhibited diffusion eliminates
exterior atmosphere effects for small samples as
well as for large. Compare with Figure 5.

The first conclusion we can reach is that commercial or custom-built instruments today generally have sensitivities far beyond the needs. And the second is that the principal attention must be centered on the experimental method.

Next consider a thin processed sample, for example a film. The DTA curve for the material would presumably represent one or more degradations. Irreversible or not, the degradation will show different curves if the film is against or separated from the heater (Fig. 8). For the separated film, not only are both sides available for escape of products but the temperature must be more nearly homogeneous. Immediate contact with a heater would require that the temperature differential between the heater and the far side of the film be in the film itself so that at reasonable heating rates the gradient within the film will be substantial; while if the film is separated, the principal gradient will exist between heater and film and a lesser gradient within the film itself. This may effect not only the clarity of observation, but even change the course of the degradation.
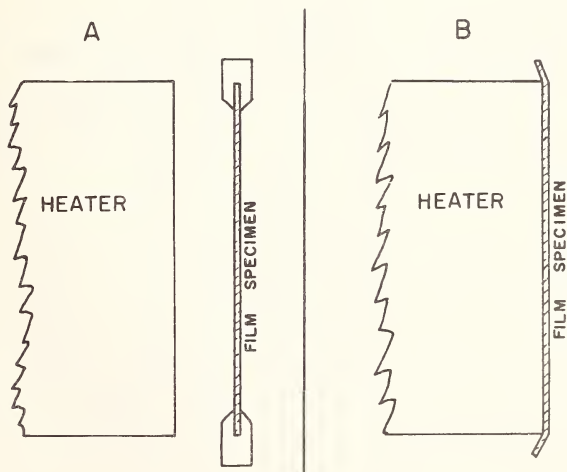
Figure 8. Heater, and A, suspended or, B, adherent film specimens. The suspended film will be heated more slowly and uniformly, for the same heater temperature, than the adherent film.

The principal example here comes from pyrolysis experiments
(Fig. 9) by Martin and Ramstad [2]. They used a flash heater to
degrade a cellulose sample directly in the inlet to a gas chromat-
ograph. They chose to bring the heater virtually instantaneously
above 600 °C by flash discharge in one experiment, but heated more
gently to 250-350 °C by arc illumination in a second experiment.
The more gentle heating is obviously a closer approach to equilib-
rium, and the "flash" heating not only produces large gradients
but brings the material to very high temperatures so quickly that
the easiest degradation reactions, presumably rate-dependent,
find themselves competing with other reactions which at near-
homogeneity of temperature might never occur because the reac-
tant had been used up in the earlier degradation.
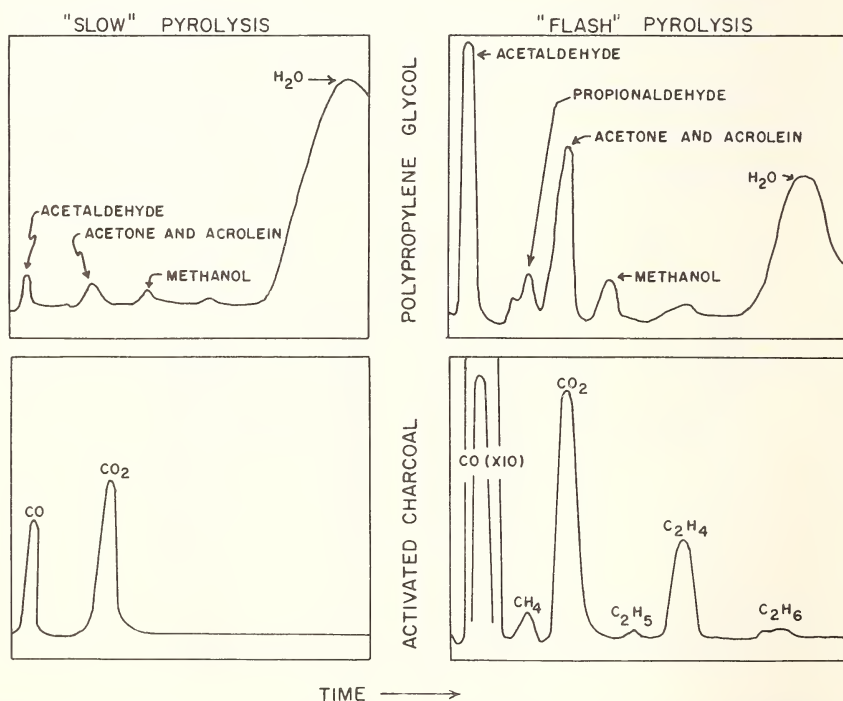
Figure 9.   Chromatographic data on cellulose pyrolysis products
            from slow and from flash pyrolysis (Martin and Ramstad
            [2],).   Different products and proportions of products
            are formed at the two temperatures.

So we may further conclude that in some cases the nature of
the reaction will be determined or influenced by the conditions
of the experiment and, hence, if the study is intended to relate
to some process outside the experimental apparatus, the experi-
mental apparatus should simulate the real process as closely as
possible.

The study of differences will certainly be a major use of DTA;
not simply differences between standard and reference but also
differences between similar -- but not identical -- specimens.
These differences may be inherent to the specimen or imparted to
the specimen by treatment. Mineral species, for example, may show
deviate behavior by reason of impurities or strains. A very marked
example is that of brannerite [3], in which the radioactivity has
apparently caused extensive disruption of the system (Fig. 10).
The disruption can be measured, perhaps, by comparison with an
annealled sample and, from the present activity and estimated
effect of the disruption, some measure of the mineralogical age
obtained.

More delicate measurements would be needed, however, for the
kind of work Keith and Tuttle [4] reported on a single crystal of
quartz. They found that from some crystals they could separate
portions which showed distinctly different $\alpha \leftrightarrows \beta$ transition tem-
peratures (Fig. 11). In other cases the separation was not feas-
ible although the existence of two forms was readily apparent
from the DTA curve. Quartz transitions have been reported over a
fifty degree range, but there is no way to assess the reality of
that range because of differences in instrumental parameters.
These can play a large part; I.C.T.A.'s Committee on Standardiza-
tion received reports varying by 22 degrees for the same quartz
sample.

Other differences arise from processing. In polymer technology
this would be a prime source of variation. The work of Schwenker
and Beck [5] showed the effect of a very necessary process upon a
very common material subjected to that process (Fig. 12). The un-
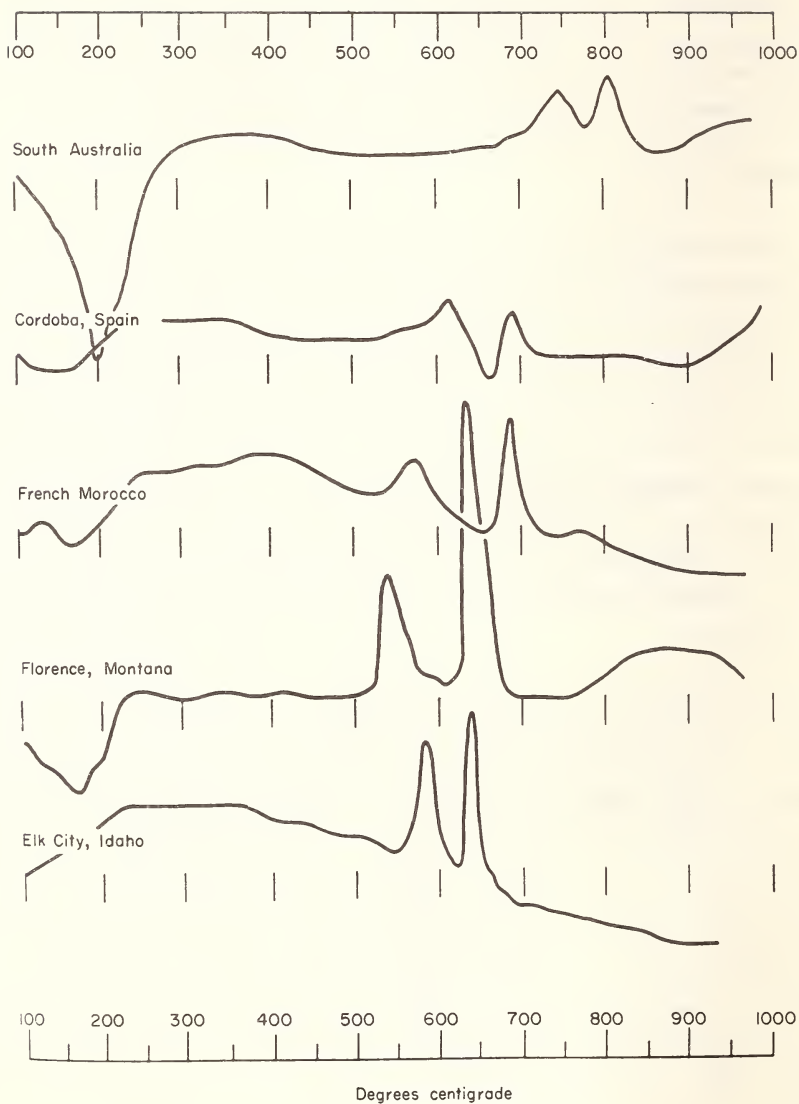
Figure 10. Thermal curves of brannerite (Adler and Puig [3]).
The variable appearance of thermograms of the
mineral is due partly to its variable composition
but partly also to its history.
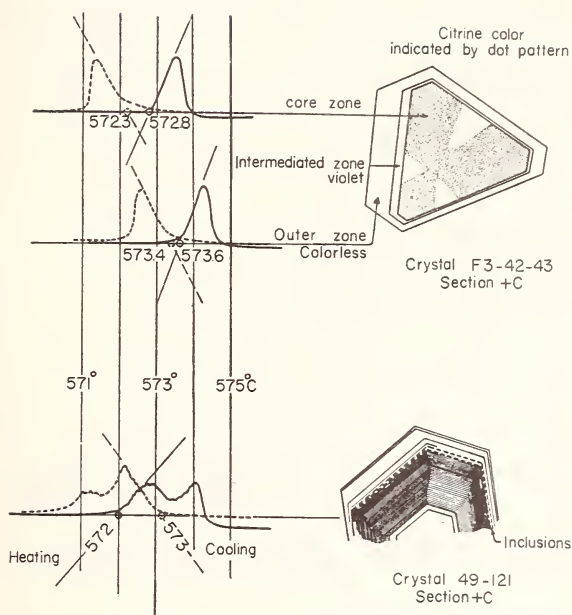
Figure 11.   Character of the heat effect obtained on two zoned
              single crystals. Crystal F3-42-43 was separated
              into two fractions as illustrated and the inversion
              of each fraction is shown (solid lines: thermal
              effect on heating, dashed lines; thermal effect on
              cooling) (Keith and Tuttle [4]). The very low
              heating rate permits clear distinction of materials
              transforming at temperatures only a degree apart.

drawn material shows the expected glass transition and crystalliza-
tion exotherm, while the drawn material, being highly ordered,
shows neither.

    Other treatment effects can also be disclosed by DTA. For
example, Balata D rubber can show a double endotherm when heated
through the 30 to 80 degree range (Fig. 13). When cooled at mod-
erate rates to *ca*. -100 °C, it apparently retains its rubbery qual-
ities to some extent. If the specimen is somewhat restrained,
mechanically, reheating will bring about mechanical relaxation at
a temperature which is presumably dependent upon the amount of
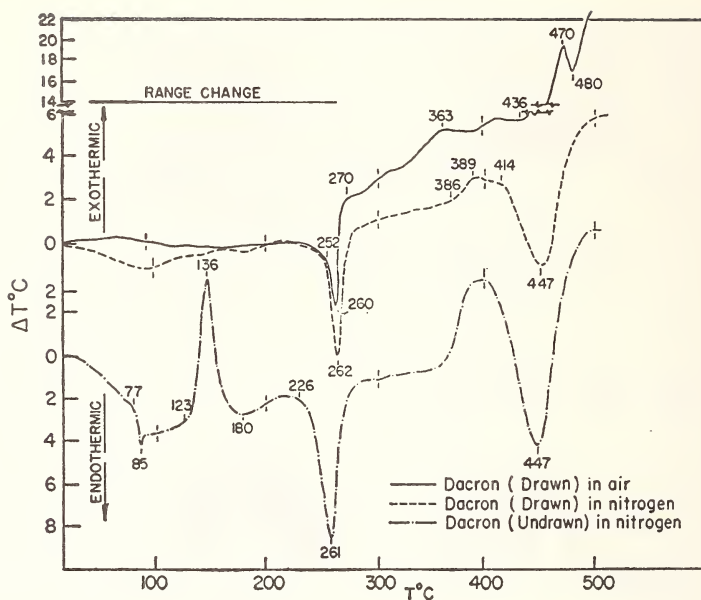
Figure 12.   Differential thermal analysis curves of Dacron
(Schwenker and Beck [5]). The undrawn fiber shows
a second order transition at 77 °C and crystalli-
zation at 136 °C.

strain. In this case the relaxation occurred *ca*. 0 °C. If this
same specimen is quenched, the material recrystallized *ca*. -50 °C
and shows no mechanical movement at 0 degree.

    The curves for brannerite, quartz and Balata rubber were run
under substantially different circumstances for very good reason.
The brannerite could be handled by virtually any DTA equipment,
large or small samples, because no very great resolution was needed.
The quartz experiment needed, above all, high resolution of tempera-
ture; sensitivity was not a problem even with this low-energy tran-
sition and an optical amplifier. The rubber required a relatively
low heat capacity system so the quenching could be done properly.

    The new uses for DTA will almost certainly call not just for
good resolution of curves, but more for good resolution of struc-
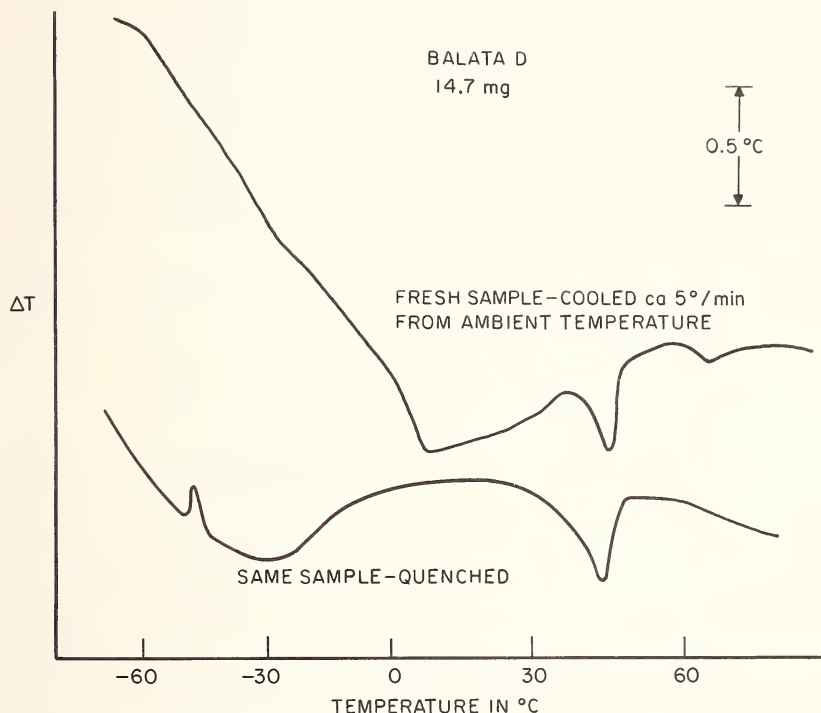
Figure 13.   Thermal curve of Balata D.

ture of peaks. Even though a few people are trying to do kinetics
calculations from DTA peaks, and others are trying to describe all
peaks by a single and simple equation by adjusting the constants,
the fact is that considerable variety exists in the shapes of peaks.
Differences exist because of differing mechanisms as well as differ-
ing thermal properties. So the equipment we shall use a few years
from now shall have to be able to reproduce faithfully some measure
of the events taking place in the sample rather than the existence
or non-existence of an event. For example it will need to detect
not only the quick departure from the base line but also the mis-
shapen leading side of the peak for potassium nitrate [6]. Laying
a straight edge alongside it leads quickly to the suspicion that
the transition is not a simple, one-step process and the cooling
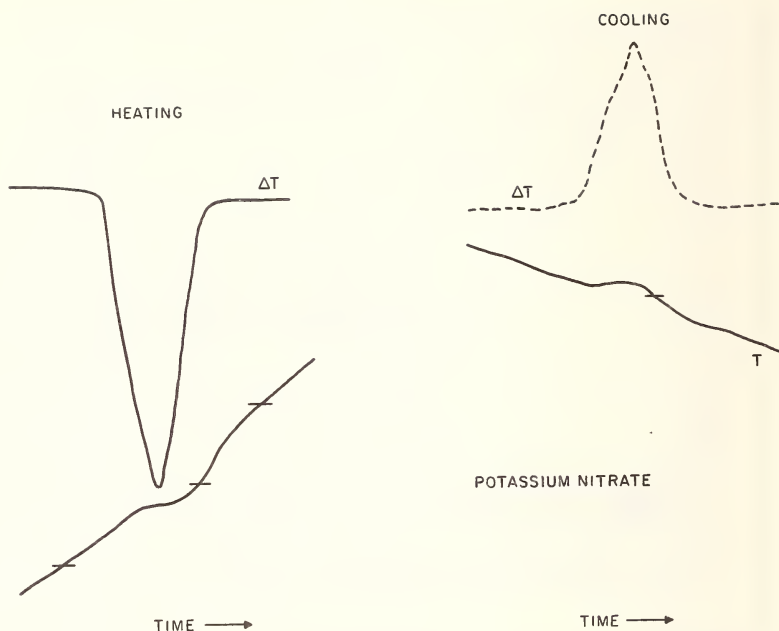
Figure 14.   Thermal curve of potassium nitrate.

curve shows clearly that it is not (Fig. 14). Potassium perchlor-
ate shows a quick departure, too, (Fig. 15) and some indication of
a rate limiting process on cooling, but no indication of a real
two-step process.

*The conclusions we may derive from these data are that (1)
there is much more to be seen that we are accustomed to seeing;
(2) good instrument design will permit us to see more structure;
(3) the disclosure of this "fine structure" will eventually lead
to interpretation and description; and (4) description will lead
in short order to some utility.*

One might postulate a composition-of-matter in which one mate-
rial was to be concentrated at the grain boundaries of the base
material. The first material might be coprecipitated in the base
material and concentrated by cycling through a phase transforma-
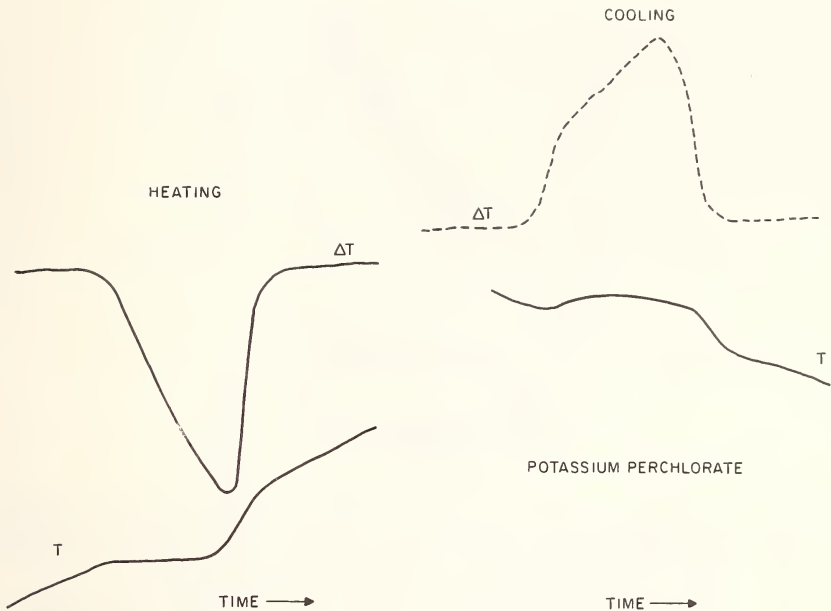
Figure 15.   Thermal curve of potassium perchlorate.

tion and the increasing homogeneity of the base material followed
by observation of the supercooling. If this seems a bit far-out
let us remember that tremendous portions of our technology depend
on such things as controlled discontinuities at levels which were
not even detectable thirty years ago.

    What about the shapes of the future? They will be like the
shapes of the past, mostly. Considerable ingenuity has been applied
to the problem of getting useful data, and much of this has been
directed to the sample holder design. New shapes will be brought
forth, but seldom; our problem will be selection from amongst the
many existing possibilities. Again, this choice will depend upon
the intended use.

    I shall advance the thesis that the major new knowledge will
come by use of a moderate-size sample with the temperature-measuring
thermocouple in the center or along the axis. The reason is simple;
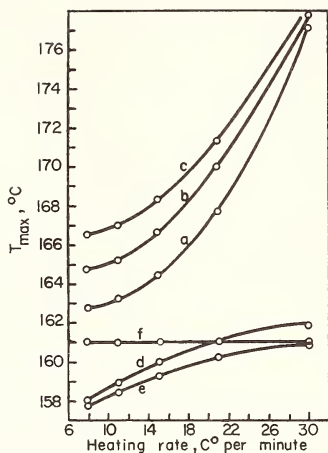
Figure 16. Peak temperature of (diluted) salicylic acid melting
            as measured in the block (a,b,c), the reference (d,e),
            and the sample (f). Curves a,d, and f refer to the
            same sample weight. (Barrall and Rogers [7]).
            Variations in thermal lag at the several locations
            will be dependent on heating rate; the actual melting
            point will not.

more of the extraneous parameters are eliminated and the heat effects
seen by the thermocouple are necessarily influenced by the sample.
An example of the elimination of a variable is the Barrall and Rogers
[7] work (Fig. 16) in which they showed that the salicylic acid peak
shifted in temperature both with sample weight and heating rate if
the temperature was measured at other points, but invariant with
heating rate if the measurement was made on the sample axis. Other
shapes will be used for measurement, and I feel sure that most meas-
urements will involve other shapes.

    *The important conclusion here is that shapes other than cylin-
ders may present some convenience in measurement, but there is no
superiority for obtaining meaningful data. The major deduction, then,
is that we should not allow ourselves to acquire a fondness for a par-
ticular type of sample holder, but pick and choose according to the
problem.*
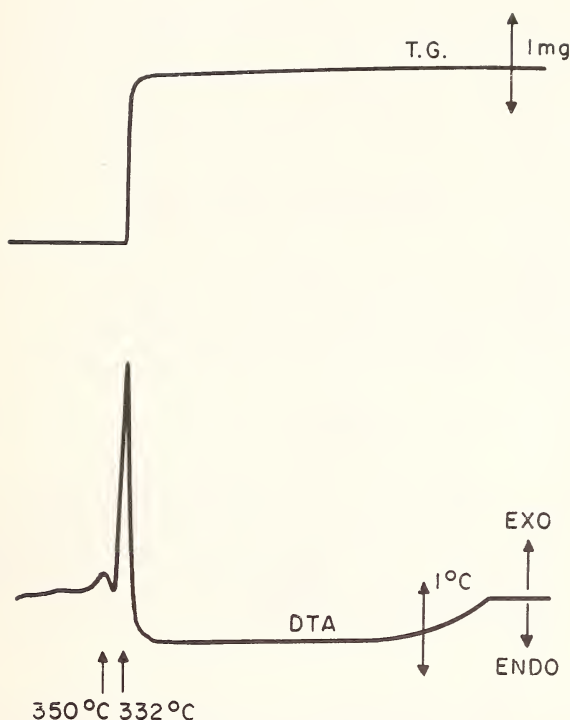
Figure 17.   DTA-TGA data for PbN6 aged 2 weeks at room
              temperature in an H_2O + CO_2 atmpsphere (Pai-
              Verneker and Maycock [8]). With the 25°/min
              heating rate, 2.0 mg of sample, the detonation
              characteristics are very obvious.

     So let us look at a further variety of problems and see why
differences are appropriate. PaiVerneker and Maycock [8] had a
good reason to use small samples of lead nitride; they wanted to use
their equipment again (Fig. 17). Here we would not become concerned
about very accurate measurement of the sample temperature; it
changes too rapidly to follow anyway. So measuring the temperature
of the sample container suffices. Besides, we can reasonably infer
that the important measurement is the temperature of the surface of
the first particle to decompose. Hence the surface on which the
particles are resting is the appropriate measurement.
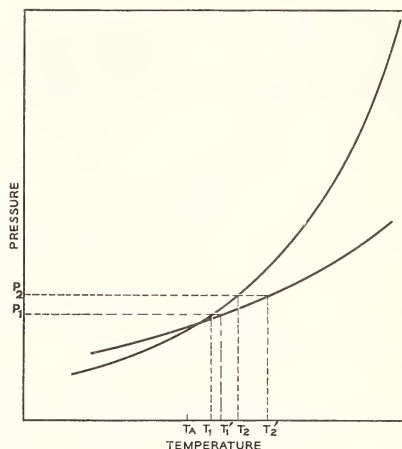
Figure 18. Van't Hoff plots for two reactions of the same
            kind. Even though the two reactions may occur
            together at some particular pressure a change
            in pressure will separate them on the tempera-
            ture scale. The separation, $T_1'-T_1$, will vary
            regularly with pressure.

     We must not neglect the utility of gases -- and pressures of
gases. I have already described the advantages to be gained by
atmosphere control [9], but let us look at it as a means of resolv-
ing peaks. The van't Hoff equation (Fig. 18) describes the vari-
ation of equilibrium vapor pressure with temperature -- or *vice
versa*. If the van't Hoff equation is plotted for each of two
materials, we can see that even if they decompose at the same tem-
perature at some pressure, by changing the pressure the reactions
can be separated. A good example here is the calcite-magnesite
system (Fig. 19) reported by Stone [10]. The reactions are resolv-
ed at 16.5 mm and higher, but if the pressure were decreased sig-
nificantly they would coincide.

     Note that the gas supplied is the one concerned in the reac-
tion. If other gases are used, special care must be taken or it
may have an adverse effect on the reaction. Helium is sometimes
used when evolved gases are to be measured, but it has particularly

TEMPERATURE IN DEGREES CENTIGRADE
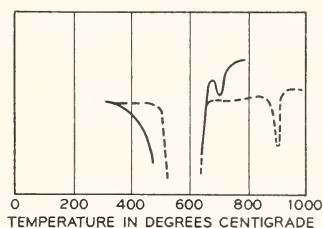
Figure 19. Differential thermal analysis of magnesite
            in carbon dioxide ——— 16.5 mm of Hg;
            ----- 750 mm of Hg (Stone [10]). The calcite
            peak is shifted much more than the magnesite.
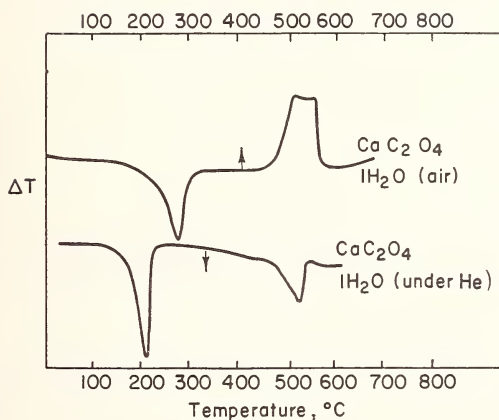
Figure 20. Differential thermal analysis curves of calcium
            oxalate monohydrate (Wendlandt [11]). The peak
            (200-300 °C) for the dehydration was used to
            calculate the activation energy by the method of
            Borchardt (Garn [9]).

bad effects. Wendlandt's [11] work shows the effect on a simple
dehydration, a very substantial peak shift downward in temperature
(Fig. 20). The reason is simple. Gases diffuse in helium with
tremendous velocity, so that the partial pressure at the surface
is low because the water moves away quickly. In air, the diffu-
sion is slower, so a significant partial pressure can accrue.

Also, there is a considerable difference between air and
oxygen. They both support oxidation but one carries with the ac-
tive ingredient a quadruple portion of inert gas. So if diffusion
of oxygen is required in the reaction the supply is quickly de-
pleted and further transfer of oxygen must take place through a
layer of nitrogen. May's [12] work on SBR rubber illustrates
this very well (Fig. 21). The need to carry along the nitrogen
as the gas moves inward slows oxidation reactions sometimes to
the point of being imperceptible.

We cannot avoid the question of atmosphere control, not sim-
ply as a blanket to avoid reaction but often as a means of supply-
ing one of the reactants. Oxidative stability studies can be
carried out under circumstances which simulate the normal atmos-
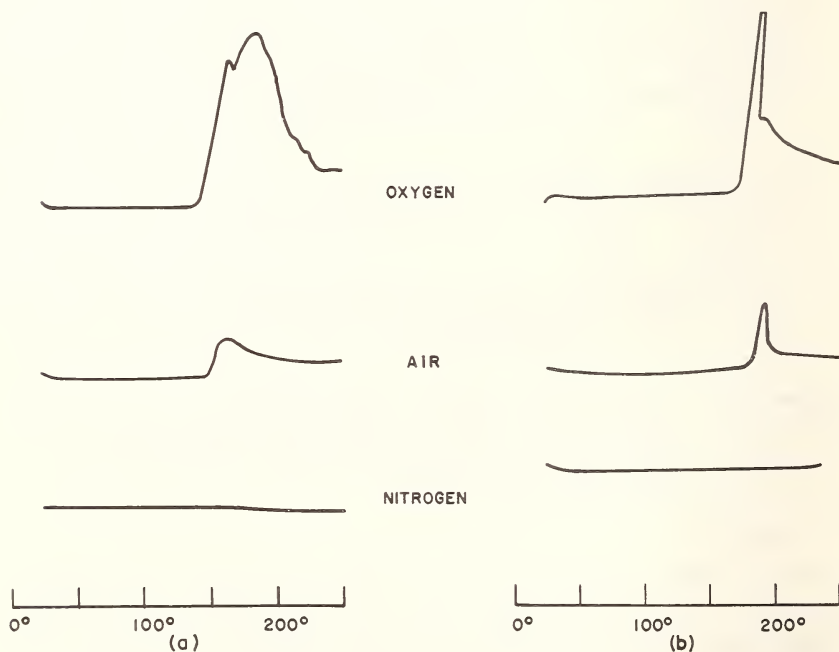
Figure 21.   DTA curves for SBR rubber. (a) Without antioxidant.
             (b) With antioxidant. (May, Bsharah and Merrifield
             [12].

phere, or the inside of a reaction vessel, or the upper atmosphere, or a deep-sea-diving apparatus without difficulty. And as we introduce new materials we must carry out the appropriate studies. But these will become more and more concerned with the structure of the peak rather than the existence or magnitude of the heat effect.

To summarize and repeat, standardization of the DTA experiment as a general procedure is unwise. In DTA we are carrying out a physical or chemical process whose heat effect is the resultant of many factors. We must design each test so that the parameter we want to evaluate has the maximum effect on the signal we obtain. This will usually require only a judicious selection from among the known types of furnace assemblies, using the same control and recording assembly for all.

REFERENCES

[1]   Garn, P. D., Thermal Analysis of Small Samples. Proc. Intern. Symp. Microchem. Techniques, State College, Pennsylvania, 1961 Cheronis, N. D., Editor, pp. 1105-1109, Wiley, New York, 1962.

[2]   Martin, S. G., and Ramstad, R. W., Compact Two-Stage Gas Chromatograph for Flash Pyrolysis Studies, Anal. Chem. $\underline{33}$, 982-985 (1961).

[3]   Adler, H. H. and Puig, J. A., Thermal Behavior of Brannerite, Am. Mineralogist $\underline{46}$, 1086-1096 (1961).

[4]   Keith, M. L. and Tuttle, O. F., Significance of Variation in the High-Low Inversion of Quartz, Am. J. Sci., Bowen Vol., Pt. 1, 203-252 (1952).

[5]   Schwenker, R. F., Jr. and Beck, L. R., Jr., The Differential Thermal Analysis of Textile and Other High Polymeric Materials, Textile Res. J. $\underline{30}$, 624-626 (1960).

[6]   Garn, P. D., On the Dissimilarities in $Solid_1 \quad Solid_2$ Phase Transformations, Anal. Chem. $\underline{41}$, 447-456 (1969).

[7]   Barrall, E. M. and Rogers, L. R., Differential Thermal Analysis of Organic Samples. Effects of Geometry and Operating Variables, Anal. Chem. $\underline{34}$, 1101-1105 (1962).

[8] PaiVerneker, V. R. and Maycock, J. N., Simultaneous Differ-
     ential Thermal Analysis-Thermogravimetric Analysis Tech-
     nique to Characterize the Explosivity of Lead Azide,
     Anal. Chem. 40, 1325-29 (1968).

[9] Garn, P. D., "Thermoanalytical Methods of Investigation,"
     Academic Press, New York, 1965.

[10] Stone, R. L., Thermal Analysis of Magnesite at Carbon
      Dioxide Pressures up to Six Atmospheres, J. Am. Ceram.
      Soc. 37, 46-47 (1954).

[11] Wedlandt, W. W., Reaction Kinetics by Differential
      Thermal Analysis, J. Chem. Educ. 38, 571-573 (1961).

[12] May, W. R., Bsharah, L. and Merrifield, D. B., Evaluation
      of Antioxidant Activity in Rubber by Differential
      Thermal Analysis, I & EC Product Research and Development,
      7, 57-61, March 1968.

MACROCALORIMETRY - HOW ACCURATE?

K. L. Churney, G. T. Armstrong, E. D. West

Physical Chemistry Division
Institute for Materials Research
National Bureau of Standards
Washington, D. C.   20234

The measurement theory of isoperibol and adiabatic
shield calorimeters operated by the method of intermittent
heating is reviewed and recent developments indicated.
Implications of the theory in terms of calorimeter design
and tests for systematic errors are discussed. Some idea
of the magnitude of calorimetric errors (as compared to
errors arising from uncertainties in the change of state
of the system under study) is outlined.

Key words: adiabatic shield; calorimetric errors;
calorimetry; isoperibol; measurement theory.

1.   INTRODUCTION

The rapid growth in the use of differential thermal methods
has been accompanied by increasing demands in the use of these
methods to measure such thermodynamic properties as heat capaci-
ties, heats of fusion, heats of transition, and heats of reaction.
For example, the recent development of differential scanning
calorimeters [1,2] of the temperature-controlled type [3] may be
viewed as an effort to improve the utility of differential thermal
methods in making thermodynamic measurements without sacrificing
the principal advantages of these techniques (small sample size
and speed) or their sensitivity.

The measurement theory of differential thermal measurements
amounts to an analysis of the operation of differential calori-
meters (see ref. [3-5]) in the dynamic mode [6]. As dynamic
processes, the methods are at a disadvantage whenever attainment
of thermodynamic equilibrium by the sample is slow relative to

the scanning rate [6d]. Also, low heat transfer coefficients
inside the calorimeter (*i.e.*, those among sample, sensor, and
calorimeter) and any large heat loss to the calorimeter environ-
ment can lead to a large uncertainty in the determination of the
temperature of the sample in spite of small sample size and low
scanning rates. Neither these ideas nor the idea of operation
of calorimeters in the dynamic mode are new to macrocalorimetry
(where by contrast the mass of sample or quantity of heat are
relatively large). When heat losses are minimized, as in adia-
batic shield calorimeters [7], and internal temperature gradients
are reduced [8], heat capacities can be obtained whose accuracy
and precision [8-10] are limited only by the inherent uncertainty
(see ref. [11], p. 338) of the dynamic mode of operation.

     A reasonable goal in calorimeter design is to make the cal-
orimetric errors less than those associated with specifying the
change in state under study. While this can be achieved for the
most part in conventional calorimetry [12,13] this is apparently
not yet generally the case in differential thermal methods.
Thus, it seems entirely relevant to review some of the concepts
used in the design and operation of certain common types of macro-
calorimeters. Such a review, more or less unencumbered by details,
can afford insight about sources of error in differential thermal
methods because, in concept, the measurement theory is identical
with that of conventional macrocalorimetry.

     Numerous reviews [6,12,14,15] of calorimetry and treatises
concerning its application to thermochemistry [16,17] and thermo-
dynamics [18] can be consulted for details of macrocalorimeter
design and use.

     We shall consider only two types of calorimeters: first,
the "isoperibol" [19] calorimeter, in which the temperature of
the calorimeter environment is independent of time, and second,
the adiabatic shield calorimeter, where the calorimeter is
surrounded by a shield whose temperature is adjusted so it matches
that of the calorimeter at all times.

In addition, we shall restrict our comments with respect to the operation of the calorimeter to the "intermittent [11,20] or interrupted [21] heating method" of operation of the calorimeter. In this method, the temperature of the calorimeter is first measured when it is in a quasi-equilibrium state, called a rating period, when there is no power input. It is then heated at constant power for a known time interval or allowed to be heated as a result of a chemical process. After a suitable time interval the temperature is again measured in another quasi-equilibrium state or rating period. The extension of the arguments to the method of "continuous heating" [20] is straight-forward.

For the purpose of illustration and simplification the various concepts will be discussed by associating them with some simple models of calorimeters. We shall classify these as one-body or two-body models of a calorimeter depending upon whether the calorimeter is considered (approximately) as consisting of one or two regions of uniform temperature.

2.   ONE-BODY MODEL OF AN ISOPERIBOL CALORIMETER

A.   Assumptions and Summary of Design Criteria

Most of the design criteria for calorimetry can be thought of as originating from this simplest model of a calorimeter. This model is sketched in Figure 1 and can be described in terms of the following three assumptions.

(1) The calorimeter, a single body having a heat capacity C_1, has a uniform but time varying temperature, T_1, and is surrounded by a jacket or environment held at a uniform temperature, T_0, which is independent of time.

(2) The rate of absorption of heat from the environment is given by $h_{10}(T_0-T_1)$ where h_{10} is the coefficient for heat transfer between the calorimeter and environment.

(3) C_1 and h_{10} are assumed to be independent of temperature and time.
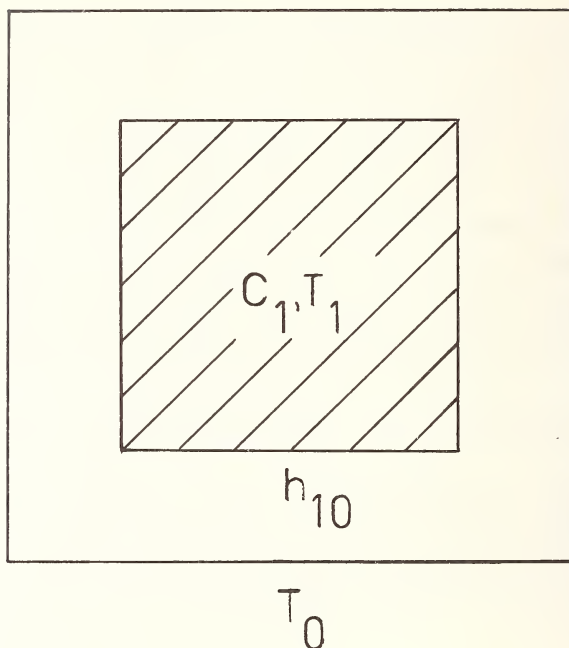
Figure 1.   Sketch of one-body model of an isoperibol
             calorimeter.

Accordingly, while this model of a calorimeter is not attain-
able in a real calorimeter, a conscious effort is made in the de-
sign of practical calorimeters to cause them to conform to the
description given above. To meet assumption (1), the jacket is
usually designed so its temperature is constant and uniform [22].
For the calorimeter itself, if it has large dimensions, we use a
closed can containing a liquid and stir so as to promote uniform-
ity of temperature of the calorimeter [22,23]. For calorimeters
of smaller dimensions, construction materials of high thermal
conductivity and diffusivity are used [23]. Within the calori-
meter, heat transfer coefficients across solid boundaries are in-
creased by small separations, large contact area, and use of
liquids, greases, or of gases such as helium between solid bound-
aries [23]. Use of vanes plus helium gas in low temperature cal-
orimetry to increase thermal contact between the sample and con-

tainer is a typical example [21,24]. In addition to improving
heat transfer inside the calorimeter, we reduce internal tempera-
ture gradients by reducing the heat exchange with the environment
(*i.e.*, minimizing h_{10} and keeping T_0-T_1 as small as is practicable).
Gaseous free convection is eliminated by evacuation of the space
between the calorimeter and jacket whenever possible or by minimi-
zing the space and temperature difference between the calorimeter
and jacket [23]. This also eliminates gas conduction. Heat trans-
fer by radiation is reduced by using materials of low emissivity
for the outer surface of the calorimeter and inner surface of the
jacket. Conduction by solids is reduced by using a minimum of
connections between the jacket and calorimeter and these are made
of small cross-sectional area and, where possible, of low thermal
conductivity. When evacuation is not practical, gaseous conduc-
tion is reduced by using the maximum separation concordant with
eliminating free convection [25].

Attempts are made to conform to assumptions (2) and (3) by
eliminating heat transfer by convection, minimizing emittances,
and keeping T_1-T_0 and the range of T_1 in any one experiment small.

B. Results Predicted by the One-body Model

Applying the principal of conservation of energy one obtains
equation (1), which is a statement that the rate of energy in-
crease of the calorimeter equals the rate at which heat is trans-
ferred from the jacket to the calorimeter and work is done on the
calorimeter. Expansion work is neglected.*

$$\frac{C_1 dT_1(t)}{dt} = h_{10}[T_0-T_1(t)] + P_1^o + P_1(t) \tag{1}$$

In eq. (1), dT_1/dt is the rate of temperature rise of the calori-
meter, P_1^o is the time invariant, and $P_1(t)$ the time- varying rate

---
* The overall expansion work done on the calorimeter will tend
to cancel in the substitution method outlined in section 2,C.
In any event, this term is small.

at which work is done on the calorimeter.

When $P_1(t) = 0$, a rating period, we find:

$$\frac{dT_1}{dt} = b(T_{1\infty} - T_1) \tag{2a}$$

where

$$b = \frac{h_{10}}{C_1} \; ; \quad T_{1\infty} = T_0 + \frac{P_1^o}{h_{10}} \tag{2b}$$

b is called the cooling constant and $T_{1\infty}$ the convergence temperature.

When $P_1(t) \neq 0$ one obtains:

$$T_1(t) = T_{1\infty} + (T_1(0) - T_{1\infty})e^{-bt} + e^{-bt} \int_0^t e^{+b\tau} \frac{P_1(\tau)}{C_1} \, d\tau \tag{3a}$$

where $T_1(0)$ is the value of T_1 at $t = 0$. For $P_1(t) = \beta[U(t) - U(t-t_h)]$, where $U(t)$ is the unit step function, β is the magnitude of the power, and t_h is the heating interval one obtains:

$$e^{-bt} \int_0^{t_f} e^{+b\tau} P_1(\tau) d\tau = e^{-bt} \frac{\beta}{b} [e^{bt} - 1] \quad 0 \le t \le t_h$$

$$= e^{-bt} \frac{\beta}{b} [e^{bt_h} - 1] \quad t \ge t_h \tag{3b}$$

A rough sketch of a temperature-time curve of a typical calorimetric experiment in which the idealized calorimeter conforms to eqs. (3a) and (3b) is shown in Figure 2. Equation (3b) indicates that at time $t = 0$ (initiation of heating) the calorimeter temperature starts to rise with a slope of β added to the previous
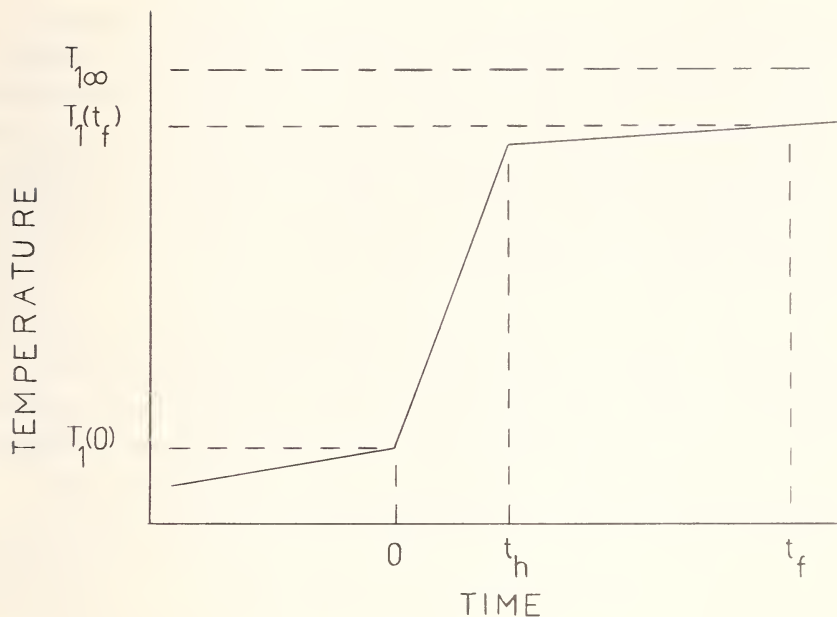
Figure 2.   Temperature-time curve for a one-body model
            of an isoperibol calorimeter for an electrical
            calibration experiment.

rate of rise, $b(T_{1\infty}-T_1)$. Because b is small this continues with
only a slight diminution until t_h, at which time the rate of
temperature rise is restored abruptly to that appropriate to eq.
(2a). Before t = 0 and any time after t_h, eq. (2) is obeyed and
the calorimeter is said to be in a rating period. For later
purposes, we take the final rating period after time t_f and call
the time between 0 and t_f the main period.

    To express our results in the conventional form for calcu-
lation, we integrate eq. (1) between 0 and t_f to give

$$C_1\left[T_1(t_f) - T_1(0) - b \int_0^{t_f} (T_{1\infty}-T_1)dt\right] = \int_0^{t_f} P_1(t)dt = W \qquad (4a)$$

$$C_1\Delta\theta_1 = W \qquad (4b)$$

Equation (4b) is the conventional "working" equation of isoperibol calorimetry--the product of the heat capacity*, C_1, times a corrected temperature rise, $\Delta\theta_1$, equals W, the work done on the calorimeter by the power source, P. The quantities $T_1(t_f)$, $T_1(0)$, b, and $T_{1\infty}$ of eq. (4a) are determined from rating period data, and the integral is evaluated from the main period data.** For the idealized one-body calorimeter $\Delta\theta_1$ will be independent of the value of t_f so long as $t_f \geq t_h$.

It is to be noted that the assumption that C_1 and h_{10} are independent of temperature makes eq. (1) a linear differential equation and allows the principle of superposition to be applied. This principle is shown explicitly in eq. (3a) where the temperature is a superposition of that due to heat transfer from the environment and that due to the power source $P_1(t)$.

C.   Limitations of the One-body Model

Real isoperibol calorimeters do not conform exactly to the assumptions and predicted performance of the one body model. During the heating interval the temperature gradient inside the calorimeter [23,24] and on the calorimeter surface [23] can be quite large compared to those when $P_1(t) = 0$. Also, the rate of rise of the temperature, dT_1/dt, does not abruptly increase by the amount β as predicted by eq. (3b) at time t = 0 or drop to $b(T_{1\infty}-T_1)$ just after t_h. Only for the time $t_f \gg t_h$ [25,27] is eq. (2) obeyed. Provided, however, we define the final rating period to be a period of time when eq. (2) is again obeyed, we do find that eq. (4) is obeyed if $\Delta\theta_1$ is evaluated from the actual temperature-time curve of the main period. That is, $\Delta\theta_1$ is independent of t_f and C_1 is independent of the heating rate β. The experimental finding that C_1 is independent of β suggests that any error in eq. (4) due to the temperature gradient during the main period is proportional to W.

---

*Heat capacity is later altered to energy equivalent.
**For details see [25-28].

A second objection to the one-body model arises because we do not know how to exactly locate the boundary surface separating the environment and the calorimeter. If a calorimeter met assumption (1) of the one-body model in section 2,A, the boundary could be located by determining the location of an infinite temperature gradient! For real calorimeters no such gradient exists. Nothing in our experimental results or one-body theory suggests an alternative method for locating the boundary experimentally. For further discussion of this point see [11]. Since the boundary of the calorimeter is indefinite, it follows that it is impossible to compute the heat capacity of the calorimeter even assuming C_1 is the sum of heat capacities. An experimental calibration must be made as outlined below.

In light of the above considerations, we can then modify the application of the ideal one-body theory to handle real calorimeters as follows:

(1) Take t_f sufficiently larger than t_h so that eq. (2) is obeyed. That is, eq. (2) will be used to define a rating period. Evaluate $\Delta\theta$ from the actual temperature-time curve of the main period after obtaining b and $t_{1\infty}$ from the rating period data.

(2) Calibrate the calorimeter experimentally in such a way that the boundary need not be known. For example, in a heat capacity experiment, determine the heat capacity with and without the sample. If C_s is the heat capacity of the sample, C_c is that of the calorimeter, and heat capacities can be added, we have for the two experiments:

$$(C_c + C_s)\Delta\theta_1 = W_1 \tag{5a}$$

$$C_c\Delta\theta_1' = W_1' \tag{5b}$$

(3) Attempt to duplicate the temperature-time curves for the various calorimetric determinations (for instance, for the full calorimeter, eq. (5a), and empty calorimeter, eq. (5b)) so that errors in evaluation of the heat exchange by means of

eq. (4) due to the temperature gradients during the main
period will tend to cancel.

The last two procedures constitute the elements of the
substitution method in calorimetry [29,30]. As will be seen
in subsequent sections, the last condition can be replaced.

Since heat capacities are assumed not to change during an
experiment, and large non-uniformities of temperature are not
provided for, the one-body model cannot handle in any simple
way the cases of a chemical reaction, drop calorimetry with an
isoperibol "receiving" calorimeter, or the measurement of a
heat of fusion. In these cases the heat capacity of the calor-
imeter plus contents does change in an abrupt way or a large
deviation from uniformity of temperature occurs during an ex-
periment so that a more sophisticated model of a calorimeter
is required.

3.   THE TWO-BODY MODEL OF AN ISOPERIBOL CALORIMETER

A.   Internal Temperature Differences

We now assume the calorimeter consists of two bodies having
constant heat capacities C_1 and C_2 and uniform but time varying
temperatures T_1 and T_2 as shown in Figure 3. We assume that
only body one exchanges heat with the environment and the rate
of this exchange is given by $h_{10}(T_0-T_1)$ as before. Applying the
principle of conservation of energy to the calorimeter as a
whole, we have:

$$C_1 \frac{dT_1}{dt} + C_2 \frac{dT_2}{dt} = h_{10}(T_0-T_1) + P_1^o + P_1(t) + P_2(t) \qquad (6)$$

In eq. (6) P_1^o, P_2^o are the time invariant and $P_1(t)$, $P_2(t)$ are
the time varying rate of doing work on bodies one and two,
respectively.
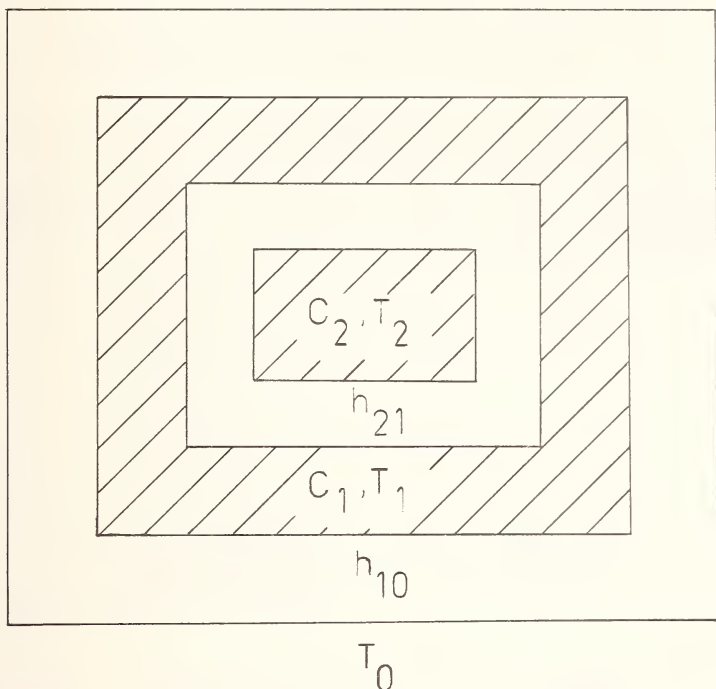
Figure 3.   Sketch of a two-body model of an isoperibol
            calorimeter involving internal temperature
            differences.

Investigating first the temperatures when $P_1(t) = P_2(t) = 0$,
we assume that heat exchange between body one and body two is
proportional to T_2-T_1. Applying conservation of energy to body
two, we have:

$$C_2 \frac{dT_2}{dt} = h_{21}(T_1-T_2) + P_2^0 \tag{7a}$$

In eq. (7a) h_{21} (equal to h_{12}) is the coefficient for heat trans-
fer bodies one and two. It is taken to be large compared to h_{10}
and is also taken to be independent of temperature and time. As
has been shown previously [31], the solution of eqs. (6) and (7a)
when $P_1(t) = P_2(t) = 0$ is as follows:

$$T_1 = T_{1\infty} + Ae^{-b_1 t} + Be^{-b_2 t} \tag{8a}$$

$$T_2 = T_{2\infty} + Aq_1 e^{-b_1 t} + Bq_2 e^{-b_2 t} \tag{8b}$$

The quantities $T_{1\infty}$, $T_{2\infty}$, q_1, q_2, b_1, and b_2 in eqs. (8a) and (8b) are defined as follows:

$$T_{1\infty} = T_0 + (P_1^o + P_2^o)/h_{12} \tag{8d}$$

$$T_{2\infty} = T_0 + (P_1^o + P_2^o)/h_{10} + P_2^o/h_{12} \tag{8c}$$

$$q_1 = \frac{(h_{12}/C_2)}{(h_{12}/C_2) - b_1} \;\; ; \;\; q_2 = \frac{(h_{12}/C_2)}{(h_{12}/C_2) - b_2} \tag{8e,f}$$

$$b_1 = \frac{h_{10}}{C_1 + C_2 q_1} \;\; ; \;\; b_2 = \frac{h_{12} + h_{10}}{C_1} + \frac{h_{12}}{C_2} - b_1 \tag{8g,h}$$

Since we have selected (*i.e.*, designed) our calorimeter so h_{10} is small and h_{12} is large, b_1 is much less than b_2*. Thus we obtain from eqs. (8a) and (8b) after a sufficient length of time so the second exponential term is negligible:

---

*For $b_1 \ll b_2$, $\dfrac{h_{12} h_{10}}{C_2 C_1} \ll \left(\dfrac{h_{10}}{C_1} + \dfrac{h_{12}}{C_2} \right)^2$ which gives

$$b_1 \sim \frac{\dfrac{h_{10} h_{12}}{C_1 C_2}}{\dfrac{h_{10} + h_{12}}{C_1} + \dfrac{h_{12}}{C_2}} \quad \text{and } b_2 \sim \frac{h_{10} + h_{12}}{C_1} + \frac{h_{12}}{C_2}$$

$$\frac{dT_1}{dt} = b_1(T_{1\infty}-T_1) \;\; ; \;\; \frac{dT_2}{dt} = b_1(T_{2\infty}-T_2) \tag{9a}$$

Equations (9a) are of the same form as eq. (2a) for the one-body model. While eq. (2a) is valid for all times when the time varying component of the rate of doing work on the calorimeter is zero, eqs. (9a) require in addition that certain transients must die out before a rating period can exist. Thus, the two-body model provides a justification of the first modification of the one-body theory to allow application to real calorimeters given in section 2,C. It also gives two new results. First, the cooling constant is the same (*i.e.*, b_1) wherever the temperature is measured in the calorimeter but the convergence temperatures (*i.e.*, $T_{1\infty}$ or $T_{2\infty}$) will be different. Second, the cooling constant is a function of ratios of heat transfer coefficients divided by heat capacities and will vary to a certain extent if the internal heat transfer coefficients (*i.e.*, h_{12}) of the calorimeter should change.

In order to investigate the temperature differences present during rating periods, we also obtain from eqs. (8) that

$$\frac{dT_2}{dt} = q_1 \frac{dT_1}{dt} \tag{9b}$$

or

$$(T_2-T_1) = (q_1-1)(T_1-T_0) - (q_1-1)\frac{P_1^o + P_2^o}{h_{10}} + \frac{P_2^o}{h_{12}} \tag{9c}$$

We see that provided one temperature is known, the other is automatically fixed during rating periods. Further, the temperature difference, T_2-T_1, varies linearly with the temperature difference between the calorimeter and jacket, T_1-T_0, as expected. Since

$$q_1 = 1 + \frac{h_{10}}{h_{12}} \frac{C_2}{(C_1 + C_2)} \tag{9d}$$

to the first order of small quantities when $h_{10} \ll h_{12}$, the model also confirms the design criterion suggested to reduce internal temperature differences, *i.e.*, $h_{10}/h_{12} \ll 1$. The internal temperature differences will not be small, however, unless P_1^o/h_{12} and P_2^o/h_{12} are small. In the intermittent heating method P_1^o and P_2^o are made small (*i.e.*, only the temperature sensor current and in the case of stirred liquid, the heat of stirring, contribute to P_1^o, P_2^o). In the continuous heating method, P_1^o and P_2^o are large and it is necessary to make h_{12} large [12].

In order to obtain working equations analogous to eq. (4), one can first integrate eq. (6) directly, using eq. (9b), to obtain:

$$(C_1 + C_2 q_1)[T_1(t_f) - T_1(0)] = h_{10} \int_0^{t_f} (T_{1\infty} - T_1)dt + W$$

where $W = \int_0^{t_f} [P_1(t) + P_2(t)]dt$. Using eq. (8g), we obtain

$$(C_1 + C_2 q_1)\left[T_1(t_f) - T_1(0) - b_1 \int_0^{t_f} (T_{1\infty} - T_1)\, dt \right] = W \qquad (10)$$

It should be noted that in eq. (6) and in deriving eq. (10) we did not make any assumption about the manner of heat exchange between body one and two during the main period. The importance of this comment will be evident in section 3,C.

For comparison, we can derive an equation analogous to eq. (10) involving only the temperature of the inner body. For this purpose, we assume that during the main period the heat exchange between bodies one and two is proportional to $T_2 - T_1$ and modify eq. (7a) as follows:

$$C_2 \frac{dT_2}{dt} = h_{12}(T_2 - T_1) + P_2^o + P_2(t) \qquad (7b)$$

Eliminating T_1 from the right hand side of eq. (6) with eq. (7b), integrating, and simplifying terms one obtains:

$$(C_1 + C_2 q_1)\left[T_2(t_f) - T_2(0)\right] = \left[h_{10}\int_0^{t_f}(T_{2\infty}-T_2)dt + \frac{h_{10}}{h_{12}}f_2 W\right] + W \quad (11a)$$

In eq. (11a) we have assumed:

$$P_1(t) = f_1 g(t); \quad P_2(t) = f_2 g(t); \quad f_1 + f_2 = 1; \quad \int_0^{t_f} g(t)dt = W \quad (11b)$$

That is, we assume the rate of doing work on the calorimeter is a product of a function of time and position. (This is reasonable for electrical calibration experiments but will not apply in general to chemical reactions.) The left hand side of eq. (11a) is the increase in internal energy of the calorimeter while the quantity in the brackets, [], on the right hand side is the heat absorbed by the calorimeter during the main period. We see that the error incurred in using the temperature T_2 to measure the heat exchange is indeed proportional to W as proposed in section 3,C. Rearranging eq. (11a), one obtains

$$\frac{(C_1 + C_2 q_1)}{(f_1 + f_2(h_{10}+h_{12})/h_{12})}\left[T_2(t_f)-T_2(0)-b_1\int_0^{t_f}(T_{2\infty}-T_2)dt\right] = W \quad (12)$$

Comparison of eqs. (10) and (12) shows that wherever the temperature is measured, the equation has the form: the product of what we will now call an energy equivalent and the corrected temperature rise is equal to the work done on the calorimeter. This is the equivalent of White's [32a] statement "when the calorimeter is calibrated, it is calibrated, lag effects and all."

A new result given by the two-body model is that the energy
equivalent is not the sum of heat capacities. For example, in
eq. (10) the energy equivalent is equal to $C_1 + C_2 q_1$. q_1 is not
equal to one and is a function of the heat transfer coefficients
h_{10} and h_{12} as well as the heat capacities C_1 and C_2. Since in
practice it is impossible to measure these heat transfer coeffic-
ients accurately, we conclude that this is a second reason (be-
sides the inherently indefinite location of the calorimeter dis-
cussed in section 2,C) for determining the energy equivalent of
the calorimeter experimentally.

A second consequence of the above result is that heat capac-
ities of materials cannot be determined with an isoperibol calori-
meter by only a single combination of an "empty" and "full" calori-
meter experiment. For example, suppose we could assume the empty
calorimeter is an ideal one-body calorimeter with heat capacity C_1
and the full calorimeter is an ideal two-body calorimeter contain-
ing a sample with heat capacity C_2. In place of eqs. (5a) and (5b),
we have

$$(C_1 + C_2 q_1) \Delta \theta_1 = W \tag{13a}$$

$$C_1 \Delta \theta_1' = W' \tag{13b}$$

Additional experiments are then required to determine q_1.

As h_{10}/h_{12} goes to zero, eq. (9d) says q_1 approaches one and
hence, the energy equivalent in eq. (13a) approaches $C_1 + C_2$. This
constitutes the basis for one method of determining q_1 - extrapo-
lating energy equivalents to zero values of h_{10} (see [24,33]).
In practice, the energy equivalents of both the empty and full
calorimeter are extrapolated to zero values of h_{10} [33] since
neither the full nor the empty calorimeter can be approximated as
an ideal one or two-body calorimeter. To illustrate the magni-
tude of this extrapolation, in one case at room temperature (where
h_{10} is large) [33] the corrections to the energy equivalents of

the empty and full calorimeter were 1 percent and 0.3 percent respectively.

An alternative use of the fact that q_1 approaches one as h_{10} approaches zero is to interpose a closed shield between the calorimeter and the environment so that h_{10} is forced to be extremely small. If the temperature of the shield is kept equal to that of the calorimeter, one has an adiabatic shield calorimeter.

Another approach to the problem of non-additivity of heat capacities is to determine experimentally whether or not, for example, the energy equivalent increases linearly with the amount of sample added to the calorimeter [34].

Equations (10) and (12) show that the energy equivalent depends in general on the location of the thermometer and the geometrical distribution of the power supplied to the calorimeter (*i.e.*, f_1 and f_2 of eq. (12)). The implication of the latter is particularly important because, if not recognized, it can lead to a systematic error. For example, suppose one wished to calibrate a calorimeter electrically for the purposes of measuring the change in energy accompanying a chemical reaction. Assume that the heat liberated by the reaction can be treated as equivalent to that generated by doing electrical work on the calorimeter and that the change in the heat capacities of the various parts of the calorimeter can be neglected. Then eq. (7b) applies. It would then be necessary to show that f_1 and f_2 are the same in both cases or that variations in f_1 and f_2 have a negligible effect on the energy equivalent. This can be studied experimentally by determining the variation of the energy equivalent for various positions of the electrical heater (see Prosen [35] or Dickinson [36]).

Both eqs. (10) and (12) state that the energy equivalent of the calorimeter is independent of the heating rate, *i.e.*, it depends on $\int_0^{t_f} g(t)dt$ instead of $g(t)$ in eqs. (11a) and (12). Thus, we can now modify our original formulation of the substi-

tution method to the following: calibrate experimentally and
also determine experimentally whether the energy equivalent de-
pends linearly upon the amount of sample added and is independent
of the geometrical distribution of the power source. These
tests must be affirmative if systematic errors are to be avoided.

B. Surface Temperature Differences

        An alternative point of view arises from a literal interpre-
tation of eq. (10). This suggests that if the temperature, T_1,
of the surface of the calorimeter is uniform and we measure it,
the energy equivalent will be independent of the geometrical dis-
tribution of the power supplied to the calorimeter. This may be
thought of as the origin of the idea of measurement of the sur-
face temperature, so to speak, of the calorimeter.

        To consider this in more detail, let us acknowledge that
there are temperature differences on the surface of the calori-
meter. We can consider, then, the two-body model portrayed in
Figure 4 and assume a term $h_{20}(T_0-T_2)$ has been added to eqs.
(6), (7a), and (7b). h_{20} is the coefficient for heat transfer
between body two and the environment. In this case, the form
of eqs. (8a), (8b), (9a), and (9b) are the same (assuming again
$b_1 \ll b_2$) but q_1 is given by

$$q_1 = \frac{(h_{12}/C_2)}{(h_{12}+h_{20})/C_2-b_1}$$

Using the method of derivation of eq. (12), one can show that,
for example, the result analagous to eq. (10), where the
temperature of body one, T_1, is measured now becomes

$$\frac{\left[C_1 \frac{(h_{12}+h_{10})}{h_{20}} + q_1 C_2\right]}{\left[f_1 \frac{(h_{12}+h_{20})}{h_{12}} + f_2\right]} \left[T_1(t_f)-T_1(0)-b_1 \int_0^{t_f} (T_{1\infty}-T_1)dt\right] = W \qquad (14)$$
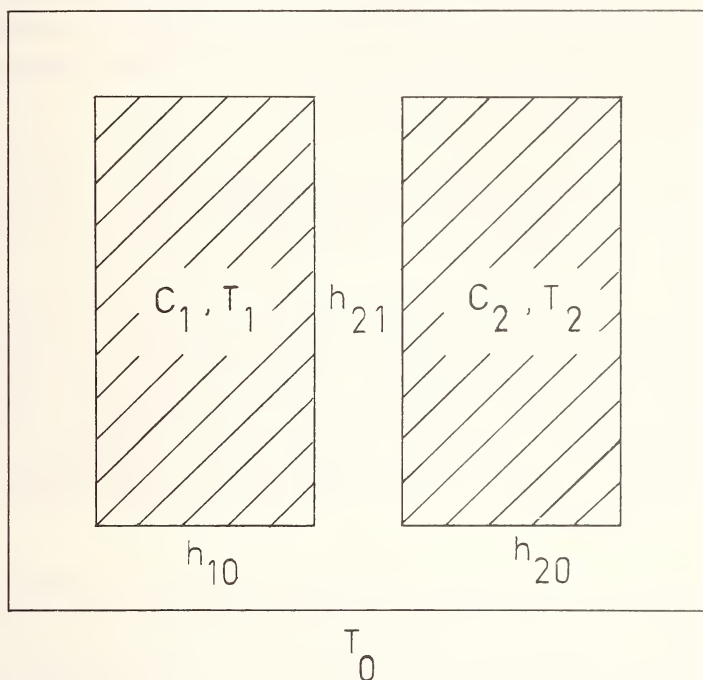
Figure 4. Sketch of a two-body model of an isoperibol
           calorimeter involving both internal and
           surface temperature differences.

A similar result will be obtained if the temperature of body
two is measured. That is, the energy equivalent in either case
is a function of f_1 and f_2.

     One can show this result is a consequence of the problem of
evaluating the heat absorbed by the calorimeter during the main
period by the measurement of the temperature of the calorimeter
in a single location. From a design point of view, the problem
can be reduced if the temperature gradient is minimized. Better,
it can be eliminated even without minimizing the surface gradi-
ents if the temperature gradient on the calorimeter surface is

independent of where heat is generated inside the calorimeter
[23]. Then the energy equivalent will be independent of differ-
ences between f_1 and f_2 for a temperature measurement made any-
where on the surface of the calorimeter.

The latter design criterion is given the title of "equivalent
sources" [37]. In light of this design criterion, the experi-
mental test for determining the dependence of the energy equi-
valent on the variation of f_1 and f_2, mentioned in section 3,A,
is called the "test for equivalent sources." The test amounts
to studying the dependence of the energy equivalent on variations
in the temperature gradients on the surface of the calorimeter
(produced by variations in the positions of the sources of energy
in the calorimeter). The design criterion for "equivalent
sources" constitutes the final revision of the substitution
method in calorimetry.

In practice, this design criterion is nearly satisfied in
stirred-water calorimeters when the stirring action of the pro-
peller mixes hot water from various sources before the water
reaches the calorimeter surface. (The temperature gradient on
the surface of the calorimeter, in any event, is usually small
[38].) It is also the origin of White's [32b] suggestion that
the dependence of the energy equivalent on the temperature
gradient on the calorimeter surface can be studied by altering
the rate of stirring to vary this gradient. Two designs, one
for a stirred-water calorimeter [38] and the other for aneroid
calorimeters [39,23] fulfill this design criterion in concept
as well as in practice.

It will be noted that the design criterion and test for
equivalent sources is associated with the desire to make temper-
ature measurements at a single location even though the tempera-
ture on the calorimeter surface is non-uniform. An alternative
approach sometimes adopted [24] is to abandon this desire and
attempt to measure some average temperature of the calorimeter
surface. In the case of the two-body model, it can be shown

that, when body two exchanges heat directly with the environment, the energy equivalent is indeed independent of f_1 and f_2 provided one is able to measure the average temperatures, S, given in eq. (15)

$$S = \frac{h_{01}T_1 + h_{02}T_2}{h_{01} + h_{02}} \tag{15}$$

As noted by White [40], the experimental difficulty with such a measurement is proving that the placement of thermocouples, for example, is such as to weight the temperatures at the various junctions in proportion to the local heat transfer coefficients to the environment. Certainly one proof might be obtained by the test for equivalent sources.

C. Change in State

The measurement of the change in energy associated with a chemical or physical (*i.e.*, heat of fusion) change in state can be handled in terms of the two-body model of Figure 3 discussed in section 3,A. Let us assume that the change in state takes place at the location of body two and replace eq. (6) by eq. (16a):

$$C_1 \frac{dT_1}{dt} + \frac{dE_2}{dt} = h_{10}(T_{1\infty}-T_1) + P_1(t) + P_2(t) \tag{16a}$$

In eq. (16a), dE_2/dt replaces $C_2 dT_2/dt$ and is the time rate of change of the energy of body two. $T_{1\infty}$ is given by eq. (8c). Integrating between the rating period ending at time $t = 0$ and the one beginning at time $t = t_f$, we have

$$C_1 [T_1(t_f)- T_1(0)] +[E_p(t_f) - E_r(0)] = h_{10} \int_0^{t_f} (T_{1\infty}-T_1)dt + W \tag{16b}$$

In eq. (16b), $E_p(t_f)$ and $E_r(0)$ are the energies of the products
at time $t = t_f$ and the reactants at time $t = 0$, respectively.
W is the work done on the calorimeter to cause or initiate the
change in state. To obtain results in a more conventional form,
let us first add and subtract from the left hand side of eq. (16b),
the quantity $E_p(0)$. $E_p(0)$ is the energy of the products at time
$t = 0$ assuming the change in state had occurred before the initial
rating period. Rearranging, one obtains

$$C_1[T_1(t_f) - T_1(0)] + [E_p(t_f) - E_p(0)] - h_{10} \int_0^{t_f} (T_{1\infty}-T_1)\,dt - W =$$

$$- [E_p(0) - E_r(0)] = -\Delta E_{\text{change in state}} \qquad (16c)$$

We make the further assumption that in the initial rating period
the actual temperature distribution in the calorimeter at time
$t = 0$ is close to that obtained if the products of the change in
state were present. This will be nearly so, if at time $t = 0$, the
calorimeter is near its convergence temperature. Then we may
write

$$E_p(t_f) - E_p(0) = C_2[T_2(t_f) - T_2(0)] \qquad (16d)$$

In eq. (16d) C_2 is the heat capacity of the products. Inserting
eq. (16d) into (16c) we obtain the familiar result

$$(C_1 + q_1 C_2)\left[T_1(t_f) - T_1(0) - b_1 \int_0^{t_f} (T_{1\infty}-T_1)\,dt\right] - W =$$

$$-\Delta E_{\text{change in state}} \qquad (17)$$

Thus, in this case, if one calibrates the calorimeter electrically when the products are present in the calorimeter, one obtains the change in energy associated with the change in state as if it took place isothermally at the temperature of body two at time t = 0.

If we had added and subtracted $E_r(t_f)$ from the left hand side of eq. (16c), we would assume that in the final rating period that the actual temperature distribution inside the calorimeter is close to that obtained if the reactants were present in the calorimeter. This assumption would be nearly fulfilled if the calorimeter is near its convergence temperature during the final rating period. Then the energy equivalent is determined electrically with the reactants present in the calorimeter and we obtain the change in energy associated as if it occurred isothermally at the temperature of body two at time $t = t_f$.

Since we measure the temperature of body one, the error in assigning the value $T_1(0)$ to the temperature of the isothermal change in state in eq. (17) will also be smaller if the calorimeter is near its convergence temperature at time t = 0 (see eq. (9c)).

Calculation of the change in energy at some other temperature requires a knowledge of the heat capacity of the products and reactants which must be determined in other experiments. If the change in energy for fusion, for example, is to be calculated, then the melting point must also be determined. Since in general the sample will contain impurities, this will involve a melting point - purity determination (see refs. [21,41]) and premelting corrections to the heat capacities (see ref. [21]).

It should be noted that, provided one can assume that body two does not exchange heat directly with the environment, eqs. (16) and (17) do not depend upon whether or not heat exchange during the main period (*i.e.*, 0 to t_f) between bodies one and two are linearly proportional to $T_2 - T_1$ or not. This is particularly important for a

chemical reaction where this is most certainly not the case.

An analogous treatment can be given for drop calorimetry with an "isoperibol" receiving calorimeter (see ref. [31]).

4.   ADIABATIC SHIELD CALORIMETERS

The need for adiabatic shield calorimeters can be thought of as arising for three reasons:

(1)   To obtain a calorimeter for heat capacity measurements whose energy equivalent is more nearly the sum of heat capacities.

(2)   To obtain a calorimeter in which the temperature distribution is more nearly uniform during rating periods.

(3)   To obtain a calorimeter whose heat exchange with the environment is small at all times so that one can study changes in state that require long times to reach thermodynamic equilibrium, without introducing excessively large corrections for heat exchange.

Two-body Model of an Adiabatic Shield Calorimeter

To see how the needs itemized above are more closely met by adiabatic-shield calorimeters, consider a model of an adiabatic-shield calorimeter as shown in Figure 5. We assume the calorimeter, itself, can be idealized as shown in Figure 3. Surrounding the calorimeter is an adiabatic shield whose temperature, T_s, is assumed to be uniform, but is varied with time so it is nearly always equal to the temperature, T_1, of the outer surface of the calorimeter. The coefficient for heat transfer between the shield and calorimeter is h_{1s}. Since this shield cannot be exactly perfect we will allow for this by assuming there is some heat exchange (*i.e.*, the value of $h_{10} \neq 0$) between the calorimeter and the environment which is held at some constant uniform temperature, T_0.

Applying conservation of energy to each of the bodies, one and two, of the calorimeter we have:
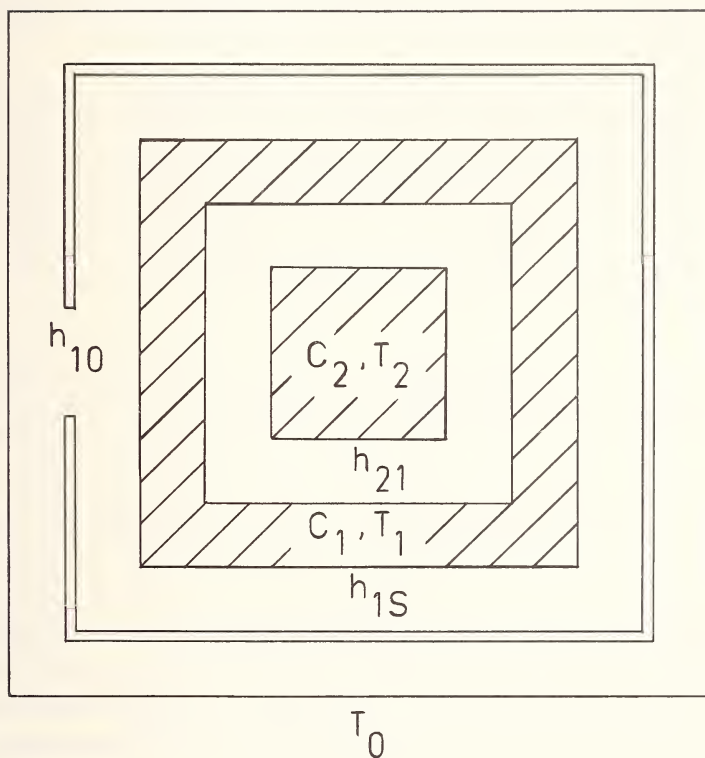
Figure 5.   Sketch of a two-body model of an adiabatic
            shield calorimeter involving internal
            temperature differences.

$$C_1 \frac{dT_1}{dt} = h_{1s}(T_s-T_1) + h_{10}(T_0-T_1) + h_{12}(T_2-T_1) + P_1^o + f_1 g(t) \qquad (18a)$$

$$C_2 \frac{dT_2}{dt} = h_{12}(T_2-T_1) + P_2^o + f_2 g(t) \qquad (18b)$$

To solve eqs. (18) it is necessary to specify how T_s-T_1
varies with time. The model shown in Figure 5 omits any consid-
eration of the details of the adiabatic shield and the associated
temperature control problem (for details see refs. [11, 20, 21]).

For our purposes it will be sufficient to appeal to experiment to specify (T_s-T_1).

During rating periods, when $g(t) = 0$, we assume that (T_s-T_1) reaches a constant very small value which we will call α. We will assume α is the same for all rating periods. Under these conditions, the form of eqs. (8) is virtually unchanged except that a term $\alpha h_{1s}/h_{10}$ must be added to $T_{1\infty}$ in eq. (8c) and $T_{2\infty}$ in eq. (8d). If, again, we assume $b_1 << b_2$ we obtain:

$$\frac{dT_1}{dt} = b_1(T_{1\infty}-T_1) = \frac{P_{20}+P_{10}+\alpha h_{1s}}{C_1+C_2 q_1} + b_1(T_0-T_1) \qquad\qquad (19a)$$

$$\frac{dT_2}{dt} = b_1(T_{2\infty}-T_1) = \frac{P_{20}+P_{10}+\alpha h_{1s}}{C_1+C_2 q_1} + b_1\left(T_0 + \frac{P_{20}}{h_{12}} -T_2\right) \qquad (19b)$$

In eqs. (19a) and (19b) we have factored out the terms in $T_{1\infty}$ and $T_{2\infty}$ that are inversely proportional to h_{10} using eq. (8g). Since α can in principle be positive or negative, depending upon how the controller for the shield operates, the physical meaning of a convergence temperature must be relinquished.

During the main period $T_s-T_1 = \delta(t)$ may vary with time. We assume that whatever this "offset", $\delta(t)$, we measure it experimentally during the main period. Then the equations analogous to those obtained in section 3,B are:

$$(C_1 + C_2 q_1)\left[\Delta T_1 - b_1 \int_0^{t_f} (T_{1\infty}-T_1)\,dt - \gamma \int_0^{t_f} \delta(t)dt\right] = W \qquad (20a)$$

$$\frac{(C_1 + C_2 q_1)}{\left[f_1+f_2\left(\frac{h_{12} + h_{10}}{h_{12}}\right)\right]} \left[\Delta T_2 - b_1 \int_0^{t_f} (T_{2\infty}-T_2)\,dt - \gamma \int_0^{t_f} \delta(t)dt\right] = W \qquad (20b)$$

where we have written:

$$\Delta T_1 = T_1(t_f) - T_1(0) \tag{21a}$$

$$\Delta T_2 = T_2(t_f) - T_2(0) \tag{21b}$$

$$\gamma = \frac{h_{1s}}{C_1 + C_2 q_1} \tag{21c}$$

It will be noted that eqs. (20a) and (20b) state that the corrected temperature rise in the case of an adiabatic shield calorimeter (the quantity multiplying $C_1 + C_2 q_1$ in eq. (20a), for example) consists of two parts. One part, $\Delta T_1 - b_1 \int_0^{t_f} (T_{1\infty} - T_1)dt$, is of the same form as that for an isoperibol calorimeter. The second part, $-\gamma \int_0^{t_f} \delta(t)dt$, is peculiar to an adiabatic shield calorimeter. It corrects for the heat transfer to the shield during the main period and is usually quite small or negligible in comparison to the first part. The parameter γ can be calculated from the change in drift rate of the calorimeter during rating periods caused by a deliberate known offset of the shield temperature as can be seen from eqs. (19) [21].

In order to convert the corrected temperature rise to the conventional form (see ref. [21]), we note that it can be shown that the term $b_1 \int_0^{t_f} (T_{1\infty} - T_1)dt$ is given by the expression [27]:

$$b_1 \int_0^{t_f} (T_{1\infty} - T_1) \, dt = \frac{dT_1(0)}{dt} (t_x - 0) + \frac{dT_1(t_f)}{dt} (t_f - t_x) \tag{21d}$$

where $(t_f - t_x) = \int_0^{t_f} [T_1(t) - T_1(0)] \, dt / [T_1(t_f) - T_1(0)]$. $\tag{21e}$

In eq. (21d) $dT_1(0)/dt$ and $dT_1(t_f)/dt$ are the time rate of change of the temperature, T_1, at times $t = 0$ and $t = t_f$, respectively. For electrical calibrations, it is found experimentally that t_x is approximately the midtime, t_m, of the heating interval (*i.e.*, $t_h/2$ of Figure 1). Thus, one can rearrange eq. (20a) using eq. (21d) to

$$(C_1 + C_2 q_1)\left[\Delta T_1 - \frac{dT_1(0)}{dt} t_m - \frac{dT_1(t_f)}{dt}(t_f - t_m) - \gamma \int_0^{t_f} \delta(t)dt\right] = W \tag{22}$$

In real adiabatic calorimeters b is two or three orders of magnitude smaller than it would be if no shield were present [42]. According to our model, b_1 approaches zero and q_1 one as h_{10} goes to zero--that is when the adiabatic shield is perfect. When $h_{10} = 0$ the rating period equations, eq. (19), become

$$\frac{dT_1}{dt} = \frac{dT_2}{dt} = \frac{P_{20} + P_{10} + h_{1s}\alpha}{C_1 + C_2} \tag{23a}$$

The temperature difference $(T_2 - T_1)$ during rating periods analogous to eq. (9c) becomes

$$(T_2 - T_1) = \frac{1}{h_{12}} \frac{(C_1 P_1^o - C_2 P_2^o)}{C_1 + C_2} \tag{23b}$$

When $h_{10} = 0$ eqs. (20a, 20b) or (22) become

$$(C_1 + C_2)\left[\Delta T_1 - \frac{dT_1}{dt} t_f - \gamma \int_0^{t_f} \delta(t)dt\right] \tag{23c}$$

$$(C_1 + C_2)\left[\Delta T_2 - \frac{dT_2}{dt} t_f - \gamma \int_0^{t_f} \delta(t)dt\right] \tag{23d}$$

dT_1/dt or dT_2/dt in eqs. (23c, 23d) are given in eq. (23a).
Thus in an adiabatic calorimeter with a nearly perfect shield
both the temperature and the rate of change of temperature dur-
ing the rating periods become more nearly equal. Further the
energy equivalent of the calorimeter becomes more nearly the sum
of heat capacities.

It is important to note that eqs. (20a and 20b) do not mean
the energy equivalent using a temperature measured anywhere in a
real adiabatic calorimeter is independent of the power distribu-
tion of the sources even though h_{10}/h_{12} may be negligible. The
reason for this is that the model considers only the internal
temperature difference in the calorimeter and not the surface
temperature difference produced by different distributions of
the power sources considered in section 3,C. Further, the ques-
tion of the temperature gradient in the shield and the effect of
where temperatures on the shield and calorimeter are controlled
to be equal have been totally neglected. Thus, for real adia-
batic shield calorimeters, the design relation for equivalent
sources must still be retained.

It should also be noted that while the correction for heat
exchange with its surroundings is greatly reduced in an adiabatic
shield calorimeter as compared to an isoperibol calorimeter, it
does not necessarily follow that the uncertainty in the measure-
ments due to the uncertainty in this heat exchange is also smaller.

5. SUMMARY: COMMENTS ON PRECISION AND ACCURACY

It can be seen that although the simple models of calori-
meters discussed in the previous sections are non-quantitative
(in the sense that they do not predict the magnitude of calori-
metric errors); they do have utility beyond providing a basis
for discussing calorimeter design. They afford valuable insight
into possible sources of calorimetric error and suggest experi-
ments to test for these errors that are predicted by more sophis-
ticated theories [37,43].

The heat exchange of the calorimeter with its environment
and the interrelation of this heat exchange with the tempera-
ture gradient in the calorimeter (and on its surface) have been
examined in the preceding material in terms of their effects on
the energy equivalent of the calorimeter. Particular attention
has been focused on possible errors in the determination of the
energy equivalents when the substitution method is used for
determining heat capacities or the change in energy associated
with a physical or chemical change in state.

In particular, we have considered an isoperibol calorimeter,
where the heat exchange between the calorimeter and environment is
large, and the adiabatic shield calorimeter, which.is designed to
reduce this heat exchange. The latter type of calorimeter evidently
has advantages for making measurements of heat capacities because
its energy equivalent is more nearly the sum of heat capacities.
Also, it has advantages in making measurements of the change in
energy associated with a change in state that takes place slowly
(*i.e.*, a slow chemical reaction) or when attainment of thermo-
dynamic equilibrium is not rapid.

Whenever the change in state is completed rapidly (*i.e.*, most
of reaction calorimetry and an appreciable part of heat capacity
calorimetry), measurements made using an isoperibol calorimeter
can yield results that are at least competitive with the adiabatic
calorimeter. This can be seen, for example, by intercomparing the
low temperature (*i.e.*, 15 to 400 K) measurements of the heat capac-
ity of benzoic acid made by Busey [44] and Cole, *et al.* [33] using
isoperibol calorimeters with those of Furukawa, *et al.* [45],
Osborne, *et al.* [46], and Busey [44] using adiabatic calorimeters.
(In Busey's work, the same calorimeter was operated adiabatically.)
In all cases, measurements were made on a standard sample, as
received, which was supplied by the Calorimetry Conference (see
ref. [47]). Also, each worker used the same temperature scale.
Except below 20 K, agreement of the various measurements was within
the overall estimated uncertainty of the measurements of Furukawa,
et al.: ±0.2 percent from 395 K to 60 K increasing to ±1 percent
at 14 K.

The overall uncertainties in heats of transition or reaction arise from those associated with the specification in the change in state and those associated with calorimetric measurements themselves. Using modern techniques of calorimetry, it is possible to make the overall uncertainty associated with the calorimetric measurements themselves less than that associated with the specification of the change in state. To determine whether this has been achieved, calorimetrists can obtain some information about the imprecision and estimated uncertainty associated with their calorimetry by intercomparing the results of their measurements on standard samples. Some idea of the current minimum values of these uncertainties can be obtained by looking at a few of the results of careful investigations.

For heat capacity calorimeters and drop calorimeters, which are used to measure differences in heat content above room temperature, these intercomparisons are made on n-heptane (25 to 523 K), aluminum oxide (15 to 1200 K), benzoic acid (15 to 400 K), and water (0 to 100 °C) [47]. Results of measurements on a standard sample of aluminum oxide [39,48] illustrate the magnitude of precision and the overall uncertainty due to calorimetric error and precision obtainable in careful work:

Adiabatic Calorimeter (13 to 380 K) [39]

Imprecision in Heat Capacity: Uncertainty in Heat Capacity:

  1 to 0.5% at 13 K   ±10% at 10 K to ±0.1%
     to 0.03% at 90K   at 90 K
  0.03% from 90 K to 380 K   ±0.1% from 90 K to 380 K

Drop Calorimeter (50 °C to 900 °C) [39]

Imprecision in H(t °C)-H(0 °C): Uncertainty in H(t °C)-H(0 °C):

  0.1% at 50 °C to   ±0.2%
  0.01% from 300 °C to 900 °C   Uncertainty in Heat Capacity:
                                      ±0.2% at 100 °C to ±0.4%
                                         at 800 °C

Imprecision in Unsmoothed Mean
Heat Capacity:
  0.1%

    Adiabatic Calorimeter (312 K to 690 K) [39]

Imprecision in Heat Capacity: Uncertainty in Heat Capacity:

  0.05% at 312 K to   ±0.1% at 312 K to
  0.14% at 690 K   ±0.2% at 690 K

    As an example of the type of precision and uncertainty obtain-
able in careful measurements of the change in enthalpy associated
with a physical change in state, we give the results of Furukawa,
et al. [49] in Table 1 on the heat of fusion of benzene. In these
measurements, benzene was deliberately contaminated with small
amounts of n-heptane (which is known not to form solid solutions
with benzene).

    In reaction calorimetry, measurements have been made on the
heat of combustion of benzoic acid (also used for calibration pur-
poses) or iso-octane (bomb calorimetry) and currently are being
made on the heat of reaction of THAM(tris-hydroxymethyl amino
methane) with HCl(aq) (solution calorimetry) [50]. A good illus-

    Table 1. Heat of fusion, triple point, and impurities
              in benzene [49].

Sample designation	Known contamination (mol %)	Measured[a] contamination (mol %)	Triple point[a] (°C)	Heat of fusion[b] (J mol^{-1})
A	.000	.0063±.0010	5.5209±.005	9844.5±2.3
B	.036	.042 ±.005	5.5199±.01	9844.2±3.0
C	.039	.053 ±.005	5.5164±.01	9842.5±6.3

[a]Stated error is overall uncertainty.
[b]Stated error is standard deviation of the mean of each set
  of determinations.

tration of the magnitude of the overall uncertainty due to calori-
metric errors (*i.e.*, excluding sample impurities, *etc.*) is given
by the intercomparison of measurements of the heats of combustion
of benzoic acid (under standard bomb conditions [27]). Measure-
ments were made on standard sample 39 (attached subscript indicates
batch number) supplied by NBS or specially purified samples (B,C,
VUS) as shown in Table 2. Precisions of a single measurement were
of the order of 0.01 percent. The uncertainties are the estimated
overall uncertainty due to calorimetric errors given by each
investigator.

Table 2. Heat of combustion of benzoic acid[a].

Author	Sample	$(\Delta E)_B$	Calorimeter[b]
Jessup, Green (1934) [51-53]	39d, 39e	26,432.0 ± 2.6	I(D)
Prosen, Rossini (1939-1941) [54]	39e	26,434.7 ± 2.2	I(D)
Jessup (1942) [51,53]	39e, 39f, B	26,433.8 ± 2.6	I(D)
Coops, *et al.* (1946-1948) [55]	39b, 39f, VUS	26,438.0 ± 4	I(C)
Coops, *et al.* (1954) [55]	39b, VUS	26,435.0 ± 4	I(C)
Challoner, Gundry, Meetham (1954) [56]	C	26,436.0 ± 4	I(A)
Churney, Armstrong (1966) [57]	39i	26,434.4 ± 3.3	I(D)
Peters, Tappe (1966) (57]	39h	26,433.3 ± 3.0	DE
Gundry, Harrop, Head, Lewis (1969) [59]	39i	26,434.4 ± 1.8	I(C)
Mosselman, Dekker (1966) [38]	39i	26,432.7 ± 1.8	I(C)

[a]Under standard bomb conditions [27].
[b]Calorimeter designations:
   I = Isoperibol calorimeter
       I(A) - Aneroid
       I(C) - Coops design
       I(D) - Dickinson design
   DE = Diphenyl ether (phase change) calorimeter

6. ACKNOWLEDGMENTS

7. REFERENCES

[1]   Eyraud, C., Groton, G., Trambouze, Y., Tran Huu The, Pettre,
         M., Compt. Rend. 240, 862 (1955).

[2]   Watson, E. S., O'Neill, J. J., Brenner, N., Anal. Chem. 36,
         1233 (1964).

[3]   O'Neill, M. J., Anal. Chem. 36, 1238 (1964).

[4]   Smothers, W. J., Chiang, Yao, Handbook of Differential
         Thermal Analysis, Chemical Publishing Company, Inc.,
         New York, (1966).

[5]   Gray, A. P., A Simple Generalized Theory for the Analysis of
         Dynamic Measurements, p. 209 in Analytical Calorimetry,
         Porter, R. S., and Johnson, J. F., Editors, Plenum Press,
         New York (1968).

[6]   Wilhoit, R. C., J. Chem. Education,
              [6a] 44, No. 7, A571 (1967)
              [6b] 44, No. 8, A629 (1967)
              [6c] 44, No. 9, A685 (1967)
              [6d] 44, No. 10, A853 (1967)

[7]   Ginnings, D. C., Introduction, Chapter 1, McCullough, J. P.,
         Scott, D. W., Editors, Experimental Thermodynamics, Vol. I,
         Calorimetry of Non-Reacting Systems, Plenum Press, New
         York (1968).

[8]   Dauphinee, T. M., MacDonald, K. C., Preston-Thomas, H., Proc.
         Roy. Soc. (London) A221, 267 (1954).

[9]   Martin, D. L., Can. J. Phys. 38, 17 (1960).

[10] Martin, D. L., Can. J. Phys. 40, 1166 (1962).

[11] West, E. D., Westrum, E. F., Jr., Adiabatic Calorimetry from
         300 to 800 K, Chapter 9, McCullough, J. P., Scott, D. W.,
         Editors, Experimental Thermodynamics, Vol. I, Calorimetry
         of Non-Reacting Systems, Plenum Press, New York, (1968).

[12] Skinner, H. A., Theory, Scope, and Accuracy of Calorimetric
         Measurements, Chapter 1, Biochemical Microcalorimetry,
         Brown, D. H., Editor, Academic Press, New York (1969).

[13] Rossini, F. D., Excursion in Chemical Thermodynamics, from
      the Past into Future, p. 95, Thermodynamics and Thermo-
      chemistry, Symposium, Lund 1963, Planary Lectures,
      Butterworths, London (1964).

[14] Sturtevant, J., Calorimetry, Techniques of Organic Chemistry,
      Vol. I, 2nd Edition, Weissberger A., Editor, Wiley-Inter-
      science, New York (1949).

[15] Kubaschewski, O., Evans, E. Ll., Alcock, C. B. Experimental
      Methods, Chapter 2, Metallurgical Thermochemistry, 4th
      Edition, Pergamon Press, Oxford, (1967).

[16] Rossini, F. D., Editor, Experimental Thermochemistry, Measure-
      ments of Heats of Reaction, Interscience, New York, (1956).

[17] Skinner, H. A., Editor, Experimental Thermochemistry, Vol. II,
      Interscience-John Wiley and Sons, New York, (1962).

[18] McCullough, J. P., Scott, D. W., Editors, Experimental
      Thermodynamics, Vol. I, Calorimetry of Non-Reacting Systems
      Plenum Press, New York, (1968).

[19] Kubaschewski, O., Hultgren, R., Metallurgical and Alloy
      Thermochemistry, Chapter 16, Skinner, H. A., Editor,
      Experimental Thermochemistry, Vol. II, Interscience-John
      Wiley and Sons, New York (1962).

[20] Cruickshank, A. J. B., Ackermann, Th., Giguere, P. A., Heat
      Capacity of Liquids and Solutions Near Room Temperature,
      Chapter 12, McCullough, J. P., Scott, D. W., Editors,
      Experimental Thermodynamics, Vol. I, Calorimetry of Non-
      Reacting Systems, Plenum Press, New York (1968).

[21] Westrum, E. F., Jr., Furukawa, G. T., McCullough, J. P.,
      Adiabatic Low-Temperature Calorimetry, Chapter 5, McCullough,
      J. P., Scott, D. W., Editors, Experimental Thermodynamics,
      Vol. I, Calorimetry of Non-Reacting Systems, Plenum Press,
      New York (1968).

[22] Skinner, H. A., Sturtevant, J. M., Sunner, S., The Design and
      Operation of Reaction Calorimeters, Chapter 9, Skinner, H. A.,
      Editor, Experimental Thermochemistry, Vol. II, Interscience-
      John Wiley and Sons, New York, (1962).

[23] Ginnings, D. C., West, E. D., Principles of Calorimetric
      Design, Chapter 4, McCullough, J. P., Scott, D. W., Editors,
      Experimental Thermodynamics, Vol. I, Calorimetry of Non-
      Reacting Systems, Plenum Press, New York (1968).

[24] Stout, J. W., Low-Temperature Calorimetry with Isothermal
      Shield and Evaluated Heat Leak, Chapter 6, McCullough, J. P.,
      Scott, D. W., Editors, Experimental Thermodynamics, Vol. I,
      Calorimetry of Non-Reacting Systems, Plenum Press, New York
      (1968).

[25] Coops, J., van Nes, K., Rec. Trav. Chim. 66, 131 (1947).

[26] Wadsö, I., Science Tools, 13, 33 (1966).

[27] Coops, J., Jessup, R. S., van Nes, K., Calibration of Calori-
      meters for Reactions at Constant Volume, Chapter 3, Rossini,
      F. D., Editor, Experimental Theromchemistry, Measurements
      of Heats of Reaction, Interscience, New York (1956).

[28] Prosen, E. J., Combustion in a Bomb of Compounds Containing
      Carbon, Hydrogen, Oxygen, Nitrogen, Chapter 6, Rossini,
      F. D., Editor, Experimental Thermochemistry Measurements
      of Heats of Reaction, Interscience, New York (1956).

[29] Rossini, F. D., Introduction; General Principles of Modern
      Thermochemistry, Chapter 1, Rossini, F. D., Editor, Experi-
      mental Thermochemistry Measurements of Heats of Reaction,
      Interscience, New York (1956).

[30] Rossini, F. D., Calibration of Calorimeters for Reactions in
      a Flame at Constant Pressure, Chapter 4, Rossini, F. D.,
      Editor, Experimental Thermochemistry Measurements of Heats
      of Reaction, Interscience, New York (1956).

[31] West, E. D., Churney, K. L., J. Appl. Phys. 39, 4206 (1968).

[32] White, W. P., The Modern Calorimeter, The Chemical Catalog Co.,
      New York (1928).
            [32a] p. 88 and section 10, Chapter 2
            [32b] p. 36

[33] Cole, A. G., Hutchens, J. O., Robie, R. A., Stout, J. W.,
      J. Am. Chem. Soc. 82, 4807 (1960).

[34] Hu, A. T., Sinke, G. C., J. Chem. Thermodynam. 1, 507 (1969).

[35] Prosen, E. J., Rossini, F. D., J. Res. NBS 33, 255 (1944).

[36] Dickinson, H. C., Bull. BS 11, 189 (1914).

[37] West, E. D., Churney, K. L., J. Appl. Phys. 41, 2705 (1970).

[38] Mosselman, C., Dekker, H., Rec. Trav. Chim. 88, 162 (1969).

[39] West, E. D., Ginnings, D. C., J. Res. NBS 60, 309 (1958).

[40] White, W. P., J. Am. Chem. Soc. 40, 1858 (1918).

[41] Westrum, E. F., Determination of Purity and Phase Behavior by
      Adiabatic Calorimetry, p. 231, Analytical Calorimetry,
      Porter, R. S., and Johnson, J. F., Editors, Plenum Press,
      New York (1968).

[42] Prosen, E. J., private communication.

[43] West, E. D., J. Res. NBS 67A, 331 (1963).

[44] Busey, R. H., J. Am. Chem. Soc. 78, 3263 (1956); ORNL-1828,
     Office of Technical Services, Dept. of Commerce,
     Washington, D. C.

[45] Furukawa, G. T., McCoskey, R. E., King, G. J., J. Res. NBS
     47, 256 (1951).

[46] Osborne, D. W., Westrum, E. F., Jr., Lohr, H. R., J. Am. Chem.
     Soc. 77, 2737 (1955).

[47] Ginnings, D. C., Furukawa, G. T., J. Am. Chem. Soc. 75, 522
     (1953).

[48] Furukawa, G. T., Douglas, T. B., McCoskey, R. E., Ginnings,
     D. C., J. Res. NBS 57, 67 (1956).

[49] Glasgow, A. R., Ross, G. S., Horton, A. T., Enagio, D., Dixon,
     H. R., Saylor, C. P., Furukawa, G. T., Reilly, M. L.,
     Henning, J. M., Anal. Chim. Acta 17, 54 (1957).

[50] Armstrong, G. T., Calorimetric Reference Materials - Status of
     the Primary Standard, Paper E-2, First International
     Conference on Calorimetry and Thermodynamics, Warsaw,
     Aug. 31-Sept. 4, 1969. To be published.

[51] Jessup, R. S., J. Res. NBS 29, 247 (1942).

[52] Jessup, R. S., Green, C. B., J. Res. NBS 13, 469 (1934).

[53] Jessup, R. S., J. Res. NBS 36, 421 (1946).

[54] Prosen, E. J., Rossini, F. D., J. Res. NBS 33, 439 (1944).

[55] Coops, J., Adrianse, N., van Nes, K., Rec. Trav. Chim. 75,
     237 (1956).

[56] Challoner, A. R., Gundry, H. A., Meetham, A. R., Phil. Trans.
     Roy. Soc. (London) A247, 553 (1955).

[57] Churney, K. L., Armstrong, G. T., J. Res. NBS 72A, 453 (1968).

[58] Peters, H., Tappe, E., Monatsberichte der Deutschen Akademie
     der Wissenschaften zu Berlin 9(11), 828 (1967).

[59] Gundry, H. A., Harrop, D., Head, A. J., Lewis, G. B., J. Chem.
     Thermodynam. 1, 321 (1969).

STATUS OF THERMAL ANALYSIS
TEMPERATURE SCALE STANDARDS

O. Menis and J. T. Sterling

Analytical Chemistry Division
Institute for Materials Research
National Bureau of Standards
Washington, D. C. 20234

Current status in the development of suitable
temperature scale standards for differential thermal
analysis is described. It involved the cooperative
effort at NBS in the collection and evaluation of
data on 12 materials studied by the Standards
Committee of the International Committee on Thermal
Analysis. In addition the results of the study
group of an ASTM Committee with the cooperation of
NBS are presented. The selected temperature values
depend on the transition temperature of a number of
compounds as well as two low temperature melting
metals. The temperature scale region of 40 to 900
°C can be covered effectively with the ten materials,
which will serve as calibration standards.

Key words: ASTM Committee; differential thermal
analysis; International Committee on Thermal Analysis;
temperature scale region of 40 to 900 °C; temperature
scale standards.

INTRODUCTION

In the field of thermal analysis, we have witnessed a tremen-
dous growth in the last few years [1]. This is evident from the
activities of new societies and organizations as well as large in-
creases in the sales and number of manufacturers of differential
thermal analysis (DTA) and differential scanning calorimetry (DSC)
instruments. Last year saw the formation of the North American
Thermal Analysis Society and the Provisional Subcommittee (in E-1)
on Thermal Test Methods of the American Society for Testing and
Materials (ASTM). In 1965 the First International Conference on

Thermal Analysis (ICTA) formed a Standards Committee to resolve disagreements on reported thermal data through the development of appropriate calibration standards for DTA instruments.

Thermal analyses, akin to all instrumental procedures, require some form of calibration. Only rarely, as in the case of coulometry, can independent physical methods be readily employed. In analytical techniques, composition materials or high purity substances are used for this purpose. NBS has therefore carefully characterized and certified materials for use as calibration standards. These standards are characterized by chemical and physical measurements to ensure that instrumental biases are not perpetuated. Ideally, an effort is made to establish a certified value which is independent of the instrument for which it is intended. In certain measurements, however, such as the determination of gases in metals and in differential thermal analyses, it is not possible to separate the measurements and certification of the true value from the method. In such cases the careful consideration of the physicochemical principles and the evaluation of the sources of errors due to various instrumental characteristics play a predominant role. In developing temperature scale calibrations for differential thermal analyses, comparison with data from adiabatic calorimetry is of great value. The two previous speakers have discussed the principles and techniques from which one can estimate the errors involved in these two types of measurements. These two methods, then, when critically applied to the measurement of selected materials, should enable us to arrive at a more accurate value for transition temperatures and enthalpies.

THE COOPERATIVE STUDY WITH ICTA

In 1966 the ICTA Standards Committee initiated a cooperative "round robin" test of twelve compounds to evaluate their potentialities as temperature scale standards. The selection of these materials was based on the following criteria: (1) only compounds with known phase transition temperatures should be selected; (2) these temperature values should be well established from literature ther-

modynamic data as reported in the NBS Circular 500, of 1952; (3) enthalpy changes at these transitions should be sufficiently large to be detected by most instruments; (4) on storage, the compounds should be stable, with known purity and homogeneity; (5) these compounds should cover a wide range of temperatures from 100 to 1000 °C; and (6) they might also serve as enthalpy standards for DTA.

These criteria were established after evaluating all the factors essential for achieving the best accuracy in these measurements. It was felt that transition temperatures are less often subject to environmental conditions and decomposition or side reactions. For these reasons melting point standards were considered less reliable. (H. McAdie discussed the latter problem fully at the American Chemical Society meeting at Houston in February 1970.) The selection of compounds based on the data in NBS Circular 500 was agreed upon in order to avoid pitfalls when lesser known values are considered. However, even in this case, preliminary information [2] indicates that the reported value for the transition temperature of silver sulphate is incorrect. The need for compounds which would cover the temperature scale of interest stems from the experience with the dynamic mode of obtaining thermal curves. Here many factors, such as the heat capacity and thermal conductivity of the tested material, may affect the shape of the curve at a given temperature. Thus, a single temperature reference point may not be sufficient to allow meaningful extrapolation to test conditions at significantly different temperatures. This presents the problem that ultimately one would like standards having physical properties (such as thermal conductivity and heat capacity) similar to the respective materials encountered in the biological, polymer and inorganic fields.

RESULTS OF THE FIRST ICTA TEST

In the "round robin" evaluation program, we have cooperated with the ICTA Standards Committee in the two tests. After a preliminary review by the Standards Committee, the data from the

first round robin, involving twenty-four laboratories from eight
nations, were evaluated by a subcommittee consisting of H. McAdie,
Chairman, from the Ontario Research Foundation, P. Garn, University
of Akron, O. Menis, NBS Analytical Chemistry Division and B. Joiner,
NBS Statistical Engineering Section, who acted as a consultant. In
the preliminary review, four compounds were rejected because of
difficulties encountered in their measurements. These were (1)
potassium bisulfate, (2) sodium sulphate, (3) potassium carbonate
and (4) sodium carbonate. In the first, the decomposition temper-
ature partially overlapped the transition temperature; in the
second, the thermal curves were not reproducible and depended on
the pretreatment of the sample. In the latter two, the materials
tended to lose CO_2 at comparatively low temperatures and the ther-
mal effects were below the limit of resolution of some instruments.

    The data from the twenty-four collaborating laboratories are
summarized in Figures 1, 2 and 3. These are plots of the data
from thermal analysis curves of eight compounds-- (1) potassium
nitrate, (2) potassium perchlorate, (3) silver sulphate, (4) quartz,
(5) potassium sulphate, (6) potassium chromate, (7) barium carbon-
ate, and (8) strontium carbonate, all of which met the specified
criteria for a standard. In Figure 1 plots of point A, the 1st
departure from the base line is recorded, point B in Figure 2
represents the intersection of the forward-extrapolated baseline
with the backward-extrapolated initial side of the peak, and in
Figure 3, point D is the peak temperature. From these plots of
data it is evident that the intersection point, B, yields values
which have the smallest deviation from the thermodynamic transition
temperatures given in the literature. About two-thirds of the lab-
oratories reported values within ±5 °C of the literature value. A
brief review of the data was reported at the Proceedings of the
Second International Conference [3].
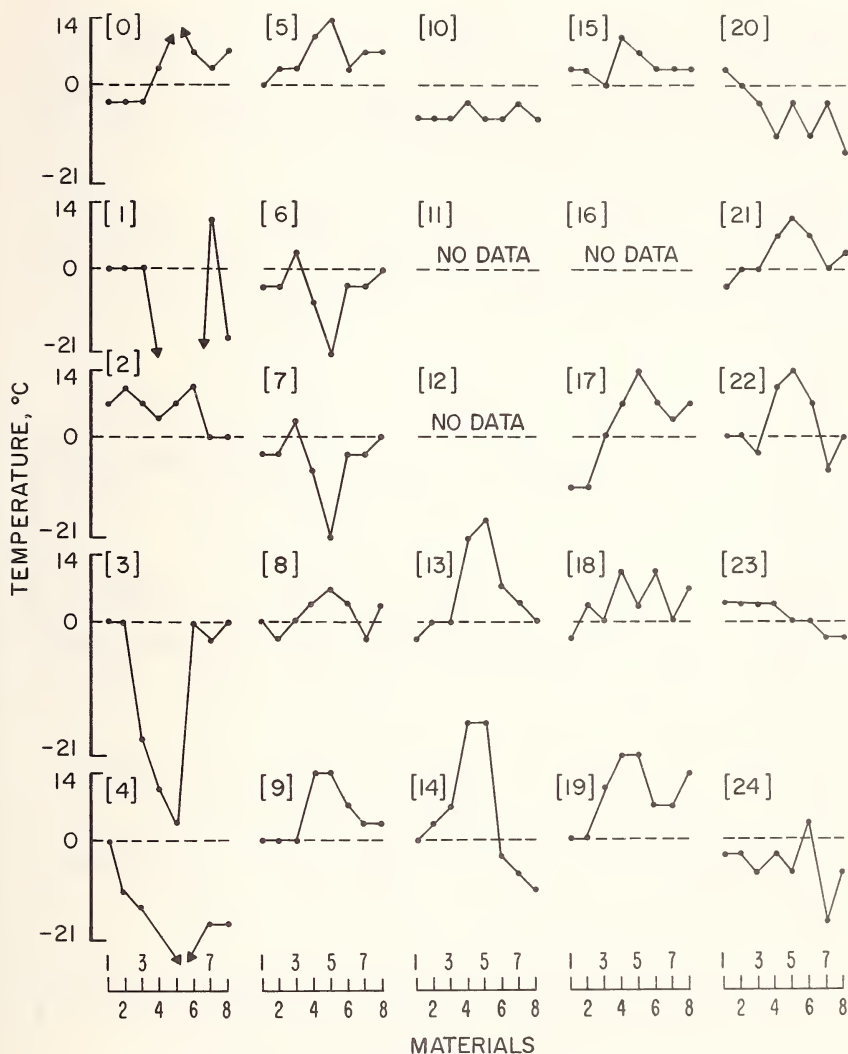
Figure 1. Data from 24 ICTA cooperating laboratories for point A heating cycle. (The numbers in brackets represent the laboratories; the groups of numbers in the abscissa represent the eight materials; the dashed lines represent the values from the NBS Circular 500.)
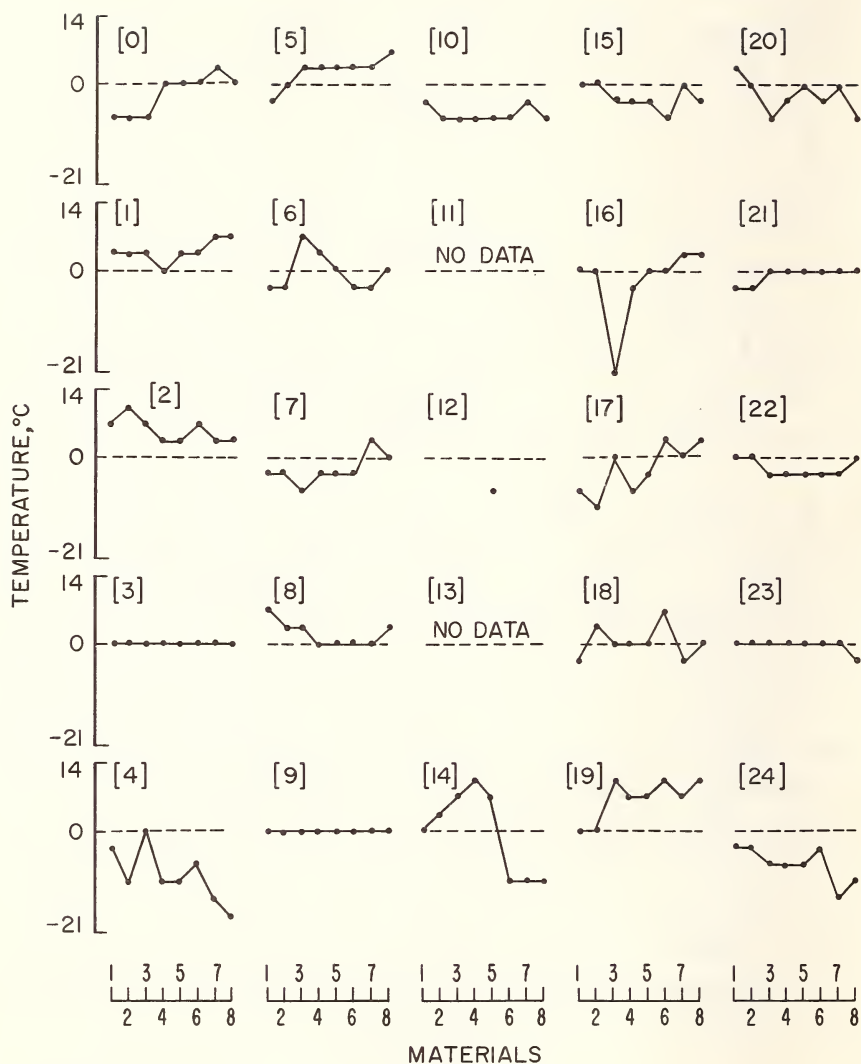
Figure 2. Data from 24 ICTA cooperating laboratories for point B heating cycle.
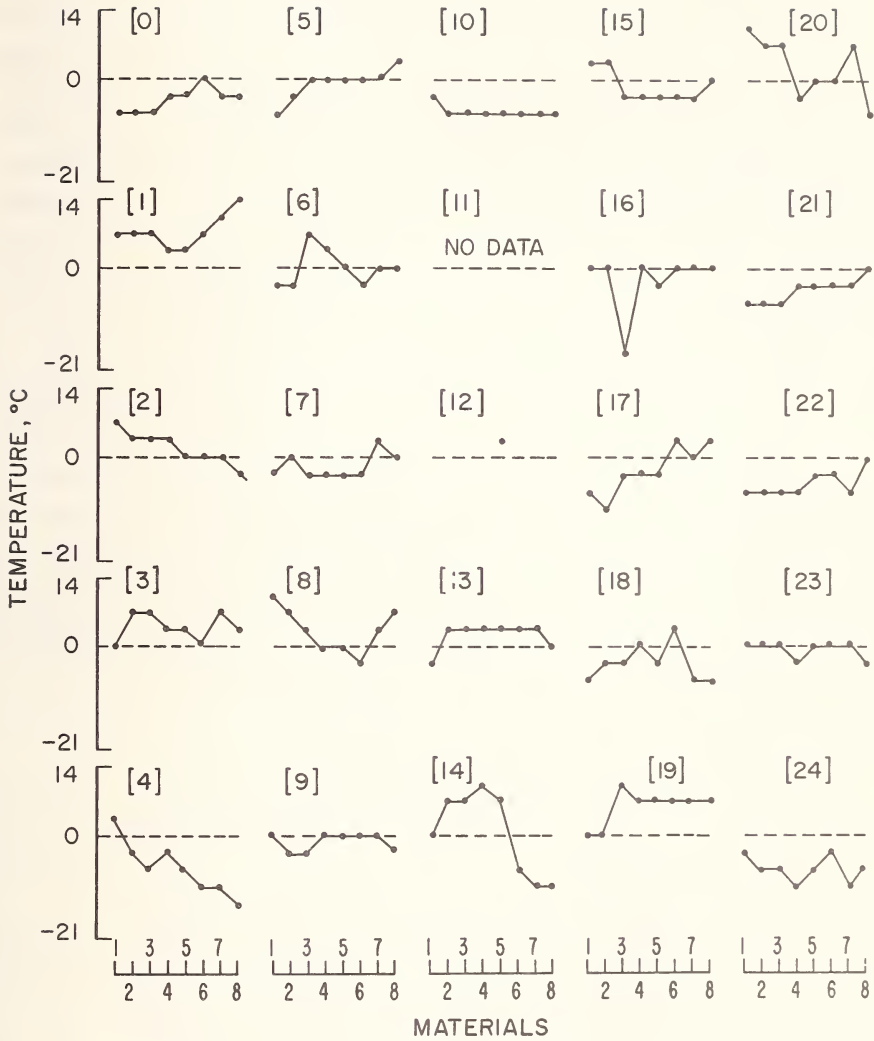
Figure 3.   Data from 24 ICTA cooperating laboratories for
            point D heating cycle.

PRELIMINARY RESULTS AT NBS FOR THE SECOND ICTA TEST

As a result of the above evaluation, the ICTA Standards Committee
initiated another cooperative study. In this case more rigorous
requirements for describing experimental conditions were included.
Mainly, however, the purpose was to characterize large quantities
(suitable for future distribution as Standards) of the eight pre-
viously screened compounds and to add indium and tin to the list as
melting point standards. The results of these tests are not yet
available from these laboratories. However, we present the data
obtained at the Analytical Division at NBS for comparison. In
Table 1, results are presented from the first and second tests and
are compared with the values in NBS Circular 500. The second series
was measured after considerable modification of equipment which will
be described in the next section. The data from the two tests are
similar, but, some of the large deviations for the transitions tem-
peratures above 500 °C have been reduced significantly in the
second test. The melting point standard behaved almost ideally on
the heating cycle. In the second set of values, there is a definite
positive bias which may be due to the rate of heat transfer which is
a controlling factor in a dynamic DTA measurement.

Table 1. NBS first and second ICTA DTA study.

Compound No.	Compound formula	NBS Cir. 500 °C	1st NBS DTA "B" °C	2nd NBS DTA "B" °C
1	KNO_3	127.7	129	129.5
2	$KClO_4$	299.5	300	300.8
3	Ag_2SO_4		426	427.5
4	SiO_2	573	570	574.4
5	K_2SO_4	583	577	586.0
6	K_2CrO_4	665	668	668.5
7	$BaCO_3$	810	791	
8	$SrCO_3$	925	905	929.3
–	Sn	231.9		233.0
–	In	157		157.8

The changes in the apparatus and procedure prior to the measurement of the second set were as follows:

MODIFICATION OF INSTRUMENT

The commercial instrument initially used in this study was limited in its capability to provide precise and accurate values. This instrument was equipped with thermocouple wires whose cold junction was dependent on the ambient temperature. Thus the temperature measurements would vary several degrees during the day. The hot junction was also located outside the sample compartment. The high programming rate, together with a low sensitive recorder, were limiting factors of the initial apparatus.

The following modifications were made to ensure its use as a research tool, especially to determine more accurately the transition temperatures of selected compounds for use as standard reference materials:

1. Simultaneous use of the same thermocouple for both sample temperature readings and delta-T readings.

2. Insertion of ice bath junctions in all temperature thermocouple circuits for voltage measurements with respect to 0 °C.

3. Simultaneous recording on an x-y recorder and two-pen strip recorder. The areas of these thermal curves correspond more, in theory, to heats of transitions than do the areas delta-T *vs.* temperature plots.

4. Slower scan rates were provided for minimizing gradients between the sample thermocouple and the sample itself, and for approximating adiabatic conditions.

5. Addition of a stable bucking voltage source was provided for use with a sensitive setting of the temperature *vs.* time recorder. This increased the precision of measurement of the sample thermocouple voltage by a factor of ten, by permitting the scanning of 5 millivolts from the thermocouple in ten one-half millivolt recorder spans.

6. Provision for temperature calibration of the apparatus:

    a. Replacement of sample thermocouple with calibrated wire.

    b. Provision for rapid comparison of calibrated thermo-couple with standard voltage source.

    c. Construction of non-metallic sample holders for use with metal freezing point standards.

EXPERIMENTAL

Modification of Thermocouple Wiring and Readout Arrangement.

The commercial unit was provided with various alloy thermo-couples together with a foam insulated box containing cold junction connections for the temperature thermocouple. However, regardless of the intermetallic junctions involved, the voltage of the hot thermo-couple was always measured with reference to a cold junction or junctions completing the circuit. The temperature of this thermocouple was thus read with respect to ambient temperature together with the temperatures in the apparatus at the junctions of the alloys. Also, the hot junction supposedly measuring the sample temperature was not inside the sample cup (this one was used for the differential meas-urement only) but was actually the furnace control thermocouple.

The following changes were made:

    a. Changes in Thermocouple Arrangement

    (1) All thermocouple wiring was removed and replaced with platinum or platinum-10 percent rhodium wires leading to an ice bath (see Fig. 4). From the ice bath, all copper leads went to the recorders and amplifiers.

    (2) The furnace control thermocouple previously used for both the temperature measurement and furnace control was now limited to furnace control. This provided the required flexibility for its optimum placement and avoided interference from the pro-grammer electronics.

    (3) The thermocouple in the sample cup was used for temperature measurement (with respect to the ice bath) rather than the thermocouple in the reference cup. (See Fig. 4.)
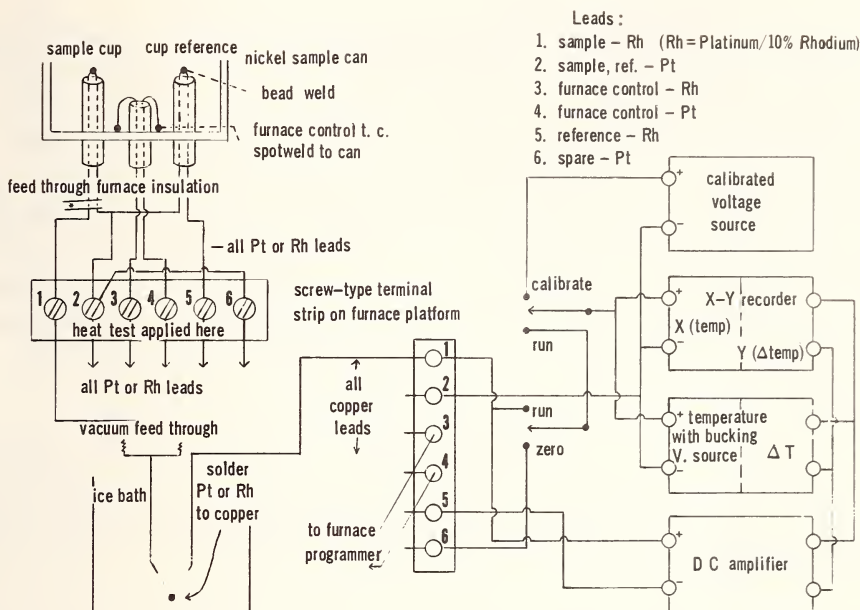
Figure 4.   Modified thermocouple wiring, calibration and
            recording arrangement.

        (4) Screw-type terminal strips were provided for direct
connections of the thermocouple leads to the ice bath leads of the
same metal.   Tests with a hot screwdriver showed a slight potential
shift due to the small dissimilarities of the Pt and Pt/Rh thermo-
couples.   These shifts, as expected, were small enough to be negli-
gible to ambient temperatures.   Since then, the terminals have been
replaced with directly soldered connections.

     All wiring was external with hookup wire for easy changes. Hum
and chatter were suppressed by shielding with wire braid and copper
screening and shunting the leads with 0.1 mfd capacitors at the
recorder terminals.

b. Recorder Changes

The two-pen recorder was used to obtain a plot of tem-
perature and differential temperature *vs.* time. To make it possible
to expand the temperature scale by a factor of ten, without intro-
ducing great distortion, bucking sources were combined with more
sensitive scales. Because of the sensitivity due to the scale fac-
tor expansion, it was necessary to thermally insulate the bucking
voltage divider and associated resistors and dry cells to suppress
drift. This was done with plastic packing material. At high sensi-
tivity, the recorder was susceptible to static electric pickup from
personnel moving nearby. It was thus necessary to surround the
apparatus with grounded copper screening.

Switches were added as shown (Fig. 4) for setting the recorders
to zero degrees centigrade without interference to the differential
circuit, and for calibrating the temperature recorders with a stand-
ardized voltage source.

c. Lower Scanning Rates

The motor controlling the heating or cooling of the
furnace had a reliable speed range of a factor of less than three
(see Fig. 5). Using the lowest reliable setting and the gears pro-
vided with the lowest ratio of potentiometer turns per motor revolu-
tions, the lowest rate available was about five degrees per minute.
Smaller motor gears were made, and the motor was moved to accommodate
them. Also, the electronics in the furnace programmer were modified
to lower the rate of temperature scan. Because this modification
also decreased the temperature range proportionately, the rate de-
crease was only a factor of 2. Using the smallest motor gears, the
minimum heating (cooling) rate was lowered to less than a degree per
minute. However, at the lower heating rates, the feedback from the
furnace sensing thermocouple was slow enough so that the furnace
would cycle above and below the proper temperature by several degrees
with periods of 10 minutes or less. To speed the feedback, the fur-
nace control thermocouple was welded to the nickel sample can (Fig. 4)
which was the closest stable point to the furnace heater windings.
Even with this modification and the optimum adjustment of the furnace
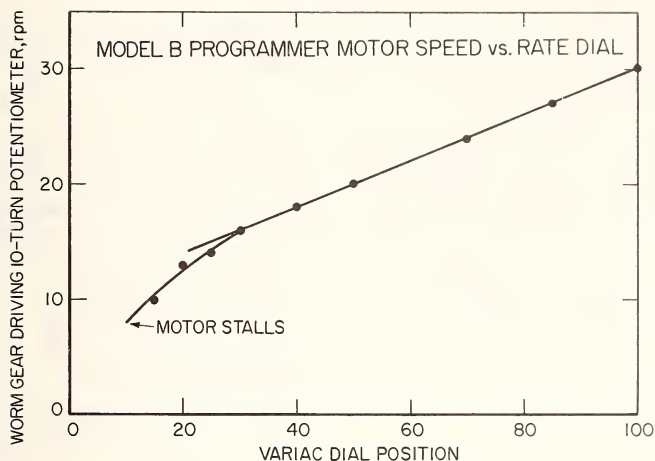
Figure 5.   Programmer motor calibration after modification.

controller, the minimum heating rate that was free of the cycling was about one degree per minute. Moving the thermocouple outside the can, thus exposing it directly to the furnace windings has further improved performance.

    d. <u>Automatic Voltage Divider for Bucking Voltage Source</u>
     A bucking voltage source of the following properties was designed and built (see Fig. 6):
     (1) Automatic - able to reset the recorder (temperature) when it went off scale in either direction.
     (2) Isolated from the ac power line and from ground.
     (3) Stable with respect to time and temperature to within at least 0.1 percent.
     (4) Able to provide 20 increments of approximately 1/2 millivolt each.

 The voltage divider was made from two percent carbon resistors and trimmer potentiometers to compensate for the expected four percent resistance variation. This portion was shielded from the control circuits, and offered no noticeable hum.
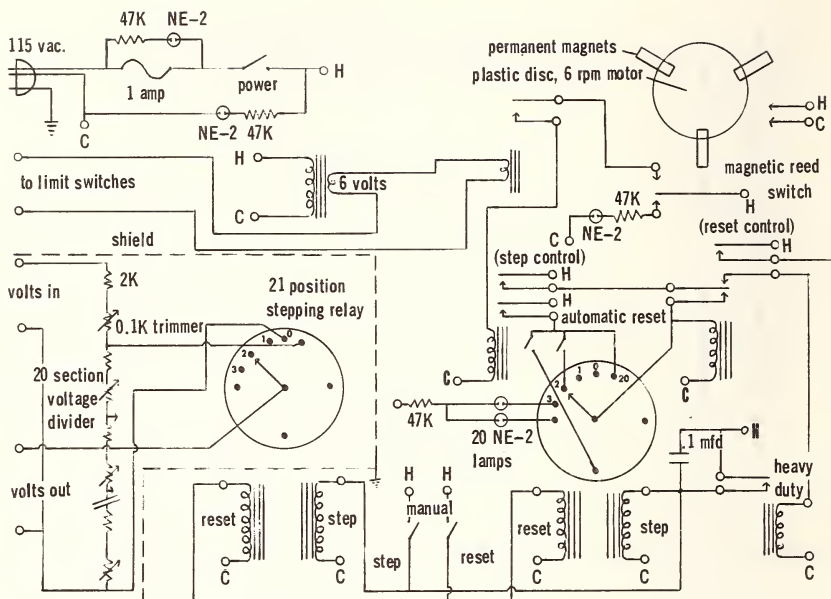
Figure 6.   Automatic voltage divider for providing bucking
             voltage.

The control circuits were made from relays because space and
speed were not at a premium and simplicity of operation was desired.
The basic control units were stepping relays that would advance and
reset, and a magnetic read switch (whose inherent hysteresis prevent-
ed chatter) that was timed to advance the stepping relays once every
two seconds. Stepping relays advance or reset continuously until
the recorder pen is on scale. Micro switches were added to both
ends of the recorder scale, and either would activate the recorder
circuit. Additional relays provided power for the steppers to pre-
vent skipping immediately after resetting, and to electrically iso-
late the limit switches for reasons of safety. Only 6 volts ac were
on the limit switch binding posts, and either one could be grounded,
if necessary.

The bucker can be set manually to any of its 20 positions and
reset from any position. When the limit switch binding posts are

connected, the position of the divider will be advanced about once
every two seconds (increasing the voltage output) until it reaches
the 4th, 9th, 14th or 20th position. It will then reset to the
zero position.

Indicator lamps were provided for monitoring the magnetic read
switch (continually driven by the motor and magnets), the position
of the voltage divider and a lamp fuse.

Because the bucker was designed for use with a potentiometric
recorder or other high-impedance device, it exhibited high impedance
(40,000 ohms) and drew very little battery current. It was there-
fore not expected to supply current. Its purpose was for a voltage
source only.

The bucking voltage source was used either with a 1.5 volt dry
cell or a mercury cell in series with an 8.2 megohm resistor so that
each step would swing a 1/2 millivolt pen recorder almost to full
scale.

Because of the scale expansion, the temperature recorder was
very sensitive to the drift of the dry cell or mercury cell. The
temperature and time stability of dry cells and size D mercury
batteries were checked separately with a potentiometer. The per-
formance varied widely except for new cells. All cells were tem-
perature sensitive. The mercury cells performed best, and remained
stable to better than 0.1 percent if insulated from ambient temper-
ature by several inches of plastic foam. To suppress further drift,
the bucker was enclosed in several inches of insulating material,
because of the temperature sensitivity of the carbon resistors in
the voltage divider. The bucker-recorder combination seldom drifted
over several microvolts per hour. Short term drift was checked and
was not apparent. The effect of long-term drift was checked and was
not apparent. The effect of long-term drifts (over 20 minutes) on
the results was not critical because the entire recorder system was
calibrated with a separate potentiometer and was provided with tem-
perature regulated standard cells, which were used frequently for
calibration.

TEMPERATURE CALIBRATION

1. Thermocouple Changes

Platinum and platinum-10 percent rhodium (15 mil) wires
were calibrated by the Heat Division at NBS.

The thermocouple over which the sample cup rested was removed,
and the calibrated wires were inserted several inches beyond the
ceramic tube. The ends of the wires were welded into a bead with an
oxy-gas torch, then placed in the same position as those of the pre-
vious thermocouple. The reference thermocouple was withdrawn slight-
ly to match the position of the calibrated thermocouple. These pre-
cautions were taken to avoid bending the leads, especially where they
enter the bottom of the ceramic tubes and where large heat gradients
were expected. The leads were directed to the ice bath containing
the copper junction.

2. Calibration Procedure

With the zero-run switch in the run position, the temper-
ature recorders were switched from the sample thermocouple to a
calibrated voltage source which in this case was a high precision
potentiometer. The approximate transition temperatures under inves-
tigation were known, so the potentiometer could be set to approx-
imately the correct potential. This allowed the fiducial marks to be
on scale, within several equivalent degrees of the thermal curve.
Fiducial marks were taken within minutes before and after the ther-
mogram. Several points gave the correct scale factor for interpo-
lating to the potential reading of the thermocouple.

As a further check on the temperature readings, NBS freezing
point standards, lead, aluminum and tin were carefully prepared.
Non-metallic cups were used with these materials to avoid alloying
with the sample. Graphite rod was chosen because of its availa-
bility, purity, and good thermal conductivity. This rod was cut to
size, drilled, rinsed several times in acetone, boiled in HCl, and
heated to incandescence before use.

3. Sample Cups

Platinum, nickel, stainless steel, aluminum and graphite cups were tested. Stainless steel was unsatisfactory because of oxidation and resultant contribution to the thermal curve. Nickel and aluminum cups were adapted and the thermocouples were inserted directly into the sample and reference. This did not improve the thermal curves perhaps because the thermocouple contacted only the small layer of sample immediately surrounding it. This layer acted as an insulator for the remainder of the samples, which were powders or small crystals having relatively poor thermal conductivity. This approach was abandoned because the thermal curves showed no improvement and since the thermocouple was not protected, the apparatus was more difficult to load and clean. Therefore, the closed well was used throughout this study.

4. Results

Scanning rates of 1 to 5 degrees per minute were used over the temperature range investigated for potassium nitrate and quartz for use as DTA standards. Temperatures could be determined to a precision of about 0.2 degree (2 microvolts). Data for several melting point standards were within 2 degrees of their certified values. Repetitive temperatures of a given sample were consistent to at least one-half degree for a particular heating rate and at all heating rates.

Typical thermal curves of two proposed Standard Reference Materials, KNO_3 and SiO_2, are presented in Figure 7a and 7b. Those for metal melting point standards are given in Figure 8. The departure point, A, and the transition peak D are marked.

INDUCTIVE PERIOD AND SUPERCOOLING

The transition temperature peak for potassium nitrate on the first programming was always several degrees higher than on subsequent repetitive cyclings (without ever going through the melting point). The displacement of the transition temperature may also be avoided by preheating the potassium nitrate crystals in a drying

DTA Standards
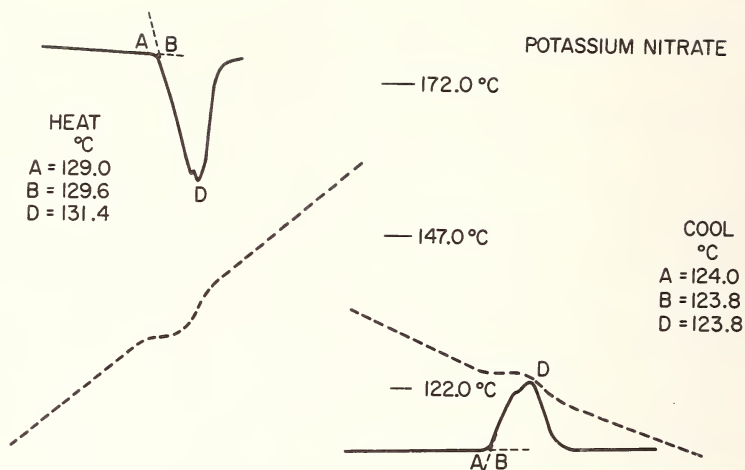
Figure 7a.   Thermal curve, heating and cooling of potassium
             nitrate.
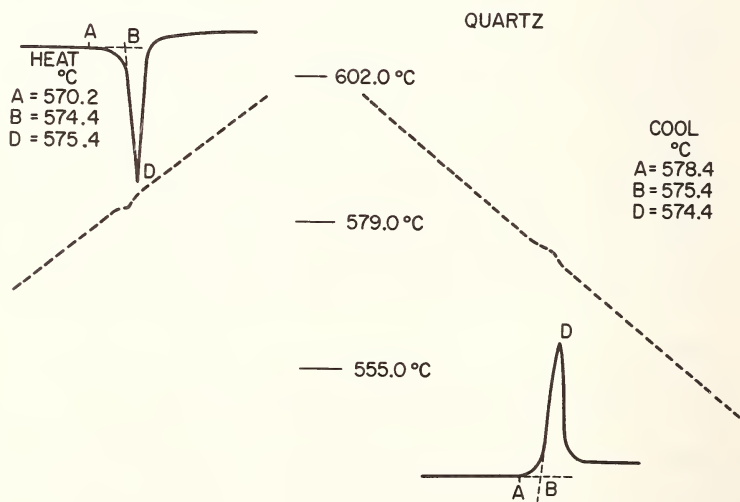
Figure 7b.   Thermal curve, heating of quartz.
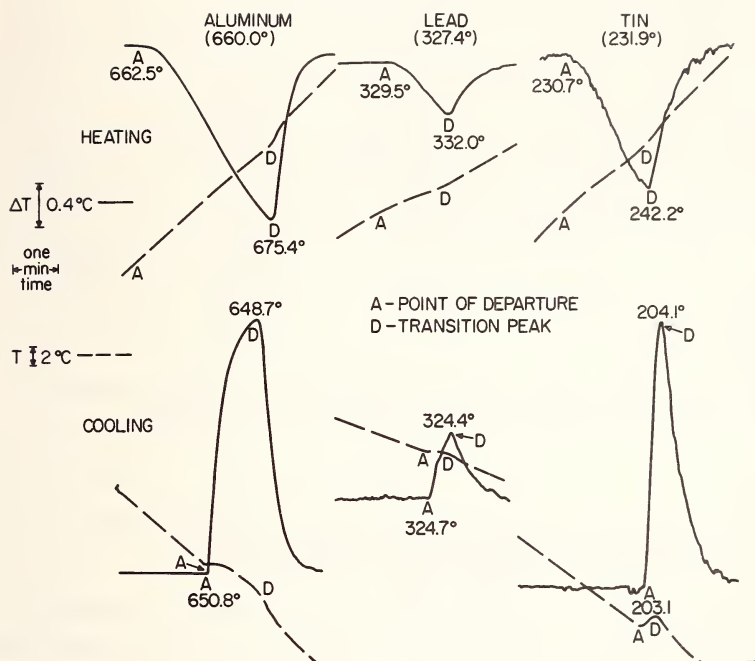
Figure 8.   Thermal curves, heating and cooling, of metals.

oven at 150 °C. This effect is probably due to the presence of
water within the crystals. Kracek [4] who investigated the effects
of water reports also its effect on the phase transition on the
cooling cycle. He observed that on cooling two peaks occur and
postulated that phase I transforms to phase III and then to phase
II. In an experiment in a sealed quartz tube in the presence of
water, he demonstrated that a rapid direct transition occurs from
phase I to phase II. Data on the cooling cycle for other compounds
are shown in Table 2. As can be noted in these examples, this type
of supercooling or induction period is not uncommon for the com-
pound and for most metals tested. In this study, quartz, potassium
sulfate and potassium chromate did not show a large induction type
temperature spread.

Table 2.   Supercooling in selected materials.

Transition temperature – °C

Compound	NBS Circular-500	NBS-DTA Heating-"B"	NBS-DTA Cooling-"B"	A.S.[a]–°C
$KClO_4$	299.5	300.8	290.4	+10.8
$KCrO_4$	665.0	668.5	671.2	-2.7
$AgSO_4$		427.5	407.0	+20.5
Sn(Metal)	231.9	233.0	213.0	+20.0
In(Metal)	157.0	157.8	155.2	+2.6

[a] A.S. = apparent supercooling = difference between average
transition temperatures on heating and on cooling.

COOPERATIVE STUDIES OF STANDARDS SECTION
OF ASTM E-1 PROVISIONAL SUBCOMMITTEE

In another effort to develop Standard Reference Materials,
studies with two organic compounds and sulfur were initiated which
covered lower transition temperatures.   This effort was carried out
with the cooperation of members of ASTM Committee E-1, Provisional
Subcommittee on Thermal Analytical Test Methods.   The results from
nine cooperating laboratories on sulfur, stearic acid and hexa-
chloroethane are presented in the three Figures 9a-11b.   Again it
is evident that point B shows the least variation in interlaboratory
comparisons.   The poorest reproducibility between laboratories can
be noted with sulfur.   It is evident from this study and the exper-
ience of others, that it would not be suitable as a standard.   The
melting point of stearic acid and the transition temperature of
hexachloroethane offers greater promise.   The latter compound, espec-
ially because of its two transition temperatures, would be very use-
ful for calibration purposes.   The cooperative values agree closely
within 1 degree of the accepted literature values of the triclinic
to cubic transformation at 72 °C and to within 5 °C to the rhombic
to triclinic at 44 °C.   Based on these data, it is planned to purify
larger quantities of hexachloroethane for certification as a Standard
Reference Material.
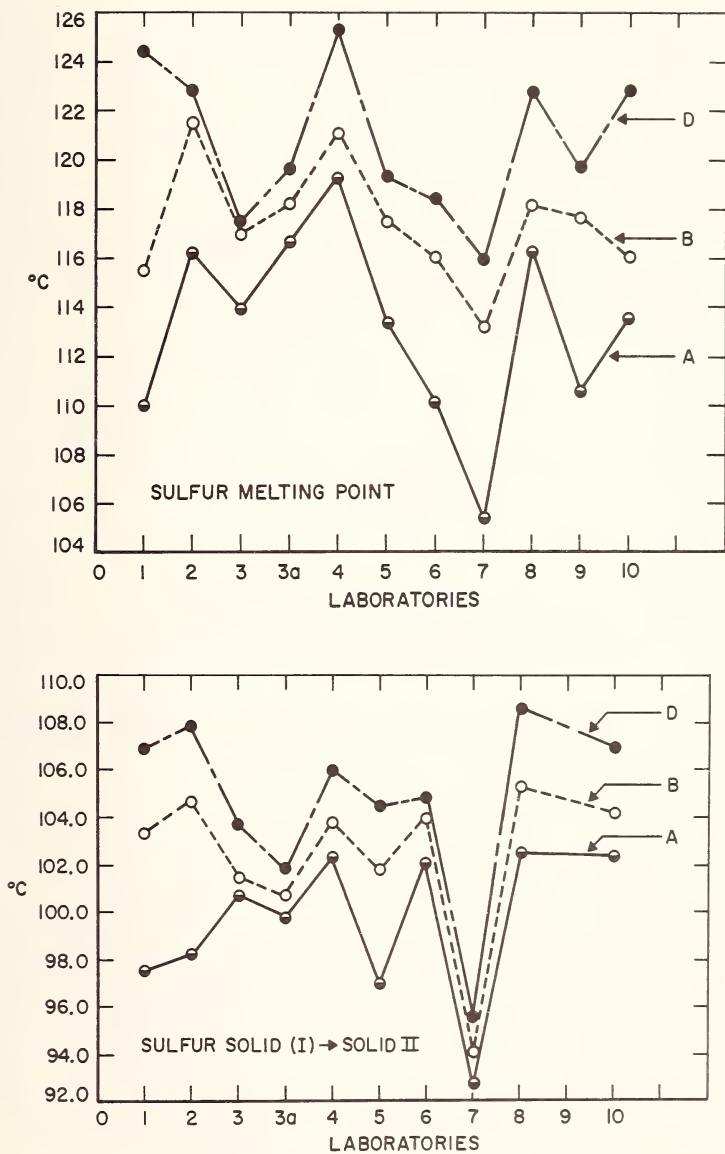
Figure 9. Cooperative data for ASTM committee members
           (one member with two data points).
                a) Sulfur Solid I→II
                b) Sulfur melting point
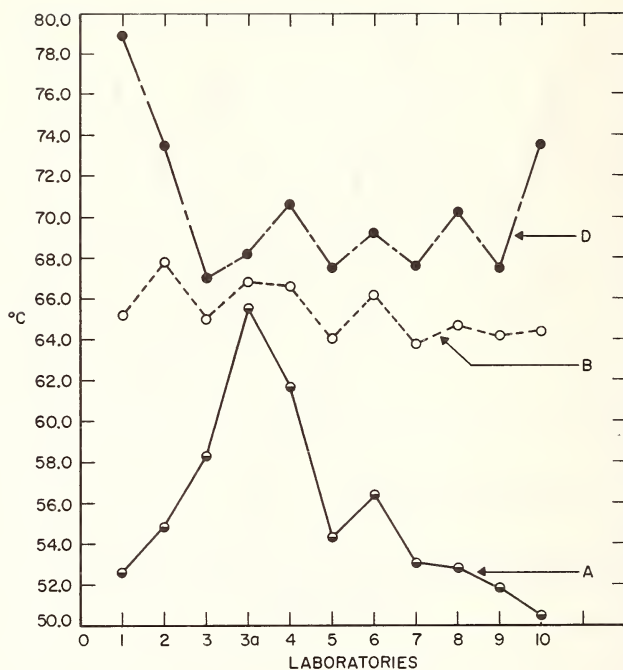
Figure 10. Cooperative data from ASTM committee members --
            for stearic acid melting point.

In conclusion, Figure 12 shows schematically a list of proposed
Standard Reference Materials which should meet the requirement for
temperature scale calibration over a temperature range from 40 to
900 °C. The peaks and the areas indicate qualitatively the relative
sensitivity and enthalpy changes of these materials. Two of these,
potassium nitrate and quartz, shown also in Figure 7, have been
issued under a provisional certificate, NBS-SRM 755 and 756.
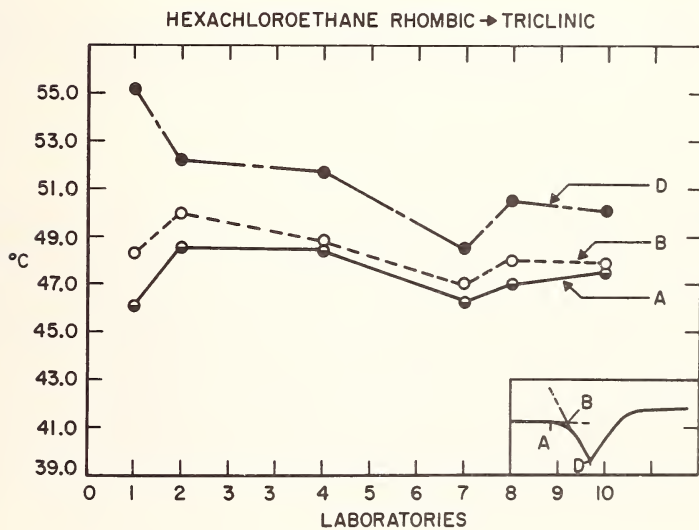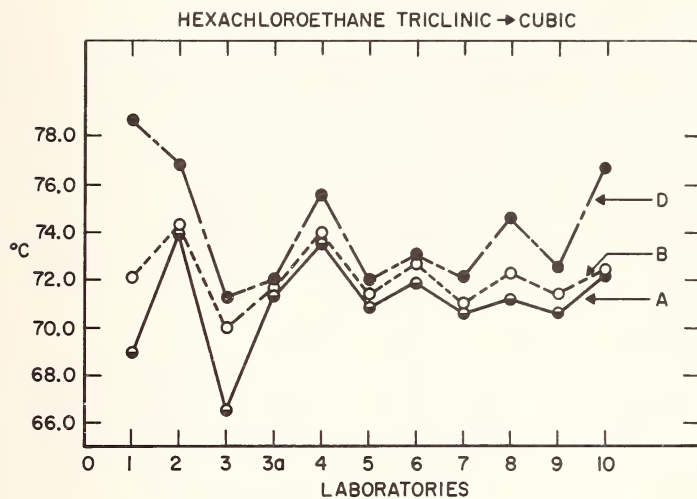
Figure 11.   Cooperative data from ASTM committee members --
              for a) hexachloroethane, rhombic → triclinic
                    b) hexachloroethane triclinic → cubic
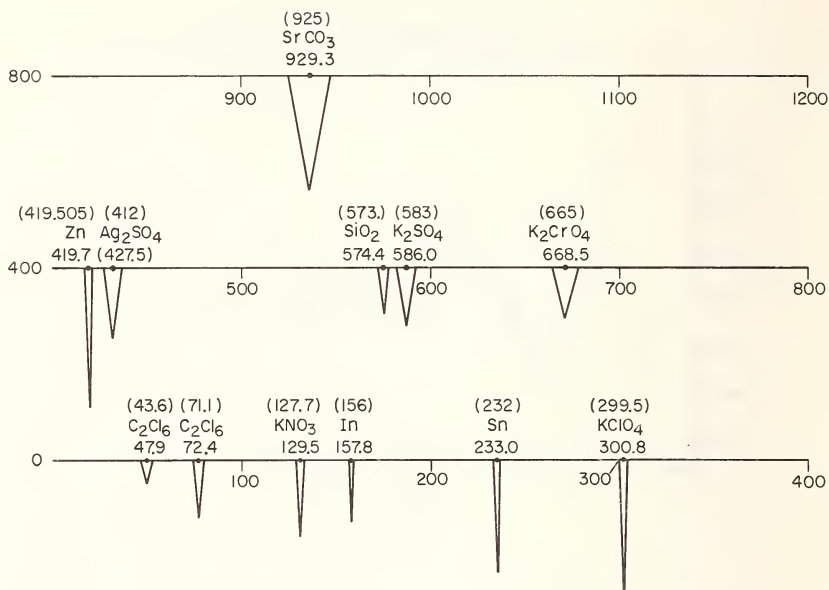
Figure 12.   Selected DTA temperature reference materials over
            the temperature range of 40 to 900 °C.

       Sample homogeneity, the effect of particle size and recycling
through the transition temperature below the melting points of the
two compounds were studied and are summarized in Figures 13 and 14.
It must be noted that KNO_3, as described previously, in its first
thermal cycle, reveals a large deviation at point D.   Subsequent
thermal curves of the same sample indicate consistent reproduci-
bility.   The transition peaks in these figures show a maximum
spread of ±0.5 °C which also reflects the variation in particle
size and source of materials.

HOMOGENEITY OF SRM POTASSIUM NITRATE
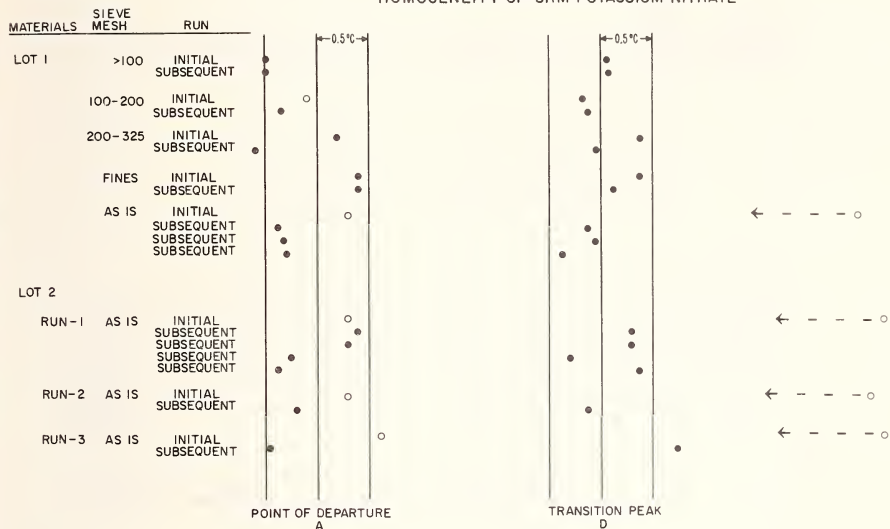
Figure 13.   Homogeneity and repetitive   cycling through the
              transition point for potassium nitrate.

Future efforts should extend to cover the subambient temper-
ature region which is of interest in bio-clinical work, and the
high temperature range, of interest in transportation and space tech-
nology.   It is anticipated also that many more organic or polymer
type standards could be useful. Finally, it can be expected that in
addition to temperature scale standards the establishment of known
enthalpy values could also aid science and technology in quantitative
analysis of various materials.
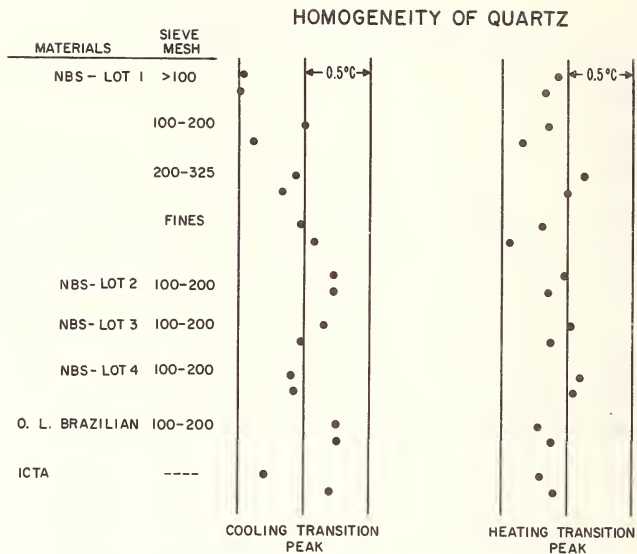
Figure 14.   Homogeneity and cooling and heating transition
              peak.

ACKNOWLEDGMENT

    The assistance of D. S. Bright in this study is acknowledged.

REFERENCES

[1]   Chemical and Engineering News, p. 46, August 18, 1969.

[2]   H. McAdie, private communication.

[3]   Schwenker, R. F., Jr. and Garn, P. D., Editors, Thermal Analysis,
      Vol. II, Appendix 3, Academic Press, New York (1969).

[4]   Kracek, F. C., J. of Phys. Chem. 34, 225 (1930).

HIGH TEMPERATURE DIFFERENTIAL THERMAL ANALYSIS

Robert D. Freeman

Department of Chemistry
Oklahoma State University
Stillwater, Oklahoma 74074

Three areas are discussed: (1) high temperature
(>1900 K) differential thermal analysis (DTA); (2)
some problems in conventional high temperature calor-
imetry, which may be relevant to high temperature dy-
namic calorimetry; and (3) a brief description of our
efforts to achieve dynamic calorimetry to at least
1300 K.

Key words: high temperature chemistry; differential
thermal analysis; dynamic calorimetry

INTRODUCTION

High temperature chemists [1] have debated at some length the
appropriate definition of "high temperature." For the purposes of
this paper I shall define "high temperature (HT)" to mean a temper-
ature higher than the range in which conventional, well-known tech-
niques and equipment produce acceptable results.

Conventional DTA (ΔT *vs.* T or t) may be more or less routinely
accomplished at temperatures up to $\sim$1900 K. The techniques and
equipment are described in books by Garn [2], Wendlandt [3], Smothers
and Chiang [4], and Mackenzie [5], and in literature readily avail-
able from the various manufacturers of DTA instruments. Therefore,
I shall consider "high temperature DTA" to indicate temperatures
above 1900 K.

On the other hand, dynamic calorimetry (*e.g.*, "Differential
scanning calorimetry") is not a well established technique above
$\sim$900 K; accordingly, for this technique "high temperature" shall
indicate temperatures above 900 K.

This discussion will focus on three areas: (1) high temper-
ature DTA (as defined above); (2) some problems in conventional
high temperature calorimetry, which may be relevant to HT dynamic
calorimetry; and, finally (3) a brief description of our efforts to
achieve dynamic calorimetry to at least 1300 K.

HIGH TEMPERATURE DIFFERENTIAL THERMAL ANALYSIS

One of the rules of thumb of high temperature chemistry [6] is:
At high temperatures, everything reacts with everything else. Like
most rules of thumb, this one is not strictly valid, but it does
serve to emphasize the problems associated with choosing suitable
thermocouples, sample holders, furnace elements and insulation,
etc., to extend conventional DTA to temperatures above 1800-1900 K.
For specific problems, one may be able to use tungsten-rhenium
thermocouples [7] and to operate tungsten, molybdenum, tantalum or
graphite furnace elements in an inert atmosphere, but the major
efforts in the development of generally applicable HT DTA apparatus
have been directed toward vacuum furnaces and radiation detectors
as temperature sensors.

One of the first of these systems was described by Rupert [8]
in 1963. A rather straight-forward vacuum system contained a ver-
tical section of 10-cm o.d. Pyrex pipe around which was located a
radiofrequency induction coil and inside of which was an "eddy
current concentrator." The crucible-sample holder was supported
in the center of the "concentrator" by a tungsten rod. Radiation
from a small hole in the top of the crucible passed through a
quartz window in the vacuum envelope, and impinged on a partially
aluminized mirror which reflected part of the light to an optical
pyrometer, and passed part to a photomultiplier tube. The output
of the PM tube, as displayed on an oscilloscope (1-2 div/s sweep
rate on horizontal axis), provided a reasonably accurate transform
of the temperature-time behavior of the crucible. This apparatus
produced reliable data from cooling curves, *e.g.*, the temperature
of phase transitions [8], but had no reference cell for differential
temperature sensing.

A couple of years later Rupert reported a major modification
to, and, improvement of his apparatus [9]. The major changes in
equipment were: (1) provision was made for two sample (or sample
and reference) containers in the crucible which was heated as be-
fore; (2) two photodiodes in "identical" light sensing circuits
replaced the PM tube and permitted cooling curves for two samples
to be recorded simultaneously or the differential output between
sample and reference to be recorded; (3) a dual-trace storage
oscilloscope was used to record and display the photodiode outputs
for long periods (hours); the display could then be studied and/or
photographed as desired; (4) electronic circuitry between the
photodiodes and the oscilloscope permitted a variety of thermal
analysis data to be recorded. These various types of data included
(1) thermal analysis (cooling curves, $\underline{T}$ $vs.$ $\underline{t}$), (2) differential
thermal analysis ($\Delta\underline{T}$ $vs.$ $\underline{T}$ or $\underline{t}$), (3) derivative thermal analysis
($d\underline{T}/d\underline{t}$ $vs.$t), and (4) "thermal derivative thermal analysis,"
($d\underline{T}/d\underline{t}$ $vs.$ T). This last mode for presentation of data appears to
be especially useful in studying the temperature range over which
phase transitions occur. With this improved apparatus thermal
effects in the range 1300-2800 K could be studied; the sensitivity
is indicated by noting that a 2.5 cal transition in 0.5 g of iron
at 1665 K produced a $\sim$4-cm deflection on the oscilloscope trace of
the $d\underline{T}/d\underline{t}$ signal.

In a parallel effort, Heetderks, Rudy and Eckert [10] developed
an apparatus similar to Rupert's, but with these differences: (1) a
low voltage, high amperage resistance furnace with a cylindrical
graphite element provides programmable temperatures from 1000 to
3900 K in vacuum or in inert gas with pressures up to 6 bar; (2) the
problem of matching radiation detectors for the sample and the ref-
erence channels was avoided by using only one photodiode which re-
ceived radiation from both sample and reference cells as a mechan-
ical chopper alternately passes and intercepts each of the two
light paths. This apparatus is now commercially available [11].

In more recent developments Baldwin, *et al*. [12] have combined radiofrequency induction heating, as used by Rupert [9], with a single radiation detector, as used by Heetderks, *et al*. [10]. The major innovation is the use of a lead sulfide photoconductor as the radiation sensor. These photoconductors, which were developed as infra-red radiation sensors, have a usable spectral response over the range 0.25 to 3.5 mm and therefore responds to changes in radiation from objects at temperatures as low as 400 K.

These various HT DTA apparatuses have been used to study a variety of chemical systems. Some examples are: Mo-C, Zr-C and U-C [8]; Th-C and UO_{2-x} [12]; Nb-C, U-C, and U-Gd-C [9]; Hf-C, Ta-C.

HIGH TEMPERATURE CALORIMETRY

There seems to be a growing desire to make DTA more quantitative *i.e.*, to obtain from peak height or peak area a value which correlates directly and linearly with the energy or enthalpy change associated with the transition/reaction. The prime example of this trend is the differential scanning calorimetry (DSC) [13,14], but a number of other approaches have also been reported [15-17]. Since this trend is certain to continue, and since there already is a desire to extend DSC-type measurements to higher temperatures than the 900 K presently available, we examine briefly some of the problems of conventional calorimetry at high temperatures and indicate where detailed discussions of these problems may be found.

There are two conventional calorimetric techniques for obtaining heat capacity and enthalpy data at temperatures above 500 K. One of these, drop calorimetry, is not particularly suited to automated, dynamic measurements; therefore, the recent publication [18] of a comprehensive discussion of the subject is noted, and our attention is directed to the other technique, adiabatic calorimetry.

As ordinarily used, the term *adiabatic calorimetry* is a misno-
mer. What is meant is the (precise measurement of changes in tem-
perature associated with enthalpy (energy) increments such that the
derived average heat capacity and enthalpy of transition is obtained
with high precision, the measurements being accomplished with the
calorimeter vessel (sample container) surrounded by an <u>adiabatic</u>
<u>shield</u> so that energy exchange between calorimeter and surroundings
is minimized. There are two techniques for producing the enthalpy
(energy) increments: (1) intermittent heating, in which the tempera-
ture is measured before and after a heating period, but no power is
supplied to the heater during the temperature measurement; and (2)
continuous heating, in which constant power is supplied to the sample
heater and the time is recorded when the thermometer indicates each
of various selected temperatures. This latter dynamic technique is
obviously closely related to quantitative DTA techniques.

West and Westrum [19] have recently discussed in detail the
problems associated with adiabatic calorimetry up to 800 K. The
problems arise primarily from the limitation imposed by the effect
of HT on possible materials of construction (*e.g*, oxidation, melt-
ing difficulties in achieving good thermal contact between components)
and from the increased rate of exchange of energy between calorimeter
and adiabatic shield as a result of the T^4 radiation law. West and
Westrum also provide a survey of some 40 intermediate and high tem-
perature adiabatic calorimeters (∼300-1800 K). Only a very few of
these operate above 1200 K; the most notable are two rather massive,
complex devices reported by Backhurst [20] (to 1870 K) and by Dench
[21] (to 1670 K).

Other very useful discussions of calorimetry at HT have appeared
in recent years [22-28]. Especially interesting is a discussion [29],
among several leaders in the field, from which the consensus appears
to be that the best approach to HT calorimetry is with heat-flow cal-
orimeters of the Calvet [30] or Wittig [31] type.

Another major effort to overcome the difficulties inherent in traditional calorimetry at HT has been made by the several developers of pulse, or high-speed, calorimetry. For example, Kollie [32] has developed an apparatus in which a dc pulse of several seconds duration is passed through a rod-shaped sample, while a high-speed (400 readings/s) digital voltmeter sequentially scans data channels connected to voltage, current, and temperature (thermocouple) probes. Accuracy within 1 percent and reproducibility within 0.5 percent in the heat capacity of pure iron over 300-1200 K was obtained.

More recently, Cezairliyan, *et al*. [33] have described a similar system in which an individual experiment, with the temperature of the specimen (*e.g.*, a molybdenum tube) changing from 300 K to near the melting point, is completed in less than one second. High-speed digital data acquisition is used, of course, and temperatures are measured by a high-speed photoelectric pyrometer which can make 1200 readings/s. It is interesting that during an experiment the pyrometer reads alternately the specimen temperature and the temperature of a calibrated tungsten filament lamp; in a sense, then, the technique is a type of high-speed DTA. Beckett and Cezairliyan [34] have recently reviewed high-speed calorimetric techniques.

DYNAMIC DIFFERENTIAL CALORIMETRY

Our initial interest in "quantitative DTA" arose from a desire to measure directly the enthalpy of a disproportionation reaction of the type: $A_{(s)} \longrightarrow B_{(s)} + C_{(g)}$ for which measurement of the equilibrium dissociation pressure [35] presented considerably more than ordinary difficulties. Our first furnace and sample/reference assembly was essentially a copy of that of Speros and Woodhouse [15]; the electronics were somewhat more sophisticated in that power to the sample heater was automatically controlled and the power dissipated in the heater was monitored by recording the output of an operational amplifier-Hall-effect multiplier circuit [36]. This apparatus required a "one-time" calibration, as proposed and discussed by Speros and Woodhouse [15], of the thermal coupling between sample, heater, and

thermocouple. Thereafter, it produced reliable data (within 1-2%) for heats of fusion of metals and for heats of decomposition of various carbonates [36]. It is worth noting that, although the sample-cell-heater assembly was considerably larger and more massive than the DSC units, the "peak" obtained for a sharp transition (*e.g.*, melting) had the same characteristics as the theoretical shape predicted by Gray [37] for DSC peaks.

From our experiences with this apparatus and from various concurrent developments, we reached the following tentative conclusions: (1) Furnace programming and control could be improved if the furnace was small (*e.g.*, 5 cm o.d. and 10 cm high) and had high thermal conductivity and low heat capacity. (2) Energy exchange between furnace and sample/reference cells is most easily controlled by minimizing that exchange, *i.e.*, operating adiabatically (or quasi-adiabatically) with the "furnace" becoming, in effect, an adiabatic shield for the sample/reference cells. (3) Achievement of near-adiabatic conditions in a small furnace (*cf.* [1]) at 1300 K is likely to be very difficult; therefore, one should retain the differential mode of operation and should make sample and reference structures as nearly symmetrical as possible, so that any nonadiabaticity produces equal effect on sample and reference.

Very few differential adiabatic dynamic calorimeters (DADC) have been described; for example, Wilhoit [38], in his survey of "Recent Developments in Calorimetry," describes five configurations for dynamic calorimeters but does not mention DADC. Clarebrough, *et al.* [39] used what is essentially a DADC apparatus to measure (up to 800 K) the energy stored in deformed metals. More recently, Bonjour [40] has described a DADC which operates over the range 75-700 K, but the sample configuration is a small rectangular strip, 0.5-3.0 mm thick, held closely to the heating element by clips.

Our ideas about DADC have led to a design in which a sample and a reference structure similar to those of Speros and Woodhouse [15] are enclosed in a small metal-walled cylindrical furnace with heating elements evenly distributed over sides and ends. The temperature
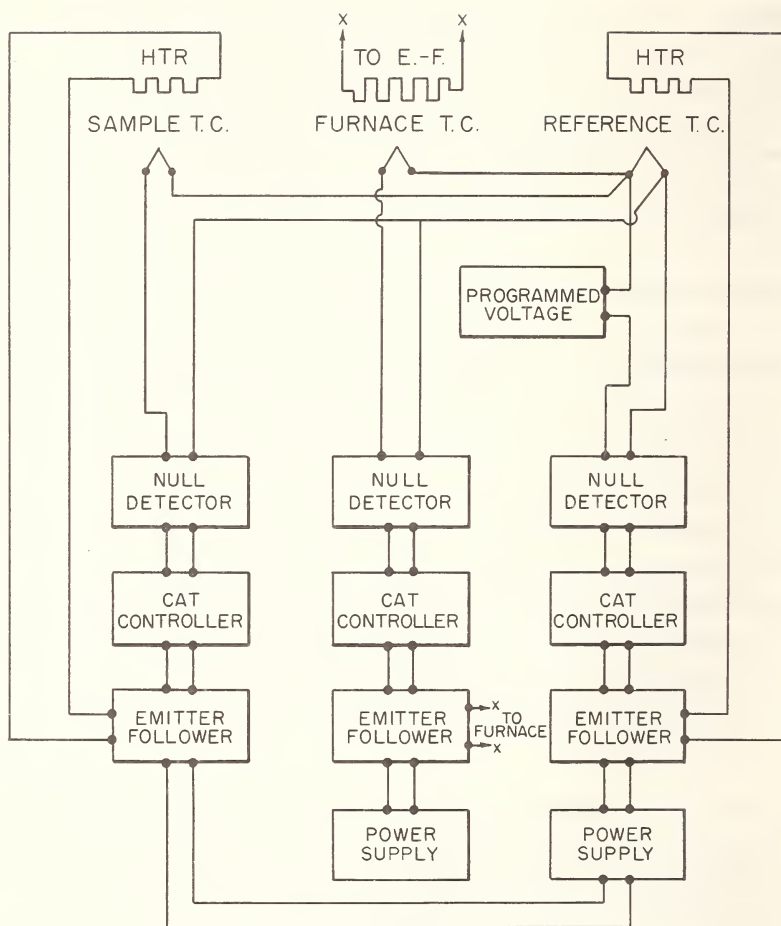
Figure 1. DADC control system.

sensing and the power control circuitry are indicated in block dia-
gram in Figure 1; the components are, more or less, conventional.
The circuit which measures the differential power between the sample
and the reference heaters is perhaps not conventional; a schematic
diagram is given in Figure 2. Details about the twin Wheatstone

Figure 2.   Analogue computation of differential power.

bridge with magnetoresistive elements ("Mistor"), which is the heart
of the power measuring circuit, are available elsewhere [41].

The apparatus is still in the development stage. It has been
established that the circuitry of Figure 2 is quite satisfactory,
and the entire apparatus has been successfully operated in the sense
that it has produced the usual "peaks" for melting samples, but we
have not yet obtained data which would establish precision, accuracy,
actual operating limits on temperatures, *etc*.

REFERENCES

[1] Goldfinger, P., A Definition of High Temperature Chemistry,
     "Advamces in High Temperature Chemistry," Eyring, L., Ed.,
     Vol. 1, Academic Press, New York (1967).

[2] Garn, P. D., "Thermoanalytical Methods of Investigation,"
     Academic Press, New York (1965).

[3] Wendlandt, W. W., "Thermal Methods of Analysis," Interscience-
     John Wiley and Sons, New York (1965).

[4] Smothers, W. J., and Chiang, Y., "Handbook of Differential
     Thermal Analysis," Chemical Publishing Co., Inc.,
     New York (1965).

[5] Mackenzie R. C., Ed., "Differential Thermal Anlaysis,"
     Vol. 1 and 2, Academic Press, New York (1969).

[6] Searcy, A. W., in "Proceedings of an International Symposium
     on High Temperature Technology," Asilomar, California,
     October, 1959, p. 336, McGraw-Hill, New York (1969).

[7] Asamoto, R. R., and Novak, P. E., Rev. Sci. Instr. $\underline{38}$, 1047
     (1967); $\underline{39}$, 1233 (1968).

[8] Rupert, G. N., Rev. Sci. Instr. $\underline{34}$, 1183 (1963).

[9] Rupert, G. N., Rev. Sci. Instr. $\underline{36}$, 1629 (1965).

[10] Heetderks, H. D., Rudy, E., and Eckert, T., Planseeber.
     Pulvermet. $\underline{13}$, 105 (1965).

[11] Aerometrics Div., Aerojet-General Corp., San Ramon, California.

[12] Baldwin, N. L., Langer, S., Kester, F. L., and Hancock, C.,
     Rev. Sci. Instr. $\underline{41}$, 200 (1970).

[13] O'Neill, M. J., Anal. Chem. $\underline{36}$, 1238 (1964).

[14] Watson, L. S., O'Neill, M. J., Justin, J., and Brenner, N.,
     Anal. Chem. $\underline{36}$, 1233 (1964).

[15] Speros, D. M., and Woodhouse, R. L., J. Phys. Chem. $\underline{67}$,
     2164 (1963).

[16] Boersma, S. L., J. Am. Ceram. Soc. $\underline{38}$, 281 (1955).

[17] Levy, P. F., Amer. Laboratory, p. 46. January 1970.

[18] Douglas, T. B., and King, E. G., "High Temperature Drop
     Calorimetry," Chapt. 8, "Experimental Thermodynamics,"
     McCullough, J. P., and Scott, D. W., Eds., Vol. 1,
     Plenum Press, New York, (1968).

[19] West, E. D., and Westrum, E. F., Jr., "Adiabatic Calorimetry
      from 300 to 800 K," Chapt. 9, "Experimental Thermo-
      dynamics," McCullough, J. P., and Scott, D. W., Eds. Vol. 1,
      Plenum Press, New York, (1968).

[20] Backhurst, I., J. Iron Steel Inst. (London) 189 124 (1958).

[21] Dench, W. A., Trans. Faraday Soc. 49, 1279 (1963).

[22] Bockris, J. O'M., White, J. L., and MacKenzie, J. D., Editors,
      "Physico-Chemical Measurements at High Temperatures."
      Butterworths, London (1959).

[23] Kubachewski, O., Evans, E. Ll. and Alcock, C. B.,
      "Metallurgical Thermochemistry," 4th Ed., Pergamon
      Press, London (1967).

[24] Eyring, L., Ed., "Advances in High Temperature Chemistry,"
      Vol. 1, Academic Press, New York (1967).

[25] "Thermodynamics," Vols. I and II, Proceedings of a
      Symposium, Vienna, July, 1965. International Atomic
      Energy Agency, Vienna (1966).

[26] Rossini, F. C., Ed., "Experimental Thermochemistry,"
      Vol. 1, and Skinner, H. A., Ed., Vol. 2, Interscience-
      John Wiley and Sons, New York (1956 and 1962).

[27] McCullough, J. P., and Scott, D. W., Eds., "Experimental
      Thermodynamics," Vol. 1, Plenum Press, New York, 1968.

[28] "Thermodynamics," Proceedings of a Symposium, Fritzens-
      Wattens, Austria, 1959. Butterworths, London (1961)
      (Reprinted from Pure and Applied Chemistry 2. Nos. 1-2).

[29] "Thermodynamics," Proceedings of a Symposium, Vienna,
      July 1965, p. 89-93, International Atomic Energy Agency,
      Vienna (1966).

[30] Calvet, E. and Prat, H., "Recent Progress in Micro-
      calorimetry," (translated by H. A. Skinner), Macmillan
      Co., New York (1963).

[31] Wittig, F. E., "Calorimetric Methods at High Temperatures,"
      in Proceedings of a Symposium, Fritzens-Wattens,
      Austria, 1959. Butterworths, London (1961) (Reprinted
      from Pure and Applied Chemistry 2 Nos. 1-2, p. 183.)

[32] Kollie, T. G., Rev. Sci. Instr. 38, 1452 (1967).

[33] Cezairliyan, K. A., Morse, M. S., Berman, H. A., and
      Beckett, C. W., J. Res. NBS 74A, 65 (1970).

[34] Beckett, C. W., and Cezairliyan, K. A., "High-speed
      Thermodynamic Measurements and Related Techniques,"
      Chap. 14 "Experimental Thermodynamics," McCullough, J. P.,
      and Scott, D. W., Eds., Vol. 1, Plennum Press, New
      York (1967).

[35] Margrave, J. L., Ed. "Characterization of High Tempera-
      ture Vapors," Chapt. 2-7, John Wiley and Sons, Inc.,
      New York (1967).

[36] Gwinup, P. D., Ph.D. Thesis, Oklahoma State University,
      Stillwater (1967).

[37] Gray, A. P., "Analytical Calorimetry," in Proceedings of
      American Chemical Society Symposium, San Francisco,
      April, 1968, Porter, R. S. and Johnson, J. F., Eds.,
      p. 209, Plenum Press, New York (1968).

[38] Wilhoit, R. C., J. Chem. Educ. $\underline{44}$, A571, A629, A685,
      A853 (1967).

[39] Clarebrough, L. M., Hargreaves, M. E., Michell, D.,
      West, G. W., Proceedings of the Royal Society, London,
      $\underline{A215}$, 507 (1952).

[40] Bonjour, E., "Thermal Analysis 1965," Proceedings of First
      International Conference on Thermal Analysis, Redferen,
      J. D., Ed., Aberdeen, Scotland, p. 56, Macmillan and
      Company, Ltd., London, England (1966).

[41] Gitlin, R. M., Analog Dialogue $\underline{1}$, (1967). Published by
      Analog Devices, Inc., Cambridge, Massachusetts.

THERMAL STUDIES ON LIPID-WATER SYSTEMS BY DIFFERENTIAL SCANNING CALORIMETRY WITH REFERENCE TO ATHEROSCLEROSIS

G. Jerry Davis and Roger S. Porter

Polymer Science and Engineering
University of Massachusetts
Amherst, Massachusetts   01002

Studies have been performed on liqid-water systems by differential scanning calorimetry. Three-component systems were investigated. The components consisted of a phospholipid, cholesterol or one of its esters, and water. The phospholipids studied included lecithin and sphingomyelin. The cholesteryl derivatives used in the ternary systems included cholesterol and its oleate, linoleate, and stearate esters. The temperatures and heats of transition for these systems were investigated. The results reveal considerable differences in the stability of complexes formed in these ternary systems with the unsaturated esters generally leading to the least stable structures. The morphologies likely represent compositions and order similar to the layered structures observed for the same and related phospholipid-cholesteryl derivative molecular organization. The results have implications concerning the nature of biological membranes and the deposition of atherosclerotic plaques.

Key words: atherosclerosis; differential scanning calorimetry; cholesterol and its fatty acid esters; lecithin; lipid-water systems; phospholipids; sphingomyelin; thermal studies.

1.   INTRODUCTION

Thermal studies on lipid-water systems provide information which have implications in biological membrane organization in connection with atherosclerosis. The origin of lipids in athero-sclerotic lesions is not known but its possible association with abnormal plasma lipids has been suggested [1]. Plasma lipids are,

99

for the most part, a mixture of triglycerides, cholesterol and its
fatty acid esters, and phospholipids, of which the main components
are lecithin and sphingomyelin [1]. These circulate as lipoproteins
which can be separated (by electrophoresis, ultracentrifugation, or
chemical fractionation) into two main divisions -- the alpha or high
density lipoproteins and the beta or low density lipoproteins. It
is the latter group which may be associated with increased deposits
in clinical atherosclerosis [1].

If the lipids in atherosclerotic plaques are compared with
those in different classes of low density lipoproteins, their com-
position is found to be closest to the S_f 0-12 or true-β-lipo-
protein [2]. The S_f 0-12 lipoprotein contains 15 to 20 percent
protein [2]. The lipid content of S_f 0-12 lipoprotein has been
analyzed to be in terms of percentages of total lipid, 58.2 percent
cholesteryl ester, 20 percent phospholipid, and 10.2 percent trigly-
ceride [3]. The most abundant fatty acids of the cholesteryl esters
are, in percentage of total fatty acid, oleic (18:1) at 24.1 percent
and linoleic (18:2) at 46.8 percent [3].

Lipoproteins are complexes of lipid and protein that have the
solubility characteristics of protein, *i.e.* are soluble in water or
aqueous salt [4]. The lipid links together with the protein, in
most instances, by the association of the non-polar regions of the
lipid molecules with similar regions of the protein molecule, such
as the hydrocarbon tails of the fatty acid moieties of lipids with
the hydrophobic amino acid side chains of the protein [4]. However,
many lipoprotein fractions contain far too much lipid for direct
association of all non-polar regions of lipid residues with non-
polar regions of protein [4]. In such cases, the lipoprotein struc-
ture must also involve lipid-lipid interaction. It is hypothesized
here that S_f 0-12 β-lipoprotein is an example of a lipoprotein
which has lipid-lipid interaction.

Lipoproteins can supply the major constituents for mammal mem-
branes, which are composed of lipids and proteins [5]. Carbohydrates
and nucleic acids are minor components at most of membranes [5].

Electron microscopic observation suggests that many different kinds
of membranes have similar molecular structures [6]. With adequate
resolution, the membranes show a trilaminar structure consisting of
two dense outer laminae separated by a faint interface [6]. Model
studies on phospholipid-water systems of low water content indicate
that the darkly stained laminae are charged and the faint inner layer
is the hydrocarbon region [7]. A trilaminar structure which would be
hydrophilic on the membrane exteriors and hydrophobic internally could
be formed by protein alone, lipoprotein or lipid alone.

Given that the β-lipoproteins contain excess lipids which inter-
act with each other, these lipids have the capacity to form membranes.
Systems of phospholipid-water [8] and phospholipid-cholesterol-water
[9] have been shown to form into discrete bimolecular layers of lipid
in which the polar regions of each phospholipid layer face outward in-
to a water layer and the hydrocarbon chains "fill" the interior of the
"sandwich." These bimolecular structures would fulfill the trilaminae
requirements of the electron microscopic observations [7].

The experimentally observed phospholipid, dipalmitoyl-L-α-
lecithin, organizes, in the presence of an equivalent weight of
water, into bimolecular layers separated by water, with the hydro-
philic groups on the surface separating the lipid and water layers
[9]. This ordering can be studied thermally on a differential
scanning calorimeter (DSC) by the observation of a measurable endo-
thermic transition at a temperature of 41 °C on heating [9]. The
addition of cholesterol to dipalmitoyl-L-α-lecithin-water systems
has been shown to reduce the heat of transition until at a mole
ratio of 1:1 cholesterol to lecithin, no transition was observed
[9]. The cholesterol appears to become a part of the lecithin
structure, as noted by x-ray examination, up to this 1:1 mole ratio,
but in doing so, causes a reduction in the cohesive forces between
adjacent hydrocarbon chains of the lecithin [9]. These hydrocarbon
chains contract in length [10].

This study is particularly concerned with the effect of choles-
teryl esters on phospholipid-water systems. A comparison is made

with previous systems involving cholesterol. A goal is to see
whether this information might help suggest a mechanism by which
lipids accumulate in arteries during development of atherosclerotic
lesions. The idea that the deposits from the plasma accumulate
through membrane formation rather than by direct deposition will be
considered [11]. The phospholipids acquired for these experiments
were dipalmitoyl-L-α-lecithin, bovine lecithin, and bovine sphingo-
myelin. From a physical-chemical standpoint, sphingomyelin is sim-
ilar to lecithin, since it has a hydrophobic region of two long-chain
fatty acyl groups and a highly polar region consisting of a phosphoryl
choline zwitterion as does lecithin [12]. The cholestery ester series
of the C_{18} fatty acids, stearic (18:0), oleic (18:1), and linoleic
(18:2) was chosen to be used in conjunction with the phospholipids
because of the presence in S_f 0-12 β-lipoprotein of large quantities
of cholesteryl oleate and linoleate.

2.   EXPERIMENTAL PROCEDURE

The dipalmitoyl-L-α-lecithin, bovine lecithin, bovine sphingo-
myelin, cholesterol, and cholesteryl esters of stearic, oleic, and
linoleic acid used in this study are 99 percent pure according to
the supplier Applied Science Laboratories, State College, Pennsyl-
vania. The phospholipids and cholesteric compounds were weighed
directly into the liquid sample pans provided for DSC testing. A
six place Mettler balance weighed the samples to 0.001 mg. Spectro-
scopic grade benzene was added to the pan to dissolve and mix the
phospholipid and cholesteric compound *in situ*. The benzene was evap-
orated under vacuum at 35 °C. The sample was reweighed as a function
of time to insure that all benzene was removed. Distilled water in
the amount of twice the phospholipid sample weight was added into the
planchet by syringe and the sample lid clamped on. The space between
the crimped sample lid and the pan was sealed with Eastman 910 adhe-
sive. Each sample contained one phospholipid and one cholesteric
compound. The sealed planchet containing the sample was placed in an
oven at a temperature of 70 °C for one hour before testing. This temp-
erature is 25 °C above that necessary to disperse the phospholipid in
the water [8,9]. The temperature choice also insured that the choles-

teryl esters would not pass through their major transition between
27 and 57 °C. The phospholipids used in this study have crystalline
melting points well above 70 °C [13].

Transitions within the samples observed on heating (all endo-
thermic) and on cooling (all exothermic) were measured on a Perkin-
Elmer Differential Scanning Calorimeter, DSC-1B. The calibration
of the DSC for temperatures and heats of transition have been de-
scribed elsewhere [14]. Equilibrium conditions for the samples were
demonstrated by repeating the heating and cooling cycle three times
over a period of one hour with observation of effectively the same
heats and temperatures of transition in the first and third cycle..
The samples were heated and cooled at a constant rate of 2.5 °C per
minute. The ordinate scale was on the maximum sensitivity of one cal-
orie per second. An accuracy in the heat of transition determination
of ± 5 percent for the dipalmitoyl-L-α-lecithin and ± 10 percent for
the bovine phospholipids is estimated. The precision in temperature
measurements is ± 0.5 °C for the dipalmitoyl-L-α-lecithin and ± 1.5
percent for the bovine phospholipids, natural materials containing a
mixture of compounds.

3. RESULTS

A. Dipalmitoyl-L-α-lecithin

The temperatures and heats of transition for the dipalmitoyl-
L-α-lecithin alone in water and with various mole fractions of choles-
terol or cholesteryl ester in water, both in heating (endotherm) and
cooling (exotherm), are presented in Table 1. The entropy of transi-
tion per mole of lecithin for the heating and cooling of each sample
has been calculated from its respective transition energy and temper-
ature. The transition energies were relatively constant over several
cycles of heating and cooling the same sample. This process is con-
sidered to be entirely reversible, since measured energy on heating
and cooling was, within the accuracy of the experimental technique,
the same. For this reason, the entropy values from the heating and
cooling of each sample were averaged. This average entropy value is

Table 1. Thermal transitions of dipalmitoyl-L-α-lecithin-water
          systems containing cholesteric compounds.

Mole fraction cholesteric compound (dry basis)	Transition	Measured ΔH Temp. °C	Cal/g. lecithin	ΔS Cal/K-mole lecithin	ΔS_{av} Cal/K-mole lecithin
None	Heating	43.2	9.36	21.7	
	Cooling	41.5	9.78	22.8	22.3
Cholesterol[a]					
0.092	Heating	42.7	8.68	20.1	
	Cooling	41.4	8.10	18.9	19.5
0.237	Heating	42.2	6.31	14.7	
	Cooling	40.8	5.61	13.1	13.9
0.320	Heating	42.4	3.14	7.3	
	Cooling	41.2	2.56	6.0	6.7
0.404	Heating	41.8	1.68	3.9	
	Cooling	40.9	1.64	3.8	3.9
Cholesterol Stearate					
0.096	Heating	43.2	9.15	21.2	
	Cooling	41.3	9.40	21.9	21.6
0.201	Heating	42.6	9.36	21.8	
	Cooling	41.2	8.91	20.8	21.3
0.329	Heating	42.3	9.15	21.3	
	Cooling	40.7	9.21	21.5	21.4
0.484	Heating	42.4	8.86	20.7	
	Cooling	41.0	8.88	20.7	20.7
Cholesterol Oleate					
0.070	Heating	42.8	9.59	22.3	
	Cooling	41.2	9.00	21.0	21.6
0.137	Heating	43.5	8.67	20.2	
	Cooling	41.3	8.43	19.7	20.0
0.300	Heating	42.5	9.70	22.6	
	Cooling	41.0	8.12	19.0	20.8
0.366	Heating	42.7	8.16	19.0	
	Cooling	41.0	7.90	18.7	18.9
0.477	Heating	42.6	8.64	20.1	
	Cooling	40.9	7.98	18.7	19.4

Table 1. (continued)

Mole fraction cholesteric compound (dry basis)	Transi-tion	Measured ΔH		ΔS Cal/K-mole lecithin	ΔS_{av} Cal/K-mole lecithin
		Temp. °C	Cal/g. lecithin		
Cholesterol Linoleate					
0.108	Heating	43.1	8.98	20.8	
	Cooling	41.4	8.36	19.5	20.4
0.244	Heating	43.2	8.10	17.7	
	Cooling	41.2	6.50	15.2	16.4
0.401	Heating	42.5	7.48	17.4	
	Cooling	40.4	6.23	14.6	16.0
0.500	Heating	42.8	7.41	17.2	
	Cooling	40.8	6.24	14.6	15.9

---

[a]At a mole fraction of 0.500 for cholesterol, no transition was detected on the DSC.

shown in the final column of Table 1. These average transition en-
tropies per mole of lecithin are plotted as a function of the mole
fraction of the cholesteric compound present in the sample, on a
water-free (dry) basis, in Figure 1. A representative DSC cooling
curve for each cholesteric compound used in the dipalmitoyl-L-α-leci-
thin-water system fraction is shown to scale in Figure 2. The choles-
teric compound was used in concentrations between 0.32 and 0.40 mole.

A rapid reduction in the transition heat with the addition of
cholesterol to the dipalmitoyl-L-α-lecithin-water system is observed
in Figure 1. This is similar to the results obtained by Ladbrooke,
Williams, and Chapman [9] for the dipalmitoyl-L-α-lecithin-choles-
terol-water system, though the heat of transition values from this
study are about 15 percent lower than those of these investigators.
The temperature of transition changed less than a degree over the
entire range of compositions tested. The transition on heating
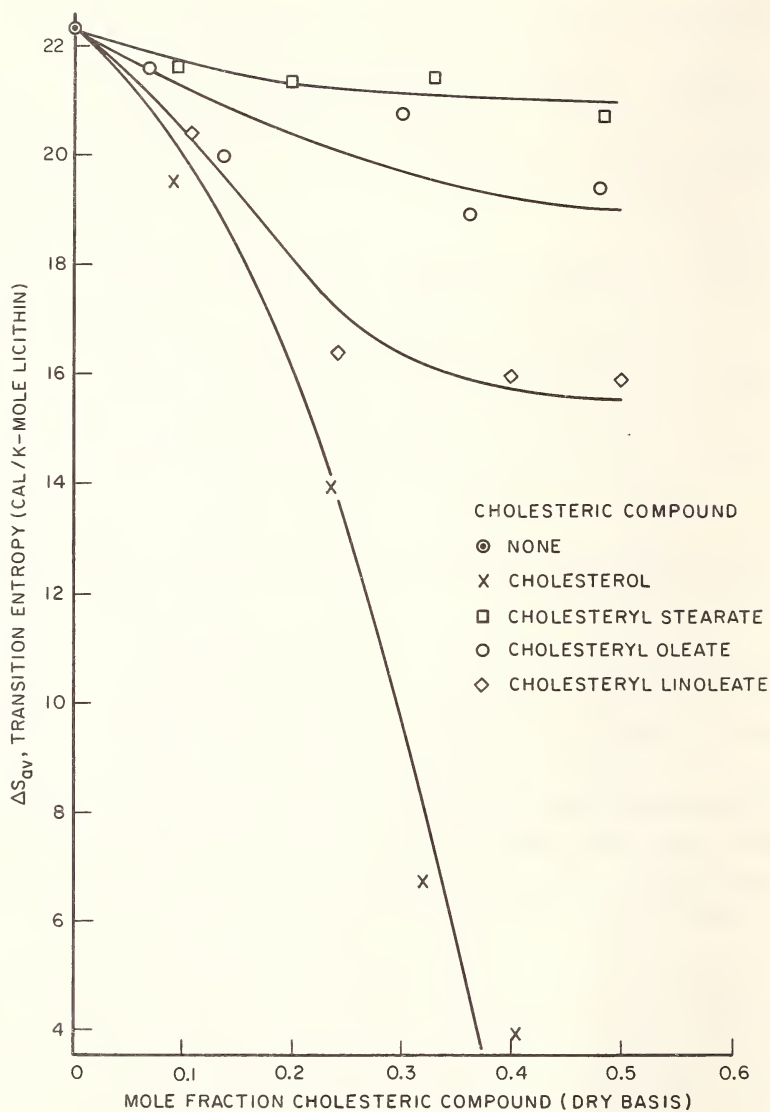occurred at a temperature about 1.5 °C higher than that on cooling.

Figure 1. (Dipalmitoyl)-L-α-lecithin cholesteric compound transition entropies (in water).

Ladbrooke, Williams, and Chapman [9] reported about 10 °C tempera-
ture decline with increasing cholesterol content. Two possible
reasons for this large temperature effect are a wider curve spread
with increasing cholesterol content than experienced by the present
investigators, and a different method of temperature calculation.
In this study, the peak temperature, corrected for difference be-
tween sample temperature and program temperature, the method recom-
mended by Perkin-Elmer, the manufacturer [15], is reported, instead
of the temperature the DSC trace leaves the baseline. The peak tem-
perature is the most significant and reproducible value. This obser-
vation is supported by Figure 2 which shows that all the transitions
have the same heat temperatures but widely varying ranges. An exten-
sive analysis of DSC curve behavior for endothermic transitions at a
heating rate of 2.5 °C/min. is presented in a complete and separate
study by these investigators [16].

     In contrast to cholesterol, cholesteryl stearate has remarkably
little effect either on the entropy or temperature of transition,
even at 0.50 mole fraction or a 1:1 mole ratio of ester to lecithin.
A plot of transition entropy per mole of lecithin *vs*. mole fraction
of cholesteryl stearate in Figure 1 indicates that perhaps a 5 per-
cent drop in entropy occurred at a 1:1 mole ratio.

     Cholesteryl oleate also has a small effect on transition en-
tropy of the system, but somewhat more than the lecithin-cholesteryl
stearate-water systems. The transition entropy decreased about 15
percent at a 1:1 mole ratio. Cholesteryl linoleate has a greater
effect, reducing the transition entropy about 30 percent at a mole
fraction of 0.35 of a 1:2 mole ratio. The presence of either choles-
teryl oleate or linoleate has little effect on transition temperature.

                         B. Bovine Phospholipids

     No thermal transition could be detected by the DSC for the
bovine lecithin-water system between the temperatures of 5 and
55 °C. However, the bovine sphingomyelin-water system exhibited
a thermal transition about 75 percent as large in energy as the
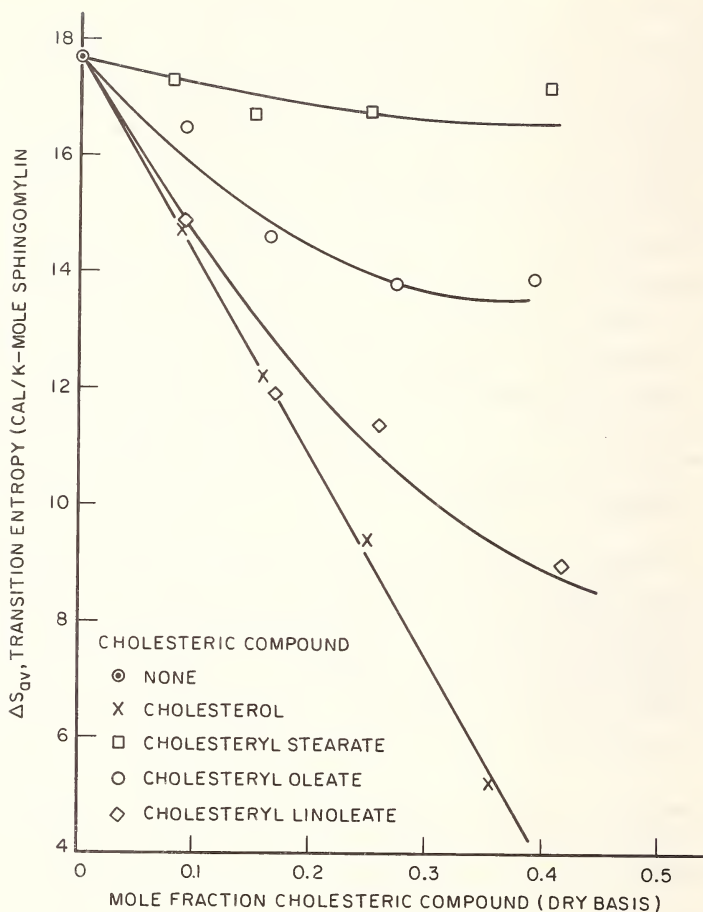
Figure 2.   Sphingomyelin (bovine)-cholesteric compound
             transition entropies (in water).

dipalmitoyl-L-α-lecithin-water system and at the same transition
temperature. This is not a crystalline-liquid transition, since
sphingomyelin melts at a temperature considerably higher than
70 °C [13], but may be similar to the type of organization exhib-
ited by the lecithin-water system [9,10]. The breadth of the
trace extended over a temperature span of 12 °C, about twice that

of the dipalmitoyl-L-α-lecithin, reflecting the difference between a natural and a single synthetic compound.

The above result is not unexpected since the bovine lecithin has two adjustable acyl groups and the bovine sphingomyelin, only one. Sphingomyelin usually has as one of its two acyl groups, the hydrocarbon chain provided by sphingosine, though some sphingomyelin contains dihydrosphingosine rather than sphingosine [5]. With two variable groups, bovine lecithin is likely to contain many more different molecules which have a broader range of physical properties than bovine sphingomyelin. These many different molecules in bovine lecithin could spread the transition energy over such a broad temperature range that the transition could go undetected by the DSC. However, the possibility exists that the transition temperature for this material is lower than + 5 °C.

The temperatures and heats of transition for bovine sphingo-myelin alone in water and with various mole fractions of cholesterol or cholesteryl esters in water, both in heating (endotherm) and cooling (exotherm) are presented in Table 2. Given that the temperature range for all samples tested, either on heating or cooling, were separated by less than 3 °C, the actual temperature variation for these systems (see Table 2) should be considered as small as that of the dipalmitoyl-L-α-lecithin systems. The molecular weight of sphingomyelin was estimated at 770 from data supplied by Applied Science Laboratories. Bovine sphingomyelin is particularly rich in the saturated C_{24} amides though about ten percent of the adjustable acyl group are the saturated C_{16} and C_{18} amides.

The average entropies of transitions of the sphinogomyelin-cholesteric compound-water systems have been calculated in the same manner as the comparable dipalmitoyl-L-α-lecithin systems. These values are shown in the final column of Table 2. These average transition entropies per mole of sphingomyelin are plotted as a function of the mole fraction of cholesteric compound present in the sample (on a dry basis) in Figure 3 (see page 112).

Table 2.   Thermal transitions of sphingomyelin (bovine)-water
systems containing cholesteric compounds

Mole fraction cholesteric compound (dry basis)	Transition	Measured Temp. °C	ΔH Cal/g sphingo-myelin	ΔS Cal/K-mole sphingo-myelin	ΔS_{av} Cal/K-mole sphingo-myelin
None	Heating	43.0	7.36	17.9	
	Cooling	41.3	7.10	17.4	17.7
Cholesterol					
0.088	Heating	41.4	5.76	14.2	
	Cooling	39.7	6.14	15.2	14.7
0.160	Heating	40.5	4.82	11.8	
	Cooling	39.4	5.10	12.6	12.2
0.250	Heating	40.4	3.42	8.5	
	Cooling	39.4	4.16	10.3	9.4
0.356	Heating	40.3	1.72	4.3	
	Cooling	38.9	2.45	6.0	5.2
Cholesterol Stearate					
0.080	Heating	41.9	7.54	18.4	
	Cooling	40.4	6.56	16.2	17.3
0.150	Heating	41.9	6.73	16.5	
	Cooling	39.9	6.83	16.8	16.7
0.250	Heating	42.9	7.27	17.7	
	Cooling	41.0	6.53	16.0	16.8
0.455	Heating	41.8	6.96	17.0	
	Cooling	39.6	7.10	17.4	17.2
Cholesterol Oleate					
0.091	Heating	42.7	6.30	15.6	
	Cooling	40.5	7.00	17.4	16.5
0.164	Heating	42.0	5.90	14.7	
	Cooling	40.3	5.80	14.5	14.6
0.272	Heating	42.0	5.66	14.1	
	Cooling	40.8	5.41	13.4	13.8
0.390	Heating	41.0	5.19	12.9	
	Cooling	39.9	6.03	14.9	13.9

Table 2.   Continued

Mole fraction cholesteric compound (dry basis)	Transi- tion	Measured ΔH Temp. °C	Cal/g sphingo- myelin	ΔS Cal/K- mole sphingo- myelin	ΔS$_{av}$ Cal/K- mole sphingo- myelin
Cholesterol Linoleate					
0.091	Heating	42.0	6.46	15.8	
	Cooling	41.2	5.66	13.9	14.9
0.166	Heating	43.6	4.97	12.1	
	Cooling	41.9	4.79	11.7	11.9
0.270	Heating	42.9	4.35	10.6	
	Cooling	41.7	5.19	12.7	11.6
0.417	Heating	43.7	3.76	9.2	
	Cooling	42.7	3.62	8.9	9.0

The results displayed in Figures 1 and 2 indicate that choles-
terol reduces the transition entropy of bovine sphingomyelin and
dipalmitoyl-L-α-lecithin in water sharply; moreover, the transition
entropy change with cholesterol concentration is quite similar in
the two systems. In contrast, cholesteryl stearate has no ability
to change the entropy of transition of either phospholipid. Choles-
teryl oleate and linoleate are somewhat more effective in reducing
the entropy of transition of bovine sphingomyelin with increasing
mole fraction than with dipalmitoyl-L-α-lecithin. The most import-
ant observation, though, is that the curves in Figures 1 and 2 for
each cholesteric compound are so similarly positioned.
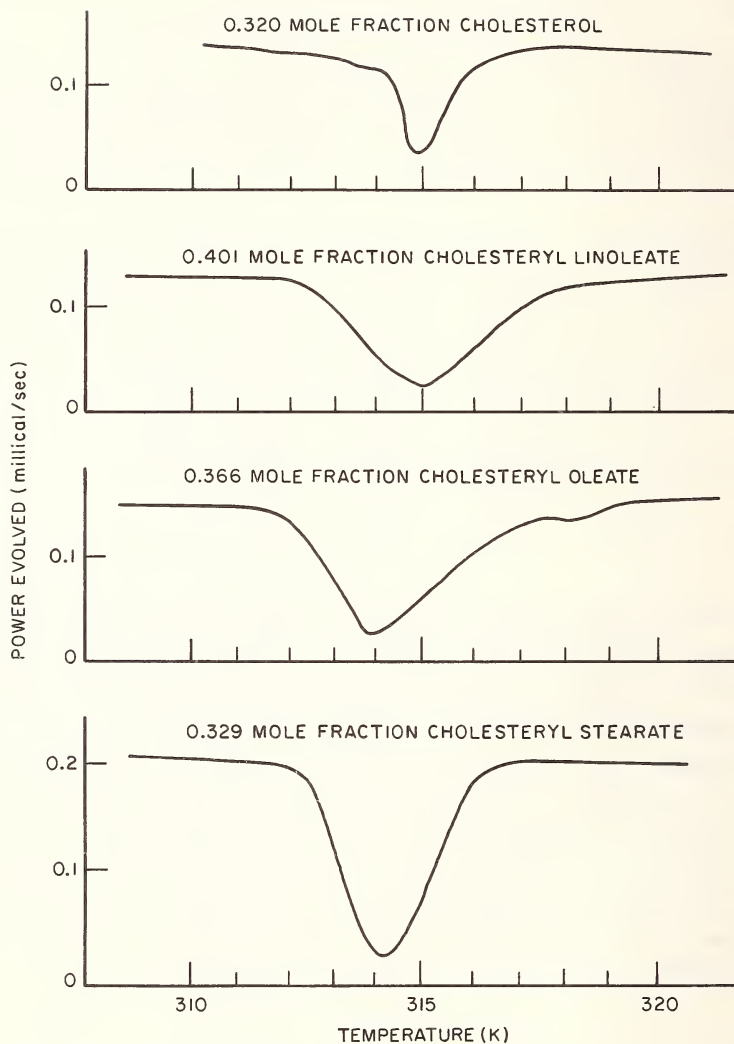
Figure 3.   DSC cooling curves of dipalmitoyl-L-α-lecithin-water
            systems containing cholesteric compounds.
            (Scaled to 1.000 mg Lecithin; Cooling Rate 2.5 °C/min)

4.   DISCUSSION OF RESULTS

A.   Significance to Membrane Formation.

When dipalmitoyl-L-α-lecithin and bovine sphingomyelin organize
structurally in water on cooling to 41 °C, heat must be removed from
the sample causing a reduction in the entropy of the system.   The
magnitude of the entropy loss is a measure of the stability of the
system, since the same amount of entropy must be returned to the
sample on heating to disrupt the organization.   As cholesterol is
added to the lecithin or sphingomyelin system, the entropy of tran-
sition is reduced until at measurements at a 1:1 cholesterol to phos-
pholipid ratio, no energy of transition is recorded by the DSC.

The above information would suggest that in the limit of a 1:1
mole ratio, a cholesterol-lecithin or cholesterol-sphingomyelin
structure is quite unstable.   However, unpublished studies by D. M.
Small [17] indicate that the 1:1 structure is stable up to 100 °C.
Organization of the phospholipid structure did not increase the over-
all stability of the system measured.   But for the cholesterol to
participate in the phospholipid structure, as described by other in-
vestigators [9,10], the crystal structure of the cholesterol must be
disrupted.   The heat absorbed by the breakdown of the crystal struc-
ture would offset the heat given off in the organization of the
water molecules and acyl groups of the phospholipid. (Water molecules
in contact with acyl chains cannot co-hydrogen bond and acyl chains
separated by water cannot join with one another by van der Waal's
forces.   At a 1:1 mole ratio of cholesterol to phospholipid, the sum
of these heat changes is zero.   This fact could indicate a rever-
sible transition between crystalline cholesterol with unorganized
phospholipid and the cholesterol-phospholipid membrane-like
structure.

In contrast to the behavior of cholesterol, cholesteryl stear-
ate has little measurable effect on the entropic change that occurs
as lecithin and sphingomyelin in water are cooled through the tran-
sition temperature.   The same heat is given off, within five percent,
whether the cholesteryl stearate is present or not.

The equilibrium temperature of 70 °C applied to all samples
causes the cholesteryl oleate and linoleate to melt. Once melt-
ed at 70 °C, the cholesteryl oleate and linoleate will not revert
to crystalline form at temperatures between 27 and 57 °C. The
cholesteryl oleate and linoleate can pass through their mesophase
transitions in the 27 to 57 °C range, but these heats are, at the
maximum mole fraction of sample present, no more than 4 to 6 per-
cent of the heat reported for their ternary transition. The
shape of the cholesteryl oleate ternary transition in Figure 2 at
46 °C does suggest the isotropic liquid to cholesteric transition
expected at this temperature from the previous data of the present
investigators. Since cholesteryl oleate and linoleate cannot be
in crystalline form at 27 to 57 °C, a change in the entropy of the
system can be directly related to the stability of the phospholipid
structure formed.

There is always present the biological possibility of phospho-
lipids (in the blood plasma) organizing to form membranes. The
sphingolipids have been reported to be major lipid constituents
of most mammalian cell membranes [18]. Sphingomyelin even when
composed of mixtures of molecules containing different acyl groups,
can organize at temperatures close to human biological environment.
It may be significant that the only sphingolipid in erythrocyte
plasma membrane in appreciable percentage is sphingomyelin [5]. In
contrast, lecithin containing unsaturated bonds may have liquid
crystalline to crystalline transitions in water many degrees below
the biological environment [19].

S_f 0-12 lipoprotein, in which lipid-lipid interaction is likely,
contains substantial quantities of cholesteryl oleate and linoleate.
A shift in the ratio of these two esters could have a significant
effect on the stability of the structure formed with phospholipids,
in particular sphingomyelin. Should the ratio of cholesteryl linol-
eate to oleate decline, structures of greater stability may form.
The saturated or monounsaturated C_{18} esters of cholesterol, would
most likely be excluded from the membrane structure owing to the
length of their acyl chain. The diunsaturated fatty esters of choles-

terol, the linoleate, could participate in the formation of the
membrane-like structure, imparting to the structure a relatively high
thermal instability. This could occur because, as has been reported
[10], the amount of unsaturation in the fatty acid is important in
determining its molecular shape. For instance, saturated and trans-
saturated fatty acids are essentially straight, but at cis double
bonds, the chain is bent. The higher the unsaturation, the more
bent a fatty acid chain can be; in arachidonic acid, the molecule
can be curved into a U [20]. The magnitude of the entropy decrease
during the organization of the sphingomyelin or dipalmitoy-1-L-α-
lecithin by esters of cholesterol is likely inversely proportional
to their ability to participate in the membrane structure and can
be expected to be, in order of decreasing effectiveness: linoleate
> oleate > stearate. Or, in other words, cholesteryl esters are
not incorporated into the lecithin structure as readily as choles-
terol, the solubilities being in the order stearate < oleate <
linoleate.

5.   SIGNIFICANCE TO ATHEROSCLEROSIS

E. B. Smith *et al.* [3] have been able to distinguish between
perifibrous lipid of the human aorta intima that thickens with
age from abnormal fat-filled cell thickening. Particularly notice-
able in comparing the chemical composition of these two types of
thickening, for the under 30, 30-40, and 40-49 age groups, is the
decrease in the percent cholesteryl linoleate and increase in the
percent cholesteryl oleate in the fat-filled membranes or cells
compared to perifibrous lipid [3]. An explanation may lie in the
potential ability of cholesteryl linoleate to inhibit the formation
of stable phospholipid structures from the plasma. The presence of
increased cholesteryl oleate could accelerate the slower natural
structure formation process in the presence of cholesteryl lino-
leate. The cholesteryl oleate, itself, could be enclosed inside
the forming structure.

E. B. Smith *et al*. [21] in a more recent technical article
describe an amorphous lipid structure in the human aorta which is
extremely high in cholesterol. It is conjectured here that this
amorphous behavior may be due to the presence of the cholesterol
causing the phospholipid to change between ordered and disordered
phospholipid structure. In this same article by E. B. Smith *et al*.
[21], has also provided a table which shows the percent distribu-
tion of the main phospholipid fractions in fatty plaques, fibrous
plaques, and amorphous lipid. The percentage of sphingomyelin in
these plaques varies from 30 to 80 percent of the total phospho-
lipid. This percentage is remarkably high, since only from 10
to 25 percent of the lipid phosphorous in plasma is in the form
of sphingomyelin [12]. It is suggested here that the reason for
this difference may lie in the ability of sphingomyelin to form
membrane structure at biological environmental temperatures.

6. ACKNOWLEDGEMENT

7. REFERENCES

[1] Smith, E. B., Lancet 1, 799 (1960).

[2] Smith, E. B., Lancet 2, 530 (1962).

[3] Smith, E. B., Evans, P. H., and Downham, M. D., J.
      Atheroscler, Res., 7, 171 (1967).

[4] Masoro, E. J., "Physiological Chemistry of Lipids in Mammals,"
      p. 179, W. B. Saunders Company, Philadelphia, Pa., 1969.

[5] Masaro, E. J., "Physiological Chemistry of Lipids in Mammals,"
      P. 276, W. B. Saunders Company, Philadelphia, Pa., 1969.

[6] Toner P. G., and Carr, K. E., "Cell Structure," p. 5, E. and S.
      Livingston, Ltd., London, England, 1968.

[7] Stein, W. E., "The Movement of Molecules Across Cell Membranes,"
      Chapter 1, Academic Press, New York, New York, 1968.

[8]   Chapman, D., Williams, R. M., and Ladbrooke, R. D., Chem.
      Phys. Lipids, 1, 445 (1967).

[9]   Ladbrooke, B. D., Williams, and Chapman, D., Biochim.
      Biophys. Acta, 150, 333 (1968).

[10] Small, D. M., Bourges, M., and Dervichian, D. C., Nature
      211, 816 (1966).

[11] Smith, E. B., Cardiovascular Res., 1, 111 (1967).

[12] Masoro, E. J., "Physiological Chemistry of Lipids in Mammals,"
      p. 161, W. B. Saunders Company, Philadelphia, Pa.. 1969.

[13] Dervichian, D. C., Progress in Biophysics and Molecular
      Biology, 14, 249 (1964).

[14] Davis, G. J., and Porter, R. S., "Thermal Transitions for
      Some Cholesteryl Esters of Saturated Aliphatic Acids,"
      to be published in Molecular Crystals and Liquid Crystals.

[15] Perkin-Elmer Corporation, Thermal Analysis Newsletter, 5,
      Norwalk, Conn.

[16] Davis, G. J., Porter, R. S., "Application of the Differential
      Scanning Calorimeter to Purity Measurements," accepted for
      publication in Journal of Thermal Analysis.

[17] Personal communication by D. M. Small.

[18] Brady, R. O., "The Metabolism of Sphingomyelin," in "Membrane
      Models and the Formation of Biological Membranes," Bolis, L.,
      and Pethica, B. A., Editors, p. 114, North Holland Publishing
      Company, 1968.

[19] Chapman, D., "Physical Studies of Biological Membranes and
      Their Constituents," in Membrane Models and the Formation
      of Formation of Biological Membranes, Bolis, L., and
      Pethica, B. A., Editors, p. 6., North Holland Publishing
      Company, 1968.

[20] Sinclair, H. M., "Lipid Pharmacology," Chapter 5, Paoletti, R.,
      Editor, Academic Press, New York, New York, 1964.

[21] Smith, E. B., Slater, R. S., and Chu, P. K., J. Atheroscler.
      Res., 8, 399 (1968).

AN ANALYTICAL EVALUATION OF DIFFERENTIAL
SCANNING CALORIMETRY (DSC)

Joseph H. Flynn

Institute for Materials Research
National Bureau of Standards
Washington, D. C. 20234

Three instrumental time constants were found in
an analysis of the (Perkin-Elmer DSC-1B) Differential
Scanning Calorimeter: an energy pulse response (1.5 s),
a temperature-averaging network response ($\sim$15 s) and a
temperature programming response (8.0 s). The first con-
stant may be determined from the decay of the response to
infrared light pulses. It affects the shape of a transi-
tion curve but not the heat of transition calculated from
the area. The second constant affects only the base line
and the third, the temperature calibration.

Application of elementary heat flow theory to a wide
range of experimental variations in the interfacial ther-
mal resistance demonstrated that interfacial time constants
are a negligible factor in determining the melting transi-
tions of many substances.

It was concluded that corrections for the various
instrumental and thermal time constants are necessary
if meaningful parameters are to be deduced, especially
at fast heating rates.

Key words: analyses of thermal apparatus; differential
scanning calorimetry; evaluation of heats and tempera-
tures of transition; instrumental time constants; inter-
facial thermal conductivity; thermal analyses.

I. INTRODUCTION

Differential Scanning Calorimetry (DSC) is a technique from
which a large quantity of experimental data on heat capacities,
heats and temperatures of transitions, reaction kinetics, *etc*., may
be obtained with an extremely small amount of effort. Therefore,

there exists a great need to assess critically the quality of the constantly growing mass of data resulting from its exploitation.

This paper summarizes some of the experimental and theoretical work in progress on the evaluation of the differential scanning calorimetry technique. The results reported here apply specifically to the Perkin-Elmer Differential Scanning Calorimetry, (DSC-1B).

The instrument is described in literature [1,2] so only a brief summary is given here. Nearly identical copper sample and reference holder cups contain heaters and platinum resistance thermometers. These holders are maintained, even at constant rates of temperature change, close to the same temperature by a temperature averaging network. The difference in power supplied to the two cups, one empty and one containing a sample, is a direct measure of the change in enthalpy of the sample as a function of time. This net enthalpy flow rate and the average temperature of the two cups are read out on a recorder.

The train by which a net thermal flux is transported from the sample and translated into a recorder readout can be divided into three sections:

1.   Instrument: the instrumental response between the surface of the sample holder and the recorder readout includes both the thermal lags between the heater, sensor and surface, and the electronic time constants of the instrument.

2.   Interface: this is the region between the surface of the sample and the surface of the sample holder. It includes heat flow through any sample container.

3.   Sample: this region is defined by the sample geometry.

The character of the energy flux may be influenced and modified in each of these regions, and, under separate conditions, any one region may be the slow, rate determining step of the sequence.

2. INSTRUMENTAL TIME CONSTANTS

It is logical to start with the instrument itself. The re-
corder response may be a limiting factor during sharp delta-func-
tion-like heat pulses which occur during some transitions such as
the fusion of a supercooled liquid. An approximate time constant is
often supplied with the recorder. The Leeds and Northrup "Speedo-
max W" used in most of these experiments had a zero order response
time of a tenth of a second per inch.

A. Energy Pulse Response

An inspection of the wiring schematic for the energy readout
indicates a time constant for energy response of about one and one
half seconds. Since the holder assembly cover has a transparent
window, this constant can be measured quite simply and unambiguously.

Rectangular energy pulses of varied amplitude and duration were
produced by shining a beam of infrared light from a heat lamp through
the transparent window onto either the sample or the reference holder
cup. Three typical readouts for pulses of 1.92, 7.92 and 15.32
seconds are shown in Figure 1.

Both the build-up curves and the decay curves were super-
imposible. Their shape and amplitude were independent of tempera-
ture and rate of heating. The build-up and decay curves closely
followed first order kinetics after an initial transitory period,
and from them were obtained time constants of the order of one and
one half seconds.

The energy pulse time constants for two instruments and three
holder assemblies are given in Table 1.

The values vary slightly for each of the three sample holders
and one reference holder. In several of the cases there is a
several tenths of a second difference between the calculated time
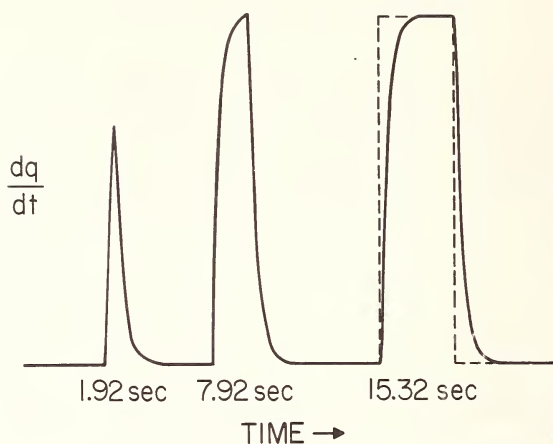constants in the endothermic and exothermic directions.

Figure 1.   Recorder response to infrared energy pulses.
Chart speed: 0.0667 in/s $\frac{dq}{dt}$ (maximum): 0.0064
cal/s (dashed line represents rectangular
energy pulse).

Table 1.   Time constants for instrumental response.

TIME CONSTANTS (seconds)

DSC	Holder assembly	Recorder (x inches)	Zero[a] knob	Energy[a] pulse	Temp. ave.	Speed selector
A	1	0.1	0.63; 1.12	1.15; 1.65 1.47; 1.55[b]	14.9	8.0
A	2	0.1	–	1.58; 1.72	18.7	–
B	3	0.1	–	1.55; 1.71	9.3	–

[a]Average values for "endo and "exothermic" directions.
[b]These two values are for reference holder; all others
are for sample holders.

If the rectangular energy pulses build up and decay according to first order kinetics over the entire time interval with time constants in the endothermic and exothermic directions, τ_{endo} and τ_{exo}, respectively, the fractional error, ε, in the area of the dq/dt *vs* t curve is

$$\varepsilon = \frac{x(\tau_{endo} - \tau_{exo})}{t} \tag{1}$$

where x is the fraction of the steady state value of the energy flux attained and t is the duration of the pulse. Since the enthalpy is calculated from the area, $\int \frac{dq}{dt} dt$, this difference in time constants could result in large errors when the pulses are of short duration.

However, in Figure 2, the integrated areas in arbitrary units are plotted against the time of the light pulse at constant intensity. The least squares straight line is for times of one and one half through twenty seconds, and is given by

$$AREA = 0.003075 \, t - 0.000027 + \varepsilon' \tag{2}$$

$$(t \leq 20 \text{ s})$$

where ε' represents a random experimental error with a calculated standard deviation of 3.4×10^{-4}.

The calculated standard deviations of the slope and intercept in equation (2) are respectively, 1.44×10^{-5} and 1.25×10^{-4}. The concurrence of the intercept with the origin is well within its calculated uncertainty, indicating that the time constant difference must be compensated for during the transitory period before first order decay becomes operative. Thus it appears that, when the course of the base-line can be accurately deduced, quite accurate relative enthalpy values are attainable with this instrument.
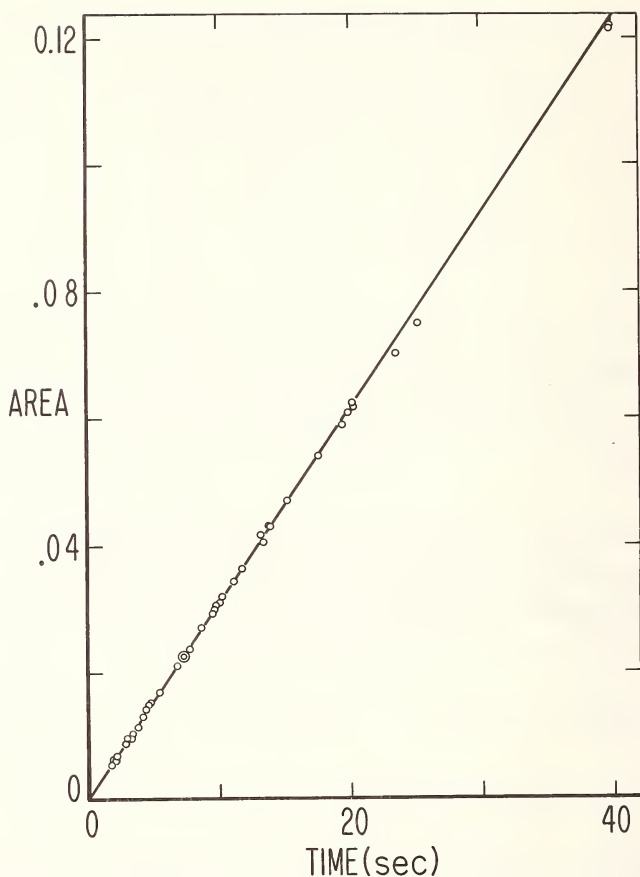
Figure 2. Area *vs*. time of infrared light pulse.
          (Solid line is least squares fit for 0 >
          t > 20 s.)

B. Temperature Averaging Network Response

The detailed energy balancing between the sample and reference holders is upset during a change in the rate of heating or cooling and a deflection of the baseline occurs. This deflection varies both in its initial amplitude and in its rate of recovery, as may be seen in the next to last column of Table 1, for the different instru-

ments and holder assemblies. For one instrument, the effect appeared
to have a somewhat damped harmonic nature.

For instrument 1, holder assembly A, the decay was kinetically
slightly greater than first order and gave an average first order
time constant of 15 seconds. The initial amplitude of the displace-
ment, X_o, obtained from the extrapolation of the first order rate
equation back to the time of the heating rate change, was found to be
related to the change in heating rate, $\Delta\beta$ (K/s) by the equation*

$$X_o = 1.67 \times 10^{-3} \ \Delta\beta \ (cal/K) \qquad\qquad (3)**$$

A relationship, such as equation (3) may be determined for each
instrument. This slow baseline decay may then be corrected for.

This temperature averaging time constant appears to be com-
pletely independent of the small exothermic and endothermic energy
pulses which occur when a sample undergoes a transition. Several
examples are shown in Figure 3.

The lower curve is a readout for empty holders for which the
temperature was changed from 320 to 380 K by rapid manual operation
of the temperature control knob. During the decay, infrared light
pulses were alternately shone on the sample and reference holders.

The upper left curve in Figure 3 shows the fusion of Wood's
Metal which was suddenly supercooled to 323 K and held isothermally
at that temperature. The upper right curve is again for Wood's
Metal which was heated quickly to 337 K and then scanned at 2.5
K/min through its melting point.

In each of these three cases the independence of the energy
response from the baseline decay is obvious.

---

* K = degrees Kelvin
** 1 cal = 4.1840 j.
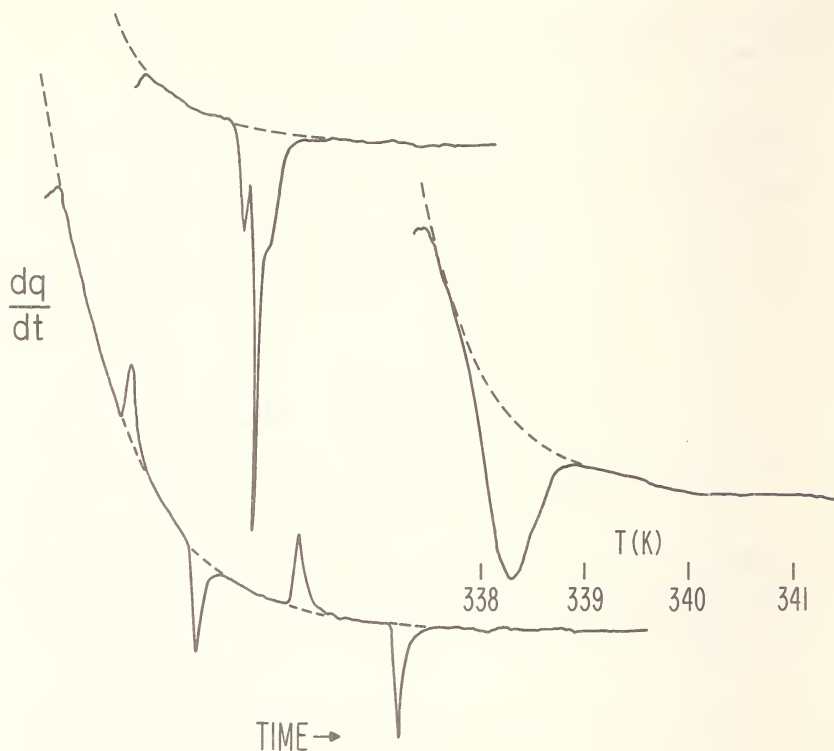
Figure 3. Three rate of enthalpy change *vs.* time curves
           illustrating the independence of "energy pulse"
           and "temperature averaging" time constants.
           ——————— recorder readout; ---------- unperturbed
           "temperature averaging" decay.

           A. Empty holders; T = 320-380 K, then
               isothermal at 380 K, infrared pulses, x 1.
           B. Fusion of Wood's Metal (in reference holder)
               supercooled to 323 K, x 1/4.
           C. Melting of Wood's Metal, heated quickly to
               337 K and scanned at β = 2.5 K/min, x 1/4.

A correction for the temperature-averaging lag should be applied to the baseline whenever the heating rate has been changed within about two minutes before the temperature range of interest is reached.

The scan speed selector time constant will be discussed later.

An instantaneous change of the "zero knob" includes only part of the readout circuit, so its response time, indicated in the fourth column on Table 1., is somewhat smaller than that for an energy pulse.

3. "INTERFACIAL" EFFECTS

For the problem involving the transport of thermal energy from or to the sample to or from the surface of the copper sample holder, some sort of assumption for a mechanism of heat flow is needed in order to compare parameters under diverse conditions.

The simplest case, utilized by Gray [3] and others, is to assume that the sample and sample holder have much higher thermal conductivities than the interfacial regions so that the temperature gradient is confined to the latter region and that, due to the small ratio of sample mass to holder mass, the holder is unperturbed by thermal effects taking place in the sample.

A number of model cases are assumed. These are illustrated in Figures 4 and 5. The curves on the left are idealized plots of temperature *vs*. time at constant heating rate where T_2 is the holder temperature, T_1, the sample temperature, T_m, the melting temperature and T_f the fusion temperature; the right-hand curves represent the resultant enthalpy flow assuming Newton's Law of Cooling.

In the first set of graphs in Figure 4, a temperature gradient is set up by heating at a constant rate starting at temperature T_A and stopping at temperature T_B. $\frac{dq}{dt}$ will approach a constant value until T_B at which point it will decay to the baseline. If, as in

Figure 4.   Idealized temperature $vs.$ time and $\frac{dq}{dt}$ $vs.$ time curves.

T_1 = sample temperature
T_2 = holder temperature
T_A,T_B = isothermal temperatures
T_m = melting temperature
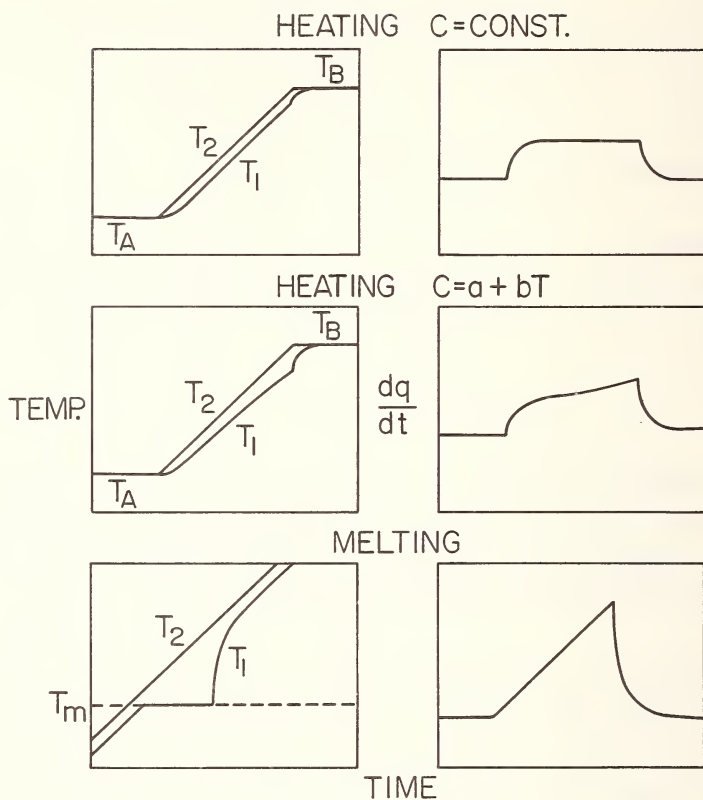β = constant
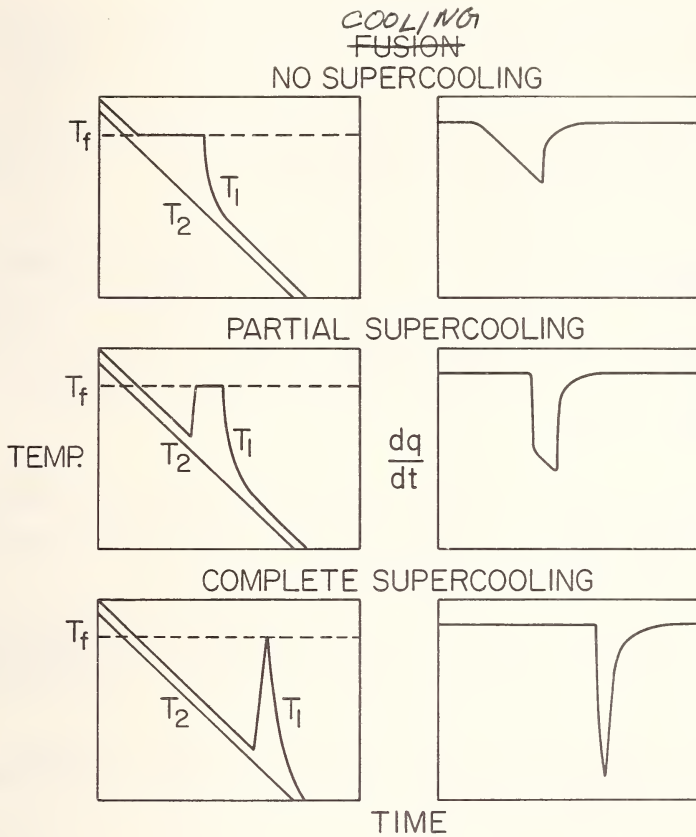c = heat capacity

Figure 5.   Idealized temperature *vs.* time and $\frac{dq}{dt}$ *vs.* time curves.
T_1 = sample temperature
T_2 = holder temperature
T_f = fusion temperature
β = constant

the second set of graphs, the heat capacity is a function of tempera-
ture, the steady value of $\frac{dq}{dt}$ will not be parallel to the baseline.

If a melting transition takes place (lower set, Figure 4), the
temperature of the sample remains constant and a steady rise in $\frac{dq}{dt}$
is approached until the melting is complete.

The first set of graphs in Figure 5 illustrate the inverse sit-
uation for ~~fusion~~. CRYSTALLIZATION If partial or complete supercooling takes place,
as in the middle and lower sets of Figure 5, there will be a sudden
jump in $\frac{dq}{dt}$, followed by the usual decay. In each of the above cases,
the decay back to the baseline will depend upon an "interfacial con-
ductivity" time constant.

All of these idealized curves approximately duplicate curves
obtained with the differential scanning calorimeter for the heating
and cooling of pure elements and compounds.

An actual melting curve for 99.99 percent Indium, encapsulated
in an aluminum sample pan with molten Wood's Metal at the aluminum-
copper interface, is shown in Figure 6.

The three critical parameters with which we concern ourselves
are shown in this figure. They are:
    1. The steady slope of a transition curve caused by a linearly
increasing temperature increment and proportional to an interfacial
conductivity term.
    2. An onset temperature of the transition, T_i, obtained from
the intersection of this slope with the baseline.
    3. A decay constant, k_i, back to the baseline at the completion
of the transition.

Some simple relationships for these three parameters may be de-
rived from the following four equations.
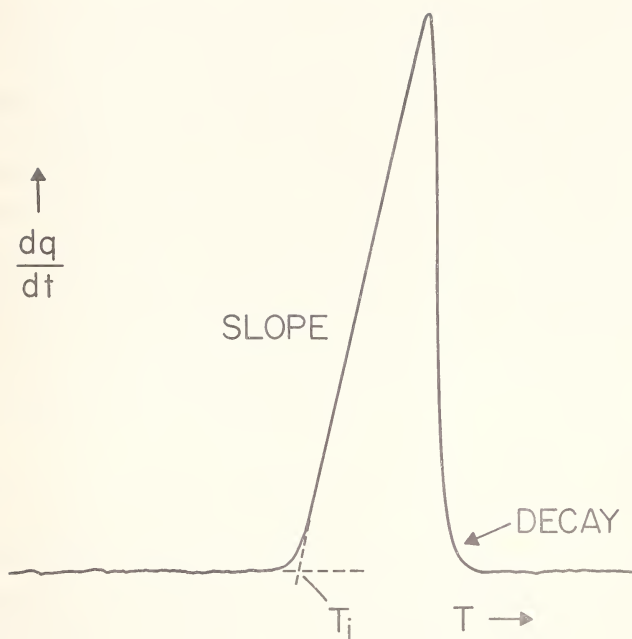
Figure 6.   Melting of 99.99 indium (molten Wood's Metal interface).
            Rate of Enthalpy Change vs. Temperature (Time).

$$\frac{dq}{dt} = Ah \ (T_2 - T_1) \tag{4}$$

$$T_2 = T_o + \beta t \tag{5}$$

$$T_1 = T_o + \frac{1}{mc} \int \frac{dq}{dt} \ dt, \tag{6}$$

$$= T_i \ (\text{during transition})$$

$$c = \text{constant} \quad \text{or} \quad c = a + bt \tag{7}$$

Equation 4, "Newton's Law of Cooling," states that the heat flow across the interface is equal to the interfacial thermal conductivity, h, multiplied by the area of the interface, A, and the temperature difference between the sample and the holder. At constant heating rate, β, the temperature of the holder, T_2, will increase, from an initial value, T_o, linearly with time eq. (5). The temperature of the sample, T_1, will depend on the rate of heat flow into it, where m is the mass of the sample and c, its heat capacity per gram, eq. (6). At a transition, T_1 will remain at the transition temperature, T_i, for a residence time, t_i, determined from

$$\int_{t}^{t+t_i} \frac{dq}{dt}\, dt = m\Delta H_i \qquad (8)$$

where ΔH_i is the heat of transition in cal/g. The heat capacity in equation (7) is assumed to be either constant or linearly increasing with time at constant heating rate. (During a transition, particularly a phase transition, h, A, and c may change considerably. This will not be taken into account in this elementary treatment.)

Solving equations (4)-(7) for constant heat capacity, the steady slope during a melting transition, the onset temperature and the decay constant at the termination of the transition are given by

$$\text{Slope} = \beta h A = k_m \beta c m \qquad (9)$$

$$T_i = T_m + \frac{\beta c m}{hA} = T_m + \frac{\beta}{k_m} \qquad (10)$$

$$\text{decay constant} = \frac{hA}{cm} = k_m \qquad (11)$$

where $\frac{1}{k_m} = \tau_m$, the time constant for the interfacial region.

The effect of a linear heat capacity increase with time considerably complicates the solutions of the equations for the three parameters. However, in steady regions, it has the effect of introducing a factor of $(1 + \frac{m\ b}{h\ A})^{-1}$ where b is the time coefficient in equation (7). mb has a value of $\sim 2 \times 10^{-7}$ cal/s K for 20 mg of indium heated at $\beta = 10$ K/min (4). From the steady slope of the melting transition of indium values of h A range from 3 to 14×10^{-3} cal/s K, depending upon interfacial conditions. It appears for this case, the correction term is quite insignificant. This applies only to the absence of transitions, such as during heat capacity determinations. During a phase transition, the heat capacity may change quite markedly with time which will introduce much larger correction terms into equations (9), (10) and (11).

Values for h A, obtained from the steady slopes of indium melting transition curves also may be used to calculate the time constant for interfacial thermal resistance at the melting point from equation (11). Thus, if c = 0.062 cal/g K at 429 K (4) and m = 0.02 g; $\tau_m = 1/k_m = \frac{c\ m}{h\ A} = 0.09$ to 0.4 s for indium for a wide variety of interfacial conditions.

These interfacial decay time constants are considerably smaller than the 1.5 s instrumental decay time constant. Under ordinary conditions, *viz.*, a sample encapsulated in a flat-bottomed aluminum cup in good contact with the copper sample holder--the perturbing effect of the interfacial resistance upon the return to the baseline following a rapid transition is negligible and the decay constant will be ~ 1.5 seconds. If the surface contact is poor, the decay time constant will increase; however, this requires rather drastic tampering with the interfacial region.

Equation (10) indicates that the heating rate, β, approaches zero, the onset temperature, T_i approaches the true melting temperature, T_m. Rearranging equation (10),

$$1/\tau_m = \frac{hA}{cm} = \frac{\beta}{T_i - T_m} = \frac{\beta}{T_i - T_{i,o}} \qquad (10')$$

where $T_{i,o}$ is the onset temperature extrapolated to $\beta = 0$. Thus the ratio of onset temperature difference to heating rate will give a "temperature lag" time constant.

Figure 7 is a plot of heating rate *vs*. onset temperature change for the fusion of indium. Curve B is a composite curve for indium metal encapsulated in aluminum sample pans. The time constant calculated from its slope is 8.0 seconds. This value is much too large to be accounted for by the interfacial time constant, whose values, determined from the slopes of the transition curves, vary over the range -- $0.09 < \tau < 0.4$ seconds. This conclusion is borne out by the other curves in Figure 7 whose time constants calculated from their slope are not greatly different from curve B even though there has
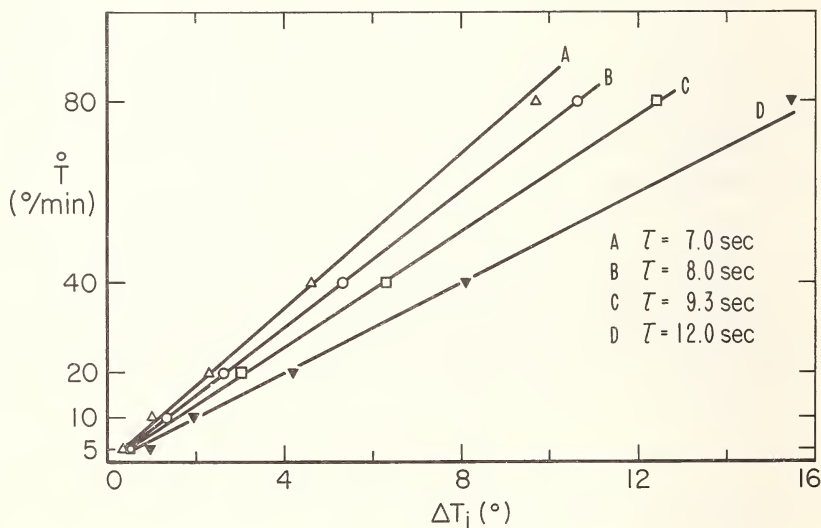

Figure 7.   Scanning rate *vs*. fusion onset temperature increment (Eq. 10').

    A.   Bare Wood's Metal, $\tau = 7.0$ s
    B.   Indium in aluminum (average of 15 determinations)
                              $\tau = 8.0$ s
    C.   Indium (2 shims) $\tau = 9.3$ s
    D.   Indium (3 shims) $\tau = 12.0$ s

been a drastic alteration of the interfaces. Curve A, for the fu-
sion of Wood's Metal resting directly upon the copper holder, yielded
a time constant of 7.0 seconds. Curve C for the fusion of encapsu-
lated indium with two aluminum sample pan covers between the pan and
the sample holder (*i.e.*, three interfaces) had a time constant of
9.3 seconds. Three aluminum sample pan covers (four interfaces) in-
creased the constant to 12.0 seconds. More importantly, a large num-
ber of similar curves for melting transition of metals, organics, and
inorganics in aluminum sample pans closely coincided with curve B for
indium. Thus an ∿ 0.15 second interfacial time constant has only a
slight effect on the temperature calibration, *e.g.*, it would bring
about an onset temperature shift of ∿ 0.2 K at β = 80 K/min.

It also appears from the coincidence of these curves that the
physical state and thermal resistivity of the samples, themselves,
do not affect greatly the temperature calibration curve.

The source of the 8 seconds time constant which overwhelms inter-
facial and material effects can be found from an inspection of the
scan-speed-selector circuit. Calculations indicate that there should
be a time constant of about 4 seconds for heating rates of 0.625 and
1.25 K/min, and about 8 seconds at 2.5, 5.0, 10.0, 20.0, 40.0 and
80.0 K/min. This is the third instrumental time constant, given in
the last column of the table. It reflects the average temperature
lag behind the temperature readout. The readout works directly from
temperature control knob.

4. EFFECT OF SAMPLE

The effects of the thermal resistance and physical state of the
sample upon the flow of heat to and from it -- especially the coup-
ling of heat transport to the process of autogeneration or dissipa-
tion of heat and the rigorous application of realistic boundary condi-
tions -- defy any simple mathematical approach [5].

It appears, however, from the results discussed in concurrence
with Figure 7 that, so far as the temperature calibration is con-

cerned, they can be relatively unimportant. Several experiments de-
signed to test the order of magnitude of these effects, involving
sandwiches and laminates of varied thickness, are being conducted
at present.

5.   CONCLUSIONS

The present state of experimental progress permits the reaching
of several tentative general conclusions concerning the reliability
of differential scanning calorimetry.

DSC can determine heats of transition within 1 percent accuracy
when the baseline is unambiguous.

The transport of heat through the sample and the interfacial
regions is not a limiting factor in the measurement of transition
temperatures for many materials.

Corrections for the several instrumental time constants must be
incorporated if temperatures of transition or kinetic parameters are
to be determined, particularly at fast scan rates.

6.   ACKNOWLEDGMENT

The author thanks Dr. Charles M. Guttman and Dr. Shu-Sing Chang
for their advice and suggestions on many phases of this work.

7.   REFERENCES

[1]   Watson, E. S., O"Neill, M. J., Justin, J., and Brenner, N.,
        Anal. Chem. $\underline{36}$, 1233 (1964).
[2]   O'Neill, M. J., Anal. Chem. $\underline{36}$, 1238 (1964).
[3]   A. P. Gray, "Analytical Chemistry", Porter, R. S., and Johnson,
        J. F., Eds., p. 209, Plenum Press, New York (1968).
[4]   K. K. Kelly, "Contributions to the Data on Theoretical Metal-
        lurgy," XIII U. S. Bureau of Mines Bulletin 584, p. 90, 1960.
[5]   Lukaszewski, G. M., Laboratory Practice $\underline{14}$, 1277 (1965);
        $\underline{15}$, 861 (1966).

APPARATUS FOR RATE STUDIES
OF VAPOR PRODUCING REACTIONS

R. J. McCarter[*]

*Office of Flammable Fabrics
Institute for Applied Technology
National Bureau of Standards
Washington, D. C. 20234*

An apparatus was developed for measuring the rate
at which vapors are evolved during the thermal degrad-
ation of materials and thereby deriving the kinetics
of such reactions. Requisite to the operating scheme
of the apparatus is the provision of a high-temperature
zone to convert condensable or tarry vapors into non-
condensable form.

The apparatus yields a direct measure of reaction
velocity, rather than the integrated indication obtained
with thermogravimetric analysis. This simplifies the
identification and calculation of kinetic parameters.
Increases in sensitivity and operating range are also
achieved. Flexibility in operation is obtained that
permits the separate recording of reactions that tend
to overlap.

Although the apparatus has been operated princi-
pally with a combustible gas indicator serving to meter
the evolved product vapors, a number of options are
available for the latter function, including flow meters
and various continuous gas analyzers. The applicability
of the method appears promising.

Key words: differential thermal analysis; DTA; kinetics;
pyrolysis; TGA; thermal analysis; thermal degradation;
thermogravimetric analysis

INTRODUCTION

Numerous limitations are encountered in the application of conventional thermal analytical methods to the investigation of the pyrolysis and combustion behavior of materials. In the use of thermogravimetric analysis (TGA), various factors tend to degrade the accuracy of recordings [1], particularly with samples of low thermal conductivity and as heating rates are increased above 10 to 20 °C/min toward those encountered in the combustion of materials. Differential thermal analysis (DTA) involves compromises in signal quality arising from the conflicting needs that must be met in design of the equipment [2]. Combining or combined TGA and DTA measurements involve further problems. Even under favorable circumstances, as when dealing with a single well-defined reaction, results from these methods are often restricted in scope and certainty by unavoidable extraneous experimental effects. When samples undergo more than one reaction proceeding in proximity on the temperature scale, the complications multiply. A clear interpretation of TGA results can then become impossibly difficult or inordinately laborious. Such limitations arise in part from the isothermal or linear-temperature rise operation that is conventional to or required by the methods. The same appears to apply to other related systems that have been reported [3-10].

The system of this report functions on a different and less restricted basis. It is designed to derive the kinetics of pyrolysis reactions from measurements of the rate of vapor evolution, rather than from weight recordings of solids. The reaction velocity is recorded directly, and does not require computation from its integrated record as in TGA. The labor, complications, inaccuracies and obfuscations of the latter step are thus avoided. Additionally and importantly, the restrictions imposed on programming of the reaction temperature are avoided. Thus the reaction temperature may be freely and usefully manipulated and be directed through any course desired within the operating limits of the apparatus.

The apparatus includes an innovation found necessary to permit general use of the system. The innovation consists of the insertion into the flow scheme of a high temperature zone. This is added to avoid the deposition of tarry products on equipment surfaces by thermally reducing such products to volatile form.

The benefits of simultaneous DTA may be obtained with the apparatus when it is appropriately operated.

PRINCIPLES OF OPERATION

The operating scheme of the apparatus is indicated in Figure 1. A flow of inert carrier gas is passed over the sample material, centered within the tube furnace. The furnace is designed to afford a slight positive gradient in temperature toward its exit end. A single fine-wire thermocouple imbedded or immersed in the sample material serves for measurement of the pyrolysis temperature. As volatiles are evolved from the sample with increasing temperature, they are carried to the "cracking" coil to be subjected to thermal decomposition and the reduction of "tars" to non-condensables. The flow is then conducted to any suitable recording instrument that will serve to continuously meter the mass flow rate of the pyrolyzed vapors or a representative portion or a component thereof. Meters that have been used, other than the combustible gas indicator* diagramed in Figure 1, include:

1. Linear mass flowmeter
2. Thermal conductivity cells, composition and flow sensitive types**.
3. Thermopile-type CO analyzer
4. Infrared analyzers-H_2O, CO, and CO_2 types

---

* A portable instrument sometimes termed a "sniffer", used by utilities and industry for the detection of flammable or explosive vapors.
** It appears possible that other gas chromatograph devices, such as electron capture and hydrogen flame detectors, could be useful with a smaller-scale apparatus (such is exemplified in part by the apparatus described in ref [9] and [10]) or with appropriate splitting of a side-stream. Possibilities appear numerous for the use of meters in the system in parallel or sequential combinations.
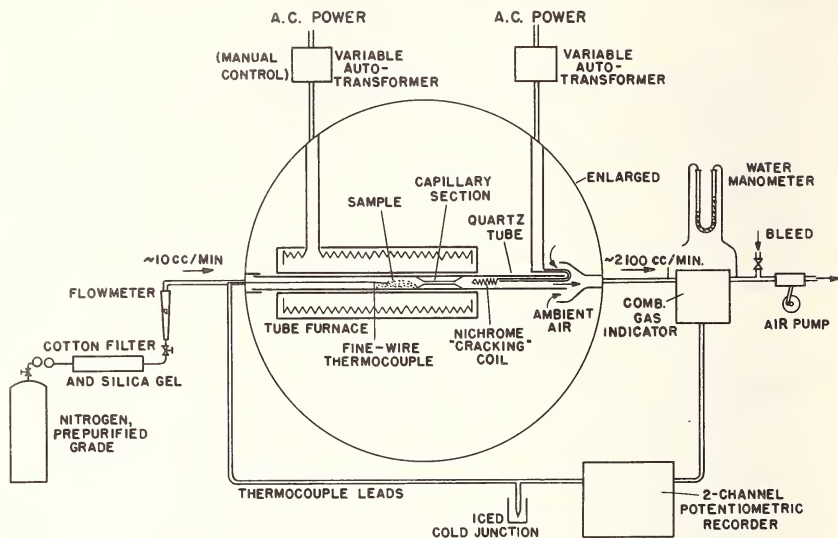
Figure 1. Schematic diagram of apparatus.

The combustible gas indicator, because of its superior response rate, has received the greater use and will be detailed. With use of this meter, the flow from the tube furnace, Figure 1, is diluted into a considerably larger flow of ambient air being drawn through the meter. This dilution is normally over a hundred-fold in volume. Therefore, the carrier gas and inert pyrolysis products are seldom of consequence to the meter response. The combustible gas indicator [10] employs a hot platinum filament within a bridge circuit. As oxygen and combustibles of the throughput gases contact the platinum filament, they are catalyzed to react on the platinum surface. The heat from this surface oxidation reaction increases the temperature and the resistance of the filament. This causes an imbalance in the bridge circuit and a consequent proportionate increase in the output potential of the meter.

In measuring the kinetics of decomposition reactions, the linearity of the meter response to concentrations of evolved vapors is

of prime concern. In this system, as a pyrolyzing compound evolves
combustible vapors, the response of the meter would be proportional
to reaction velocity insofar as:

    1. The transit time of the evolved vapors to and through the
filament cell of the combustible gas indicator is appropriately
brief.

    2. Absorption and desorption of product vapors in the conduit
tubes is not of significant magnitude.

    3. Oxidation of product vapors or secondary reactions of dis-
proportioning effect do not occur in transit.

    4. The decomposition performed by the "cracking" coil is uni-
form and does not introduce disproportioning effects in the product
vapors in regard to meter response.

    5. The response of the meter is linear to the concentration of
combustibles in the filament cell.

    6. The recorder registers linearly to its input.

The temperature record would represent the reaction temperature
insofar as thermocouple registry is accurate and temperature grad-
ients within the sample are minor. Tests and a variety of operating
results indicate that these criteria have been met.

It was also found in operating the system that when the furnace
temperature was uniformly increased, departures of the sample tem-
perature from a corresponding increase could be clearly detected and
serve to indicate reaction exotherms and endotherms.

DERIVATIONS

For typical simple reactions, the calculation of kinetic param-
eters from the recordings is straightforward. For example, the meter
recording for a single first-order reaction with a linear reaction
temperature increase would be of the nature indicated in Figure 2.
The total gas-evolving reaction is represented by the area under the
meter curve. At temperature T (K) where the meter output is V (mv),
the curve area to the right of the V ordinate, F (mv sec), repre-
sents the proportion of the sample material that has not yet decom-
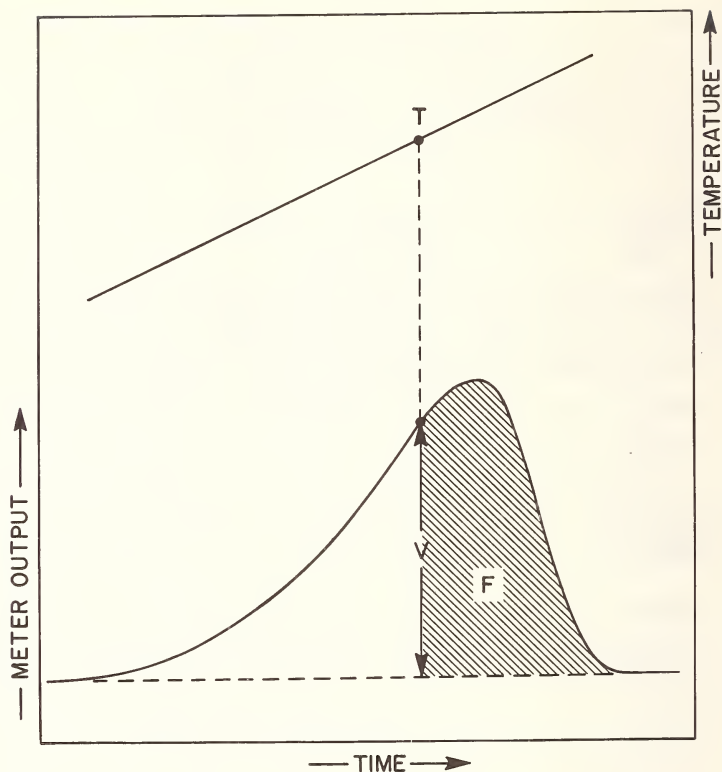
Figure 2. Simple reaction curve.

posed, and the specific reaction rate, k (sec^{-1}), is equal to V/F.
Any convenient selection of points along the curve can then be used
to assess compliance to an Arrhenius equation by plotting ln k *vs.*
1/T. The goodness of fit to this equation, particularly for reac-
tions conducted over a varied and irregular temperature history, is
taken to validate the derived reaction constants, *e.g.* Figure 5.

DETAILS OF APPARATUS

The apparatus is diagrammed in Figure 1. The nitrogen
(Matheson prepurified grade), was passed through silica gel and a
cotton filter before entry to the flow meter (Fischer and Porter

Minirator or Brooks Type 1355), at a rate generally of about 10
cc/min. Helium was found to be less satisfactory as a carrier
gas in use with the combustible gas indicator because it caused
excessive base-line drift in this meter. Flow through the com-
bustible gas indicator (Johnson-Williams Model G or Model SS-P)
was maintained at 2.1 liter/min by bleed valve adjustment before
the air pump (Model 2 Neptune diaphragm-type). Recordings were
taken with a two-channel potentiometric recorder (Moseley Model
7100B or Honeywell Electronik 194).

    Chromel-alumel thermocouple leads of 28 B&S gage wire were
used, with a 2 cm extension of 40 B&S gage wire to the hot junc-
tion. The "cracking" coil, maintained at "orange" heat in use,
was a 3.5 mm o.d., 3 cm long helix of 24 B&S gage nichrome wire
of about 2 ohms resistance (cold) with a ceramic inner core.
Various tube furnaces have been used. One furnace was 20 cm long,
constructed with a 7.5 mm i.d. copper tube bore which was wound
with about 160 cm of asbestos-covered nichrome wire, with closer
windings toward the tube ends to compensate for end heat losses,
and enclosed with ceramic fiber insulation and a 3.2 cm D. chrome-
plated brass cover. Another furnace, without insulation and heat-
ed by a radiant source within a reflective shell, had less thermal
inertia. This version was less stable in operation but permitted
faster changes in temperature.

    Tests of the apparatus' response rates have included:
    1. Imposition of a full-scale square-wave input to the com-
bustible gas indicator by connecting and disconnecting a premixed
gas sample to the inlet, to which the meter indicated a 70 percent
response in 2 seconds.
    2. Measurements indicating a vapor transit time from sample
to meter of 1 second.
    3. A perturbation in power to the radiant-type tube furnace
was observed to effect a change in both the sample temperature and
the meter recordings in less than 3 seconds.

    The system's responsiveness and linearity is also indicated by

the degree of correlation obtained in kinetic parameters, *e.g.*
Figure 5. Temperature gradients within sample material are mini-
mized by the convective heat transfer supplied by the inert carrier
gas, and by adjustments in sample size and geometry when required.

PROCEDURES

Samples are weighed and loaded into a standard quartz tube for
insertion into the furnace, Figure 1. A small plug of glass wool
inserted ahead of the capillary section of the tube can be used to
help in the loading and retention of pulverized or powdered samples.
Circuitry and flows are activated and run until base lines are stabi-
lized and air is flushed from the upstream section. The cracking
coil is then activated and, a minute or two later, power to the tube
furnace is switched on and manually advanced. Predetermined voltage-
time schedules are used when uniform advances in furnace temperature
are desired. Such a schedule can be useful in initial or explora-
tory pyrolysis runs. Meter outputs resulting from reactions then
appear in a standard recognizable form, and departures of the sample
temperature from the furnace temperature are apparent, indicating
reaction heat effects. At completion of pyrolysis, the quartz tube
is removed and cooled, and the sample residue weighed.

Sample size requirements vary inversely to the pyrolysis rates
to be used. Samples of 10 to 20 mg weight have yielded adequate
meter outputs at heating rates in the order of 1 °C/sec. Samples
up to 200 mg weight have been used with lower heating rates.
Samples in pulverized, sheet, fabric, and chunk forms have been
used, with the difference in form not of apparent consequence to
the results (*e.g.* a 20 mg block of wood yielded essentially the
same meter recording as 20 mg of sawdust of the same sample.)

Liquid samples and samples of materials that melt before pyrol-
ysis have been pyrolyzed in the apparatus using quartz or metal
boats for sample support. Some materials of this type indicated
excessive wetting or "creep" tendencies. Dispersion of such samples
in a plug of glass wool has served in some cases to provide suffic-
ient wettable surface to contain the material.

EXPERIMENTAL EXAMPLES

To obtain a direct comparison of the system's performance to
that of thermogravimetry, some well-characterized polymers were
pyrolyzed in the apparatus. The meter recordings for these mate-
rials and the respective Arrhenius plots are diagrammed, Figure 3.
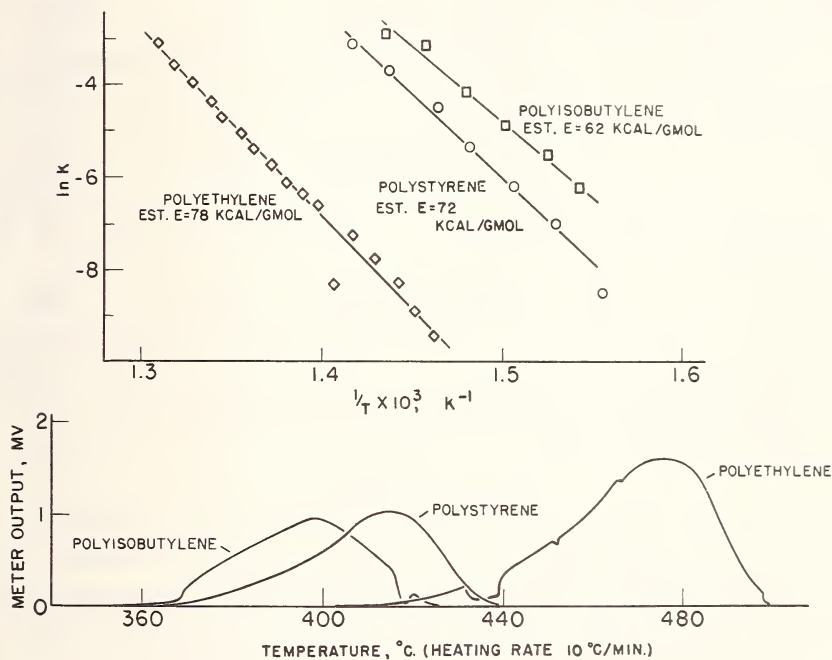
Figure 3.   Pyrolysis recordings and Arrhenius plots of data
            for polymer samples.

The derived reaction parameters are compared in Table 1 to those
obtained [12] with thermogravimetry. The values for activation
energies and the temperature datum points are judged to be within
the limits of experimental error for the respective thermogravi-
metric results.

A more informative comparison is afforded by the recordings
for the pyrolysis of a cellulosic material, Figure 4. Thermograv-

Table 1.   Comparison of results from thermal methods.

Material	Estimate of	Combustible gas indicator[a]	DuPont 950 Thermograv. Analyzer[a,b]
		Thermal Method	
polyisobutylene (Enjay Chemicals L80-B)	E, kcal/mol	62	62
	temp, °C,@20% reacted	381	375
	°C,@50% reacted	394	400
polystyrene (Styron 66)	E, kcal/mol	72	75
	temp, °C,@20% reacted	398	390
	°C,@50% reacted	411	408
polyethylene (Marlex 6002)	E, kcal/mol	78	71
	temp, °C,@20% reacted	453	445
	°C,@50% reacted	468	460

[a] With heating rate of 10 °C/min.
[b] Activation energies, E, estimated by Broido method [13].
 averaged from 3 or 4 runs.

imetric analysis had not been helpful in defining the pyrolytic
reactions of this material. The thermogram for this material was
judged undecipherable, as was its first derivative, recording A
of Figure 4. However, the comparable output curve of the combus-
tible gas indicator, recording C of Figure 4, clearly indicated the
curve form of Figure 2 for the principal decomposition. The record-
ing was found on calculation to conform closely to first order reac-
tion kinetics, with an apparent activation energy of 40 1/2 kcal/mol,
after subtraction of the minor tail area of the curve as represent-
ing a secondary decomposition.

    The differences between recordings A and C were resolved by
various experiments, including the use of other meters in the appara-
tus. It was found that the initial pyrolysis reaction of the mate-
rial (with precautions in sample desiccation) evolved only non-
combustible vapors. The combustible gas indicator was not responsive
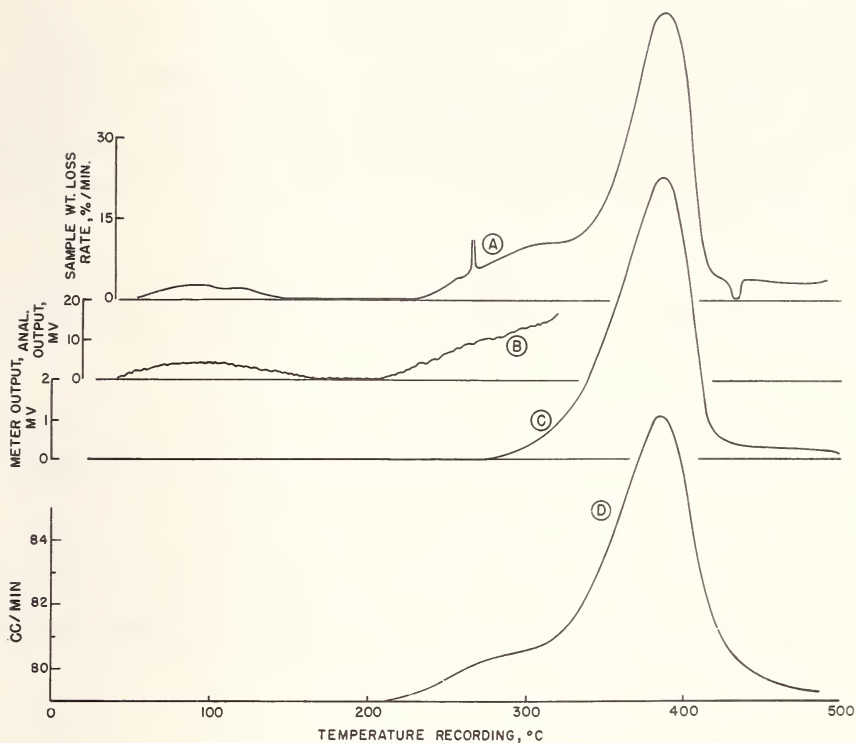
Figure 4.   Comparison of system recordings, pyrolysis of treated
             cellulose. Materials: Standard grade Whatman Ashless
             cellulose powder (<0.01 % ash) with 1.5 Wt % $KHCO_3$, add-
             ed from aqueous solution. Heating rate: All 60 °C/min.
             A. First derivative of thermogravimetric recording,
             DuPont 950 Thermogravimetric Analyzer, 11.4 mg sample.
             B. Output of water analyzer, Model 300 LIRA Infrared
             Analyzer, N_2 flow 280 cc/min, tube furnace outflow direct
             to analyzer w/o air dilution, analyzer responds to water
             and hydrocarbon vapors, 19.5 mg sample. C. Output of
             combustible gas indicator, Johnson-Williams Model G,
             19.8 mg sample. D. Output of flowmeter, Model LL-100
             Hastings Linear Electrical Mass Flowmeter, 13.8 mg
             sample.

to these vapors. Thus this reaction had been conveniently "filtered"
out of recording C. The reaction was recorded by the infrared H_2O

analyzer, recording B of Figure 4, and by the linear mass flowmeter, recording D of Figure 4. The kinetics of the initial reaction could then be separated by obvious means: (1) by calculation and subtraction of the principal decomposition from recording D, (2) by difference, from recordings C and D, and (3) by recording the reaction separately with the linear mass flowmeter using an appropriate temperature limit.

The above illustrates capabilities of the apparatus system provided by options in the metering function that are not available with TGA.

The kinetics indicated by recording C of Figure 4 was confirmed by a variety of other pyrolysis runs of the material, including the one represented in Figure 5. In this case, the pyrolysis temperature has been cycled through an irregular course and held below 370 °C to repress secondary decomposition during the principal reaction. The secondary reaction was then recorded as the temperature was subsequently increased to 500 °C, an example of separating reactions by appropriate temperature control.
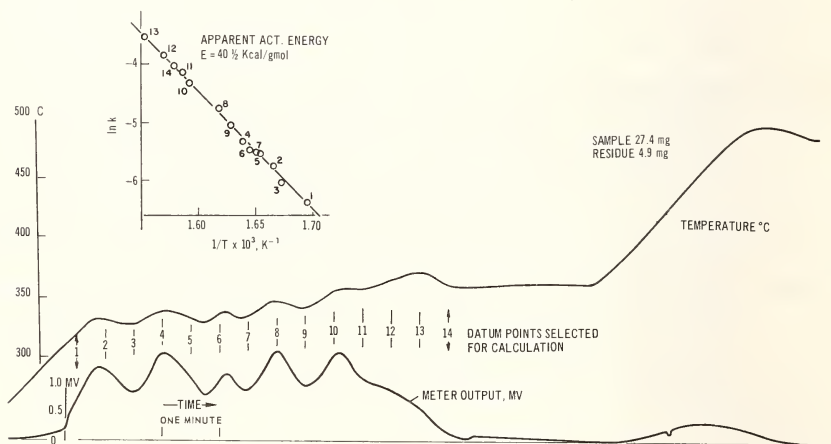

Figure 5. Recordings and Arrhenius plot, pyrolysis of treated cellulose.

DISCUSSION

Other advantages of the system may be noted. There is little
"noise" in the recordings. Dynamic effects from evolved vapors,
convection, *etc.* are not of consequence to the measurements. A
wide range of reaction rates may be accommodated by the apparatus.
Heating rates up to 2 °C/sec have been used without apparent impair-
ment of the recordings. Sensitivity of up to 2 orders of magnitude
greater than that of conventional thermal methods is obtained. The
direct contact of the low-mass temperature sensor with the sample
material is advantageous. For example, during pyrolysis some cellu-
losic samples have indicated excursions of up to 30 °C from the tem-
perature of the immediate environment. This indicates the inaccur-
acies that can occur in thermal methods where the temperature sensor
is bulky, or is detached from the sample.

Of particular merit is the simplicity of the system. The
apparatus is simple and expeditious to operate. It does not in-
volve the complications and delays of vacuum operation. The re-
sults are generally simple to interpret. The "visibility" of the
recordings is such that effects can sometimes be recognized and
explored by adjustments in temperature during the course of pyrol-
ysis runs, in the manner of operating an analog computer. The data
are simple to translate into kinetic terms. The equipment is
relatively inexpensive.

CONCLUSIONS

The described apparatus is an efficient means for measuring
the kinetics of vapor producing reactions and has performed ki-
netic measurements not attainable by conventional thermal methods.
The system permits a variety of options in effluent sensing and
mode of operation, such that the applicability of the method
appears promising.

ACKNOWLEDGMENT

REFERENCES

[1]   Newkirk, A. E., Anal. Chem. <u>32</u>, 1558 (1960).

[2]   Barrall, E. M. II and Rogers, L. B., Anal. Chem. <u>34</u>, 1101 (1962).

[3]   Wilson, Abraham, Rev. Sci. Instr. <u>38</u>, 1757 (1967).

[4]   Ramiah, M. V. and Goring, D. A. I., Cellulose Chemistry and Technology <u>1</u>, 277 (1967).

[5]   Murphy, E. J., J. Polymer Sci. <u>58</u>, 649 (1962).

[6]   Bryce, D. J. and Greenwood, C. T., Applied Polymer Symposia No. 2, 149, Interscience, New York (1966).

[7]   Bryce, D. J. and Greenwood, C. T., Die Starke No. 10/15, 359 (1963).

[8]   McNeill, I. C., "Application of Thermal Volatility Analysis with Differential Condensation to Some Problems in Polymer Chemistry," 2nd International Conference on Thermal Analysis, Holy Cross College, Worcester, Mass., August 1968.

[9]   Eggertsen, F. T., Oki, H. M., and Stross, F. H. "A Pyrolysis-Flame Detection Technique for Thermal Analysis", Second International Symposium on Thermal Analysis, Holy Cross College, Worcester, Mass., August 1968.

[10]   Stapp, A. C. and Carle, D. W. "A New Thermal Analysis Instrument", Pittsburgh Conference on Analytical Chemistry and Applied Spectroscopy, Cleveland, Ohio, March 1969.

[11]   Johnson, K. W. and Bruce, E. L., Instruction Manual, Johnson and Williams Model G Combustible Gas Indicator.

[12]   Barrall II, E. M., Private communication.

[13.]   Broido, A., "A Simple, Sensitive Graphical Method of Treating Thermogravimetric Analysis Data," Spring Meeting of Western States Section, The Combustion Institute, Univ. of Southern California, Los Angeles, California, April 1968.

DIFFERENTIAL THERMAL ANALYSIS OF
PRIMARY EXPLOSIVES - A MODIFIED TECHNIQUE

R. J. Graybush, F. G. May*, A. C. Forsyth

Solid State Branch
Explosive Laboratory, FRL,
Picatinny Arsenal
Dover, New Jersey

The usefulness of differential thermal analysis (DTA) in the study of metastable materials has been hindered by the tendency of samples to explode during the experiment. A description is given of modifications which have been made to the remote cell used in conjunction with a Dupont 900 DTA such that the possibility of explosion is minimized. Using lead azide to evaluate the technique it is shown that complete curves for the exothermic decomposition

$$PbN_6 \rightarrow Pb + 3N_2$$

are reproducibly obtained. The endotherm in the curve corresponding to the fusion of the product lead serves as a confirmation of the reaction. Illustrations are given to show extensions of the system to other sensitive compounds, namely lead styphnate, mercury fulminate, and potassium dinitrobenzfuroxan.

Key Words: differential thermal analysis, Dupont 900 DTA remote cell, lead azide, lead styphnate, mercury fulminate, metastable materials, potassium dinitrobenzfuroxan, primary explosives.

INTRODUCTION

The application of thermal analysis to decomposition studies of very sensitive materials, such as primary explosives, has been hindered by the possibility of explosions of samples within the apparatus.

Although specimens can be sufficiently small to ensure little risk
of instrument damage this is an undesirable situation since the
amount of significant data which can be extracted from such a curve
is minimal.

Krien [1] investigated the application of combined differential
thermal analysis and thermogravimetry (DTA/TG) to the decomposition
of explosives. Problems associated with this TG apparatus restricted
him to slow heating rates (5 °C/min or less) and as a consequence
the DTA peaks obtained were spread out.

In more recent work PaiVerneker and Maycock [2,3] described
the application of simultaneous DTA-TG to lead azide. They were
able to observe thermal decomposition which they attributed to the
reaction

$$PbN_6 \rightarrow Pb + 3N_2 \tag{1}$$
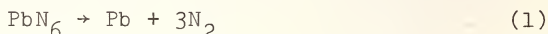
Since the DTA and TG traces are recorded from the same sample it is
correct to assume that analysis obtained for the TG will also be
incorporated in the DTA results. The nitrogen content of lead azide
is 28.8% therefore it would be expected that if this reaction were
to take place the weight loss recorded by thermogravimetry would be
28.8%. The curves which they obtained show very slow thermal decom-
position over a wide temperature range with loses of 21.9 - 27.5%.
Thus the decrease in weight found experimentally indicates conclu-
sively that the products of reaction consist of a mixture of metallic
lead and its oxide. The results can be more adequately explained
from a consideration of reactions of the type

$$PbN_6 \xrightarrow{\text{trace } O_2} PbO + 3N_2 \tag{2}$$
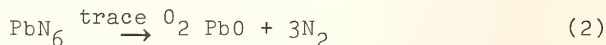
or formation of higher oxides of lead depending on oxygen concentra-
tion. The weight losses predicted for reactions of this type would
be 23.4% for formation of PbO or less for a mixture of PbO plus
higher oxides of lead. The experience of the present investigators
has been that such slow reactions invariably yield oxide mixtures,

or, at best, metal plus oxide mixtures. It is more tenable to pro-
pose that the decomposition which was reported was not the formation
of metal plus gaseous nitrogen but decomposition in the presence of
trace amounts of oxygen to yield an ill defined product consisting
of a variable mixture of metal plus oxides with no assurance that
the same reaction path will be followed in any two (2) experiments.

Lead azide is of interest because of its wide use. A study of
the decomposition reaction (eq. 1) is most suitable since it is known
to occur in the detonation process [4] yielding basic lead and nitro-
gen and therefore can be easily characterized. Thus, it was consid-
ered ideal to use for the evaluation of the modified cell.

EXPERIMENTAL

Remote Cell Modifications

A typical remote cell as currently supplied by E. I. DuPont
(Fig. 1) differs from earlier models in that the heating block has
been raised and is separated from the thermocouple connections by
a large insulating disk of pressed asbestos. Experience with earlier
designs of the cell had shown that it is imperative to protect these
connections from exposure to stray thermal currents. The need to
protect samples from the slightest oxidizing environment necessitated
the cell being evacuated to 10^{-6} torr. This required removal of the
porous disk and redesign of the support. It was also necessary to
seal the electrical connectors, relocate the gas inlets, and modify
the base plate and locking clamps.

The modified cell is shown in Figures 2 and 3, where Figure 2
shows an overall view and Figure 3 gives the dimensions. It was
necessary to reconstruct the original cell starting with a new base
having four (4) holes to accomodate vacuum tight cartridge bushings,
supplied by Glass Tite Industries (A-2622), which were in turn
soldered into the base. The pins from the original plug were sol-
dered into the new cartridges to adapt them to the existing thermo-
couple and heater connections. The new heating block holder and
support consisted of a single unit fabricated from heavy walled glass
and silver coated to minimize thermal losses. The thermocouple con-

Figure 1. Remote cell as supplied by E. I. Dupont.

nections were further protected from the development of thermal
gradients by shielding with glass tubing. Evacuation and gas flow
was effected through two (2) pressure-vacuum stopcocks attached to
the top of the pyrex dome. The pyrex dome was made vacuum tight by
fastening it to the base with a ring seal and metal ring clamp.
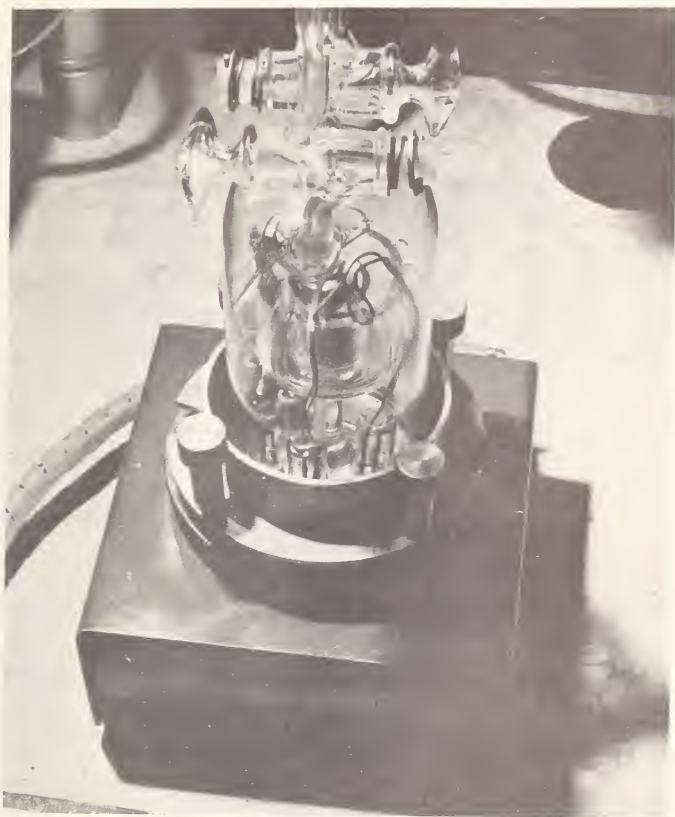
Figure 2.   Modified remote cell.

DTA Procedures

Samples investigated were in the form of fine crystalline powders.   Glass beads were used as reference materials and in the tube containing the heater control thermocouple.   Standard heating blocks of silver or aluminum were used with specimens contained in either 2 mm or 4 mm capillary tubes.   With 2 mm tubes sample weight was approximately 0.5 mg, in 4 mm tubes a maximum of 2.5 mg was used;

Figure 3.   Schematic diagram of components in the modified remote
DTA cell.

however, the weight could be increased to 5 mg if the sample was diluted with an equal volume of glass beads [5]. In all cases samples were compacted by mild tapping. The cell was evacuated to 10^{-6} torr for several minutes before backfilling and purging with dried helium gas. A flow rate of 400 cc/min was maintained throughout the experiment. Standard chromel-alumel thermocouples were employed. Heating rates up to 10 °C/min and maximum differential temperature sensitivity, 0.1 °C/in, could be used.

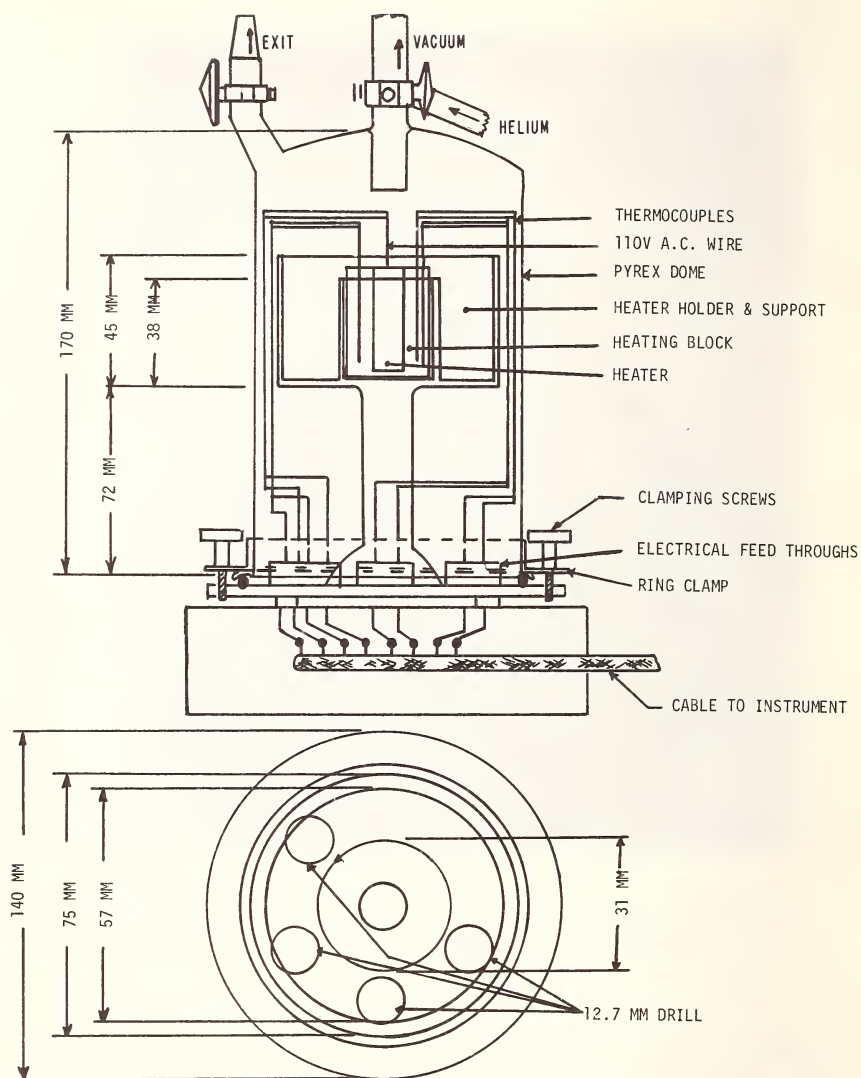Fisher Scientific "Thermetic" standards and high purity lead (99.999%) supplied by Electronic Space Products, Inc. were selected for instrument calibration. Lead azide of high purity was prepared by reaction of lead nitrate with hydrozoic acid [6]. Other explosive samples were of commercial or military production grade stock.

RESULTS AND DISCUSSIONS

The instrument was calibrated through the lead azide temperature range using melting point standards and was in agreement with the old cell. The results of pure lead melting at 318 °C under the high helium flow rate is shown in Figure 4a. The lead fusion peak is indicated as an exotherm at 318 °C in Figure 4b when lead is placed in the reference tube and analyzed simultaneously with lead azide in the sample tube. The differences in the peak sizes of the product lead from that of the added lead is due to differences in amount.

DTA curves for lead azide obtained prior to cell modifications are shown in Figure 5. Two (2) unacceptable curves, sample detonation (Fig. 5a) and sample oxidation (Fig. 5b) are shown. It is readily apparent that very little information other than onset temperature can be extracted from those curves in which high order detonation occurred.

The presence of trace amounts of oxygen causes nonreproducible distortion of the decomposition exotherm. Depending on the oxygen concentration this distortion can range from gross deformation and
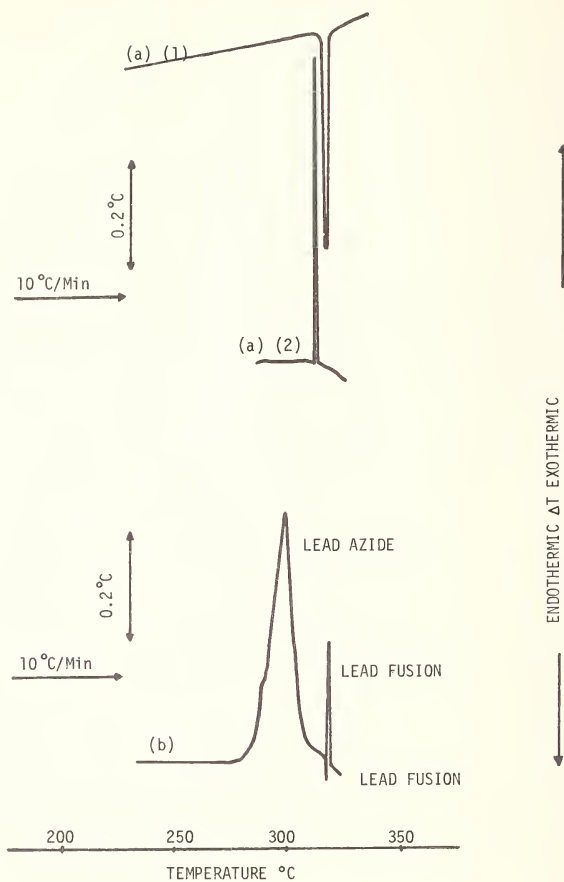
Figure 4.   DTA curves showing the position of the lead m.p.
            (a) (1) lead fusion (a) (2) supercooled solidification
            of lead (cooling curve).   (b) Pb metal in reference
            tube + PbN_6 in sample tube.

extended tailing of the peak to a reduction in peak area in the
presence of extremely minute traces of oxygen.   When lead azide
specimens were placed in the modified cell at varying vacuum pres-
sures before backfilling and purging with helium it was found that
the exotherm trace configuration was a function of pressure becoming
constant at 10^{-6} torr.   Although the peak height and shape is affected,
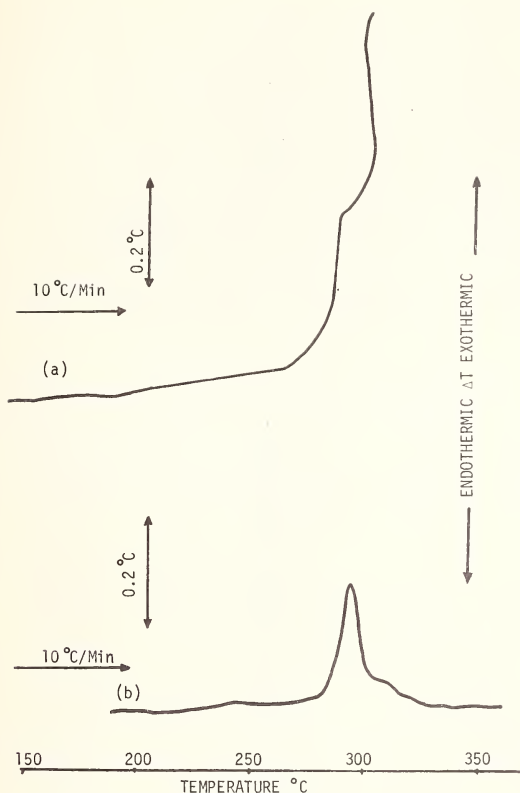
Figure 5.   DTA curves for lead azide.   (a) sample detonated.
            (b) sample decomposed in the presence of trace amounts
            of oxygen.

this treatment did not influence either the onset or peak temperature
except in cases of gross deformation of the trace.

    Figure 6 shows decomposition of high purity lead azide to metal-
lic lead as obtained in the modified system.   Features of importance
are the decomposition exotherm in the region 287 - 302 °C and the
lead fusion endotherm at 318 °C.   Subsequent cooling of the sample
gives the exothermic solidification of lead supercooled to 315 °C.
The products of reaction (eq. 1) are confirmed by the lead fusion.
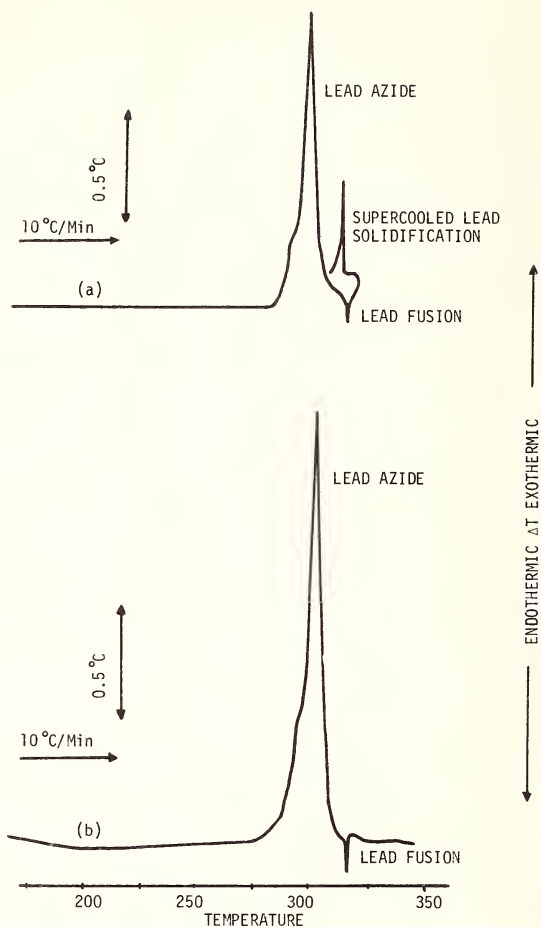
Figure 6. DTA curves for lead azide using modified remote cell.
           (a) 2.6 mg lead azide. (b) 3.1 mg lead azide diluted
           with glass beads

The extent to which the fusion point is displaced at a constant
heating rate depends on the amount of azide used. Using varying
quantities of lead azide to check out the cell the average deviation
of the lead fusion was ± 1.9 °C at 318 °C. This could be signifi-
cantly reduced by use of a constant mass of sample. Similarly values
of the decomposition onset and apex temperatures could be obtained

with greater accuracy if all experimental parameters were held con-
stant during a set of experiments. It would also be desirable to
sieve samples for constant particle size but with sensitive materials
such as lead azide this proves to be extremely time consuming. The
onset and peak temperatures are used for trace description. These
values are given in Table 1 and were obtained from experimental
curves using various instrument settings and sample sizes. This
data gave an average $T_{(onset)}$ 287 °C with a deviation of ± 1.0% and
an average $T_{(max)}$ 302 °C with a deviation of ± 0.8%.

Table 1.   Results of thermal decomposition of lead azide
           under various experimental conditions.

T °C$_{(onset)}$	T °C$_{(max)}$	Lead mp °C	Sample weight mg	ΔT (°C/in)	Glass beads	Size of capillary tube
287	305	317	2.4	0.5	No	4
289	305	316	2.6	0.5	No	4
288	305	320	1.1	0.2	No	4
293	305	320	1.0	0.2	No	4
294	306	321	0.8	0.2	No	4
290	304	320	0.5	0.2	No	4
288	304	320	0.4	0.2	No	2
290	304	316	0.4	0.2	No	2
287	302	316	0.5	0.2	No	2
290	303	320	0.3	0.2	No	2
287	302	320	0,3	0,1	No	2
288	300	316	3.0	0.5	Yes	2

It can be seen from the table that considerable flexibility in
choice of instrument settings and sample configuration is possible.
It was found essential to provide for efficient conduction of heat
away from the sample area since the reaction is highly exothermic
and can result in detonation. Helium was employed as the preferred
carrier gas. When the sample size was increased to the point where
helium gas alone was not sufficient; dilution of the sample with
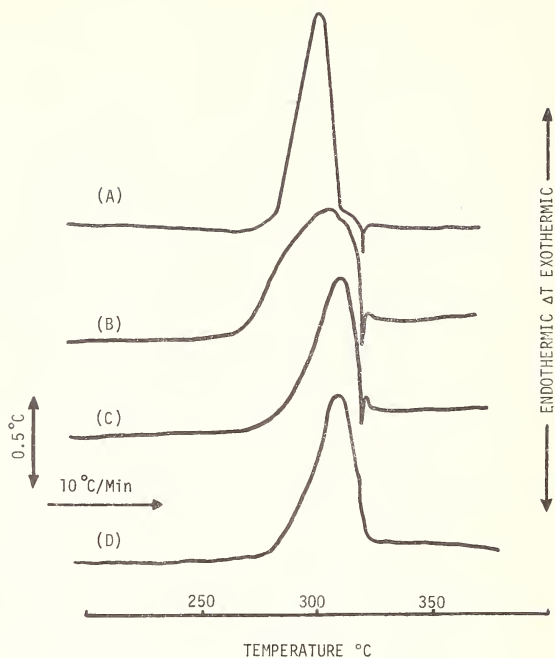
Figure 7. DTA curves for iron doped lead azide. (A) PbN_6 + FeI_3.
(B) PbN_6 + $FeBr_3$. (C) PbN_6 + $FeCl_3$. (D) PbN_6 + FeF_3.

glass beads, commonly used for reference material, provided a heat
sink. This use of glass dilution affects peak magnitude but not
position as shown in Figures 7a and 7b.

The new cell and the experimental procedure were evaluated
further using doped lead azide samples and other primary explosives.
From another study [7] it is known that lead azide prepared in the
presence of various dopants has related defect structure. Figure 7
shows curves for a series of lead azide samples doped with ferric
chloride salts. Work is in progress in interpret these results in
terms of observed electron spin resonance phenomena. In general,
initiating compounds were difficult to analyze without the modifica-
tion of the remote cell. Figure 8 shows some results of the exten-

Figure 8.   DTA curves for other primary explosives. (a) potassium
            dinitrobenzfuroxan (KDNBF). (b) lead styphnate.
            (c) mercury fulminate.

sion of the method to several other metastable compounds. In all
instances complete curves are obtained and it appears that the
method can be successfully applied to other sensitive materials.

     Effort is currently being directed to modifying the accessory
DuPont 950 TG apparatus to enable equivalent thermogravimetric data
to be obtained.

REFERENCES

1. Krien, G., Explosivstoffe 13, 205 (1965).

2. PaiVerneker, V. R., and Maycock, J. N., Anal. Chem. 40, 1325
        (1968).

3. PaiVerneker, V. R., and Maycock, J. N., Proc. of 2nd International
        Conference of Thermal Analysis (1968).

4. Garner, W. E., Trans. Farad. Soc., Symposium on Solid Phase
        Reactions (1938).

5. Smith, J. R., and Forsyth, A. C., private communication.

6. Reitzner, B., and Manno, R. P., Nature 198, 991 (1963).

7. Downs, D. S., Forsyth, A. C., and Fair, H. D., ESR Studies of
        Doped Lead Azide, to be published.

THERMOGRAVIMETRY OF VULCANIZATES

John J. Maurer

Enjay Polymer Laboratories
Linden, New Jersey

Thermogravimetric analysis provides an important
advance in the analysis of elastomer compounds and
vulcanizates. This paper reviews the current state
of such investigations including a consideration of
key experimental variables, precision and accuracy for
estimating basic composition of different types of
practical formulations. Additional information can
be obtained by careful study of the oxidation charac-
teristics of the carbon black in the formulation.
The latter is influenced by both physical (*e.g.*, sur-
face area) and chemical (type of cure system or poly-
mer) effects. Finally, an isothermal oxidation pro-
cedure is discussed for demonstrating differences in
carbon black(s) and/or curatives in routine compari-
sons of samples.

Key words: carbon black; curatives; elastomer com-
pounds and vulcanizates; oxidation; thermogravi-
metric analysis.

INTRODUCTION

Elastomer compounds are complex mixtures of polymer(s), carbon
black(s), mineral filler(s), curatives, plasticizers, and miscel-
laneous additives. This complexity is increased by the frequent
use of blends of carbon blacks or elastomers. Because of this
situation, it is a challenging task for the manufacturer to deter-
mine the cause of various problems which may arise in the pro-
cessing and curing operations leading to the finished product,
and also for manufacturer and customer to conduct quality control
analyses on the finished rubber products.

Methods exist for conducting highly detailed analyses of rubber formulations, but these are often too expensive or time-consuming to be justified and/or useful for routine application [1]. Our first-stage TGA objective [2] was to develop rapid practical procedures for use in certain factory and technical service related problem areas. Later, it became evident that the basic concepts could be extended to provide additional information by careful analysis of the oxidation characteristics of the carbon black in the formulation [3]. The objectives of this paper are to present a critique of the present methods [4]; demonstrate current strengths; consider refinements to improve precision and accuracy; discuss factors which may influence the results; suggest new areas of application and new types of information which may be obtained; and show the potential of the current methods for Quality Control analysis and "trouble shooting" activities.

EXPERIMENTAL CONSIDERATIONS

Considerations of instrument design, *etc.*, are not included in this discussion since it will be assumed that one has available a TGA instrument of sound basic operating characteristics. References to such matters are available elsewhere [4]. As a basis for commenting on several important procedural details, the basic method adopted in our laboratories for routine inspections of butyl rubber vulcanizates is presented below.

TGA Conditions for Compositional
Analyses of Vulcanizates

Instrument   : DuPont Model 950 TGA
Sample   : 20 mg (usually in one piece)
Thermocouple: Chromel/Alumel
Atmosphere   : purge with nitrogen for 15 minutes prior to run
Decomposition sequence: heat at 15 °C/min to constant weight
                in nitrogen; admit air, continue at 15 °C/min
                to constant weight
Calibration : Monitor daily *via* standard vulcanizate to
                check reference temperatures and composition.

The conditions listed above were selected because of a desire
to have a relatively rapid analysis, and because a dynamic method
(as opposed to several possible isothermal approaches) would lead
to information about oil and carbon black variations in some sys-
tems. An important consideration, regardless of the specific steps
employed, is to insure reliable instrument operation. This was
done in the present case by means of daily checks of an extracted
vulcanizate known to contain 48.8 weight percent polymer and 51.2
weight percent carbon black plus ash. Some representative data are
shown in Figure 1, which shows the degree of variation experienced
in the terminal decomposition temperature (T_t) for the polymer and
in estimated total polymer content for one such sample. Long-term
data on this type can be translated into a quality control chart
which provides a reference point for judging instrument stability.
Of course, such a procedure also reflects any variations in opera-
tor technique and uniformity of the standard, both of which must be
evaluated and controlled. It is useful to point out that the preci-
sion of quantities such as shown in Figure 1, especially reference
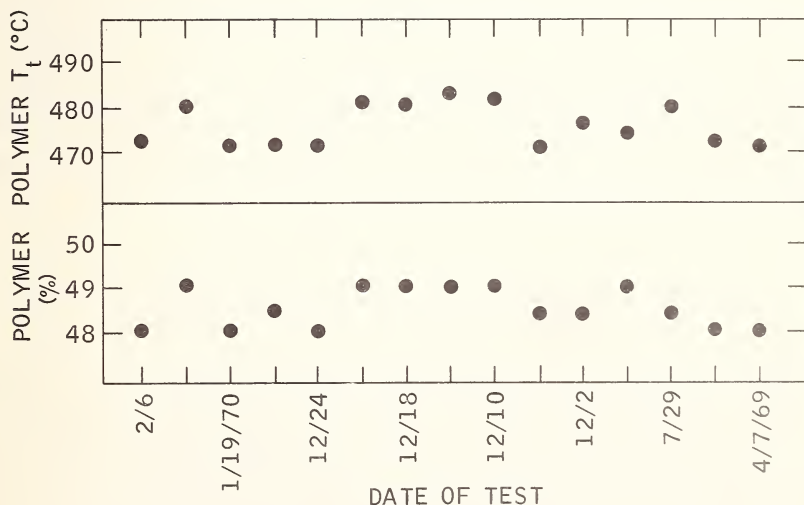temperatures, is influenced also by the scale used on the thermo-

Figure 1.   Analysis of TGA standard sample (extracted).

gram. In the present instance, each minor chart division on the
weight scale represented 2 weight percent, and on the temperature
scale represented 5 °C. Expansion of these scales would contribute
to improved precision and accuracy.

ANALYSIS OF "BASIC COMPOSITION" OF VULCANIZATES

The original goal of this work was to provide a rapid estimate
of the "oil," polymer," "carbon black," ash, or mineral filler plus
ash in the formulation. For general unknowns, use of an unextracted
sample would not enable separate determination of the oil content,
thus, the sum of oil and polymer would be obtained in the decomposi-
tion in nitrogen. Extraction of the sample prior to TGA can provide
an estimate of the "oil" content but lengthens the time for the
analysis of the vulcanizate.

The kinds of data obtained from this analysis are illustrated in
Figure 2. The upper thermogram depicts the weight losses due to
polymer + oil, to carbon black oxidation and the residual weight due
to ash. The lower thermogram (for an extracted sample) shows the
weight losses due to polymer and carbon black, and the large residue
(after achieving constant weight in air) due primarily to mineral
filler but with a small contribution from the ash content as well.
The precision and accuracy of such determinations, as well as a meth-
od for estimation of oil content in a "known" system, will be taken
up later in this report.

EXPERIMENTAL VARIABLES INFLUENCING THE ANALYSIS

Other than instrument considerations, the three TGA variables
which could influence the present analysis are heating rate, sample
size and atmosphere control. The first of these is considered in
Table 1, which contains data taken on an extracted commercial vul-
canizate. It is seen that the calculated composition in terms of
polymer, carbon black and ash is not significantly influenced by
this range of heating rates. This is an interesting result for two
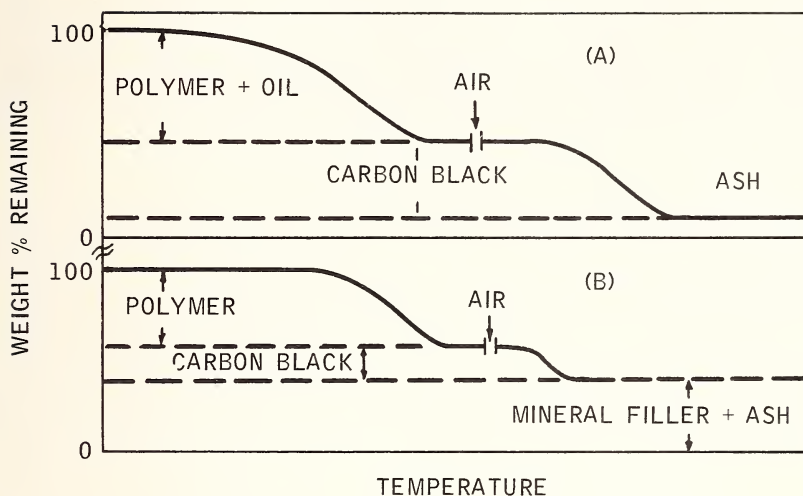
Figure 2.   Analysis of carbon black and mineral filler.

Table 1.   Influence of heating rate on vulcanizate analysis.

Rate (°C/min)	Vulcanizate composition (Wt %)[a]		
	Polymer	Carbon black	Ash
15	57.0	27.0	3.0
6	55.7	27.8	3.5
0[b]	56.0	27.5	3.5

---

[a]Commercial sample; 13 percent "oil" removed by extraction.
[b]Isothermal (532 °C).

reasons.   First, one may use a rate as high as 15 °C/min if a dy-
namic test is desirable (reasons for this will be illustrated sub-
sequently).   Second, a very rapid estimation of vulcanizate compo-
sition is possible in terms of (a) polymer plus oil, and (b) carbon
black plus ash, or mineral filler plus ash.   This may be easily
accomplished for the system in Table 1 by isothermal degradation in

nitrogen at 532 °C. The total time for this isothermal analysis
was less than 5 minutes. It should be noted that heating rate does
influence the decomposition characteristics of polymer and carbon
black, and this effect may be useful in analyses of blends of these
materials.

The influence of particle size is demonstrated in Table 2 for
several vulcanizates, some of which contained polymer blends, of
the same "basic composition." The pulverized samples were obtained
by crushing vulcanizate sections which had been shock cooled in
liquid nitrogen. The data indicate no advantage for using smaller
pieces in this test; therefore, the one piece, solid sample was
adopted for convenience. Similar experience was observed for other
vulcanizates.

Table 2. Influence of sample size[a] on vulcanizate analysis.

| Formulation[c] | Sample type | Composition (Wt %)[b] | |
		Polymer	Carbon black + ash
A	Solid	49	51
	Pulverized	49	51
B	Solid	49	51
	Pulverized	49	51
C	Solid	49	51
	Pulverized	49	51

[a] 20 mg in all cases; known:
[b] 48.8% polymer; 51.2% black + ash
[c] Samples differed in elastomer type.

The atmosphere control during the basic TGA procedure consists
of purging the system with nitrogen for 15 minutes prior to initia-
tion of the heating rate. The nitrogen, which is piped to the labor-
atory from a large, central supply is known to contain a very low
level of oxygen (4-5 ppm). To date, this has presented no apparent
problem in our TGA studies of basic vulcanizate composition, as in-

ferred from precision and accuracy data of the type cited elsewhere
in this report. However, rigorous nitrogen purification to remove
trace oxygen would enhance absolute accuracy of the method, and may
assist in other studies which rely on the temperatures at which cer-
tain events take place rather than on total weight changes, as such.

FACTORS INFLUENCING ACCURACY OF VULCANIZATE ANALYSIS

As previously noted, the initial objective of this work was to
provide a procedure applicable to problems where both time and cost
of the analysis were important factors. It will subsequently be
shown that the standard TGA conditions successfully meet these ob-
jectives. For completeness, we first take up the assumptions and
approximations involved in calculating the Basic Vulcanizate Compo-
sition. Some of these are also involved in other methods of vulcan-
izate analysis. These point to the areas where additional work is
required to enable even greater utility of the method.

• Estimation of Oil Content by Preliminary Extraction
Solvent will also remove accelerators, sulfur, resins, waxes, *etc.*;
also some low ends from the polymer.

• Estimation of Polymer from Weight Loss in Nitrogen
  (Extracted Sample)
Polymer is assumed to degrade completely. Organic materials, insol-
uble in *e.g.* MEK, and also those of high thermal stability (*e.g.*,
certain resins) will interfere.
Note: DTA may be useful to detect systems containing major amounts
       of these ingredients [2].

• Estimation of Carbon Black Content From Weight Loss in Air
Any residues from polymer, resin, *etc.*, will interfere. Small
weight losses due to certain mineral fillers interfere.

• Estimation of Ash Level from Residue After Weight Loss in Air
Residue contains all non-volatile metallic residues (from ZnO,
accelerators, resins, process aids, *etc.*).

PRECISION AND ACCURACY OF BASIC TGA PROCEDURE

In this section we examine the degree to which the technique
may provide reliable information about basic vulcanizate compo-
sition. In Table 3, data are shown for four laboratory-prepared
vulcanizates, each of which contained a different elastomer type.
Visual inspection of these data indicate the excellent precision of
the analysis. The accuracy is also quite good, recalling that, be-
cause of the assumptions involved, exact agreement between known
and observed values will not be obtained. It is interesting to note
for the NR system that incomplete polymer loss may have been in-
volved, with a resulting increase in the apparent carbon black con-
tent. Such problems are usually not major, but illustrate the type
of variation in the analysis which must be considered in treating
"unknown" samples. It should also be noted that major differences
in compounds are readily detected; and it is this type of data which
is generally most significant.

Table 3. Precision of vulcanizate analyses for
different elastomers.

Polymer type	Vulcanizate composition (Wt %)[a]	
	Polymer	Carbon black + ash
Ethylene propylene terpolymer	49.0	51.0
	49.0	51.0
	50.0	50.0
	50.0	50.0
Butyl rubber	49.0	51.0
	49.0	51.0
	49.0	51.0
	49.0	51.0
Chlorobutyl rubber	66.0	34.0
	66.0	34.0
	66.0	34.0
	66.0	34.0
Natural rubber	64.0	36.0
	65.0	35.0
	64.0	36.0
	64.5	35.5

[a]Four separate samples analyzed for each system.

The vulcanizates referred to in Table 3 also provided additional information regarding the characteristics of the polymer decomposition in nitrogen (Table 4). It is noted that there is a wide range of temperatures over which the 50 percent weight loss (T_{50}) and the terminal decomposition temperature (T_t) occur. This suggests that for some systems TGA procedures might be devised to determine the composition of elastomer blends in the vulcanizate. We hope to report on this kind of study at another time. For this type of analysis, it will be necessary to determine whether the effect on polymer decomposition, of the fillers, curatives, *etc*., in the system varies with elastomer blend composition. Of course, once having established the pattern for a known compound, T_{50} and T_t of the polymer are two additional quality control statistics which may be monitored.

Table 4. Decomposition characteristics of different elastomers[a].

Polymer type	Polymer decomposition temperature (°C)	
	$T_{50\%}$	$T_{terminal}$
Ethylene propylene terpolymer	479	504
	472	496
	472	498
	472	498
Butyl rubber	417	452
	417	449
	417	452
	416	450
Chlorobutyl rubber	407	445
	411	454
	406	449
	404	447
Natural rubber	388	462
	386	462
	388	470
	388	471

[a]Same vulcanizates as Table 3.

A more interesting demonstration of the accuracy of the basic
TGA method is to examine the data obtained for different types of
practical elastomer formulations. As shown in Table 5, the method
appears highly useful, even in its simplest form, for studying the
composition of a variety of commercial compounds. However, systems
are known where particular ingredients in the formulation will
interfere with the analysis to varying extents [2]. Examples of
these would be cases where (a) all of the polymers did not degrade
completely in the nitrogen step, or (b) resins, waxes or miscel-
laneous processing aids are present in substantial amounts.
Further, the latter materials are not readily removed completely
from some formulations during extraction procedures prior to TGA.
It should be noted that even in these cases, the carbon black, ash,
mineral filler plus ash, or "oil plus polymer" values are often
reasonably close to the true values. Of course, the degree to which
such formulations are a problem depends upon the purpose of the anal-
ysis. For determinations of the exact composition of unknown formul-
ations, the problem is a serious one, but for routine quality control
considerations it may be insignificant. Those interested in the for-

Table 5. Accuracy of TGA method for unextracted commercial
                        vulcanizates.

Formulation		Oil	Polymer	Carbon black	Mineral filler	Ash
Inner tube	known	12.5	50.0	35.0	--	2.5
	observed	13	49.5	34.5	--	3.0
			Oil + Polymer			
Weather strip	known		49.4	49.5	--	1.1
	observed		50.0	49.0	--	1.0
Sponge	known		55.0	14.5	29.0	1.5
	observed		56.0	15.0	← 29.0 →	
Engine mount	known		62.0	35.4		2.6
	observed		62.0	35.0		3.0
Electrical insulation	known		49.2	8.6	← 42.2 →	
	observed		49.0	9.0	← 42 →	

mer area may find Differential Thermal Analysis a useful complementary
technique since it can detect the presence of significant amounts of
resins, waxes, *etc.*, in some formulations [2].

EXTENDING THE ANALYSIS TO PROVIDE ADDITIONAL INFORMATION

Oil Content of a System Containing a Known Elastomer

The oil content of a vulcanizate cannot generally be estimated
directly from the thermogram because the oil weight loss region
overlaps that due to the polymer. A method of circumventing this
problem has been found for butyl rubber systems and should also be
applicable to others (including oil-extended polymers). The
approach involved is to establish a reference temperature (T_R) at
which essentially all of the oil plus only a small amount of poly-
mer have been volatilized from the system. A series of vulcanizates
differing in oil/polymer/carbon black ratio is then extracted and
analyzed in the standard manner. Based upon the resulting thermo-
grams, a correction curve of "Polymer remaining at T_R" *vs.* "Polymer
Weight Loss at T_R" is constructed (Figure 3).

For an "unknown" system, after completing the polymer decomposi-
tion step in nitrogen, one can read the amount of polymer remaining
at T_R from the thermogram. Reference to the correction curve then
allows an estimation of the polymer content in the system and thus,
from the knowledge of the total weight <u>loss</u> at T_R, an estimate of
the oil content as well. Potential methods for improving the anal-
ysis of oil content consist of lower (including isothermal) heating
rates, and reduced pressure to facilitate vaporization of the oil.

An example of the possibilities of this method is the first
formulation in Table 5; here, the oil content was estimated by the
T_R technique. Our experience indicates that the oil content can
usually be estimated within about three weight percent of the known
value for butyl rubber compounds. This is sufficiently accurate for
some purposes, and avoids the use of a lengthy extraction step to
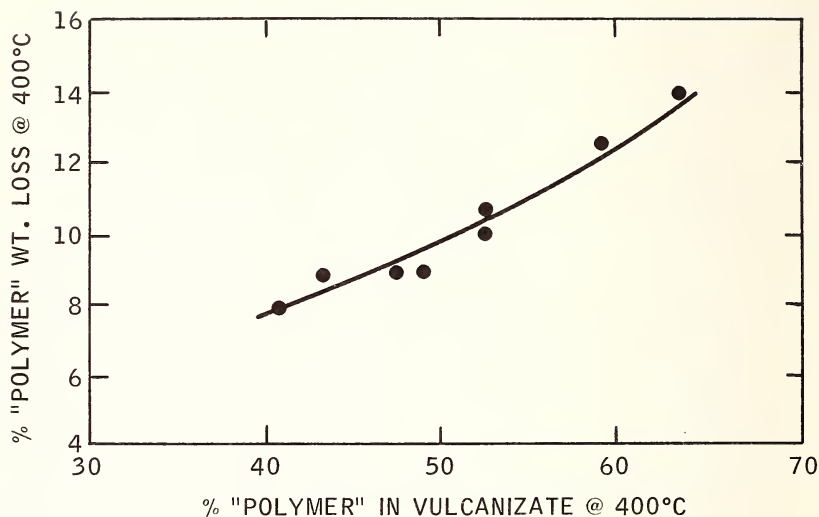estimate oil content. In order to use this approach, one must know

Figure 3. Polymer weight loss correction at T_R.

the decomposition characteristics of the polymer and oil of interest
(assuming isothermal and/or reduced pressure conditions do not enable
the oil to be directly "separated" from the polymer. Here again,
waxes, resins, *etc.*, may interfere if present in large and/or varying
quantities.

DETECTION OF CARBON BLACK DIFFERENCES
IN STANDARD FORMULATION

It has been found that a slight modification of the basic TGA
procedure permits discrimination among several carbon black types
in a standard butyl formulation [3]. This modification consists
of cooling the system to 275 °C (after bringing it to constant
weight in nitrogen) before admitting air, and then continuing the
analysis at 15 °C/min in the usual manner. An example of this
approach is shown in Figure 4. Both chemical and physical effects
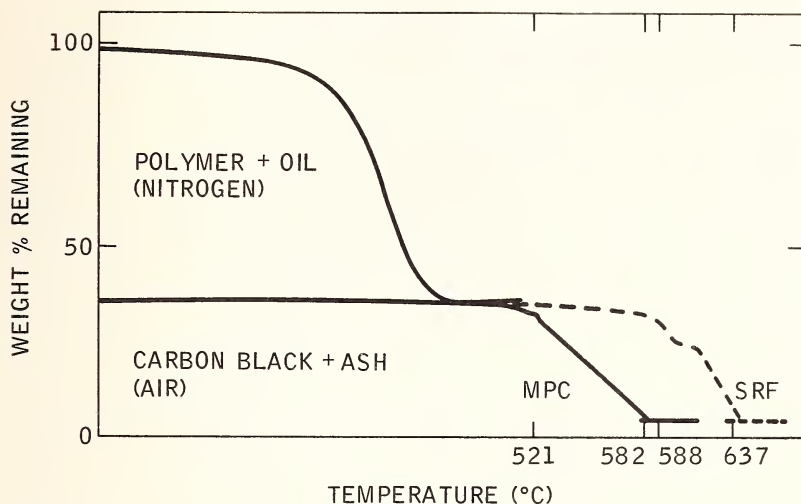can influence the decomposition characteristics of carbon blacks

Figure 4.   Detection of carbon black differences in "standard
            formulation.

in this procedure. Thus, for a known formulation containing a
single accelerator system and differing only in carbon black type,
a relationship between decomposition characteristics and surface
area has been demonstrated (Fig. 5).

   Information concerning the degree of chemical effects on carbon
black decomposition was obtained by examining a set of different
types of cure systems for butyl rubber in combination with each of
several different carbon black types. Tables 6 to 9 indicate the
repeatability of the analyses, and Table 10 summarizes the data for
the study. It is evident that the components in the cure system
can influence decomposition of the carbon black. These data suggest
that replicate examination of carbon black decomposition character-
istics could be useful to detect unusual carbon black types and/or
acceleration systems in a "known" formulation.
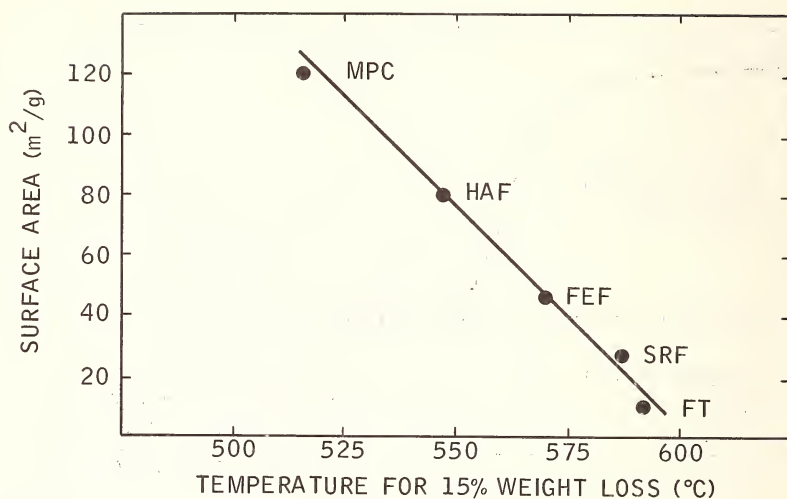
Figure 5.   Carbon black decomposition *vs*. surface area.

Table 6.   Influence of cure system on butyl rubber –
MPC vulcanizate.

Cure System[a]	% Polymer	% Black	% Ash	Polymer decomposition (°C)		Carbon black decomposition	
				Temp. for 50% loss	Terminal temp.	Onset temp.	Terminal temp.
	66	31	3.0	422	462	490	557
	65	31	4.0	421	455	492	542
1	65	31	4.0	419	454	499	554
	64	31	5.0	419	453	508	560
	65	31	4.0	422	457	504	558
	65	32	3.0	417	452	507	554
2	65	32	3.0	417	450	518	555
	65	32	3.0	416	452	521	564
	65	32	3.0	424	464	531	563
	66	31	3.0	420	450	522	563
3	65	32	3.0	420	457	527	554
	65	32	3.0	419	455	531	562
	63	30.0	7.0	417	464	423	454
4	64	30.0	6.0	421	462	431	468
	63	30.0	7.0	412	466	426	460

[a]See Table 10.

Table 7.   Influence of cure system on butyl rubber –
           HAF vulcanizate[1].

Cure System[a]	% Polymer	% Black	% Ash	Polymer decomposition (°C)		Carbon black decomposition	
				Temp. for 50% loss	Terminal temp.	Onset temp.	Terminal temp.
1	65.5	30.5	4.0	415	452	526	577
	65.0	31	4.0	419	457	530	584
	65.0	31	4.0	421	457	530	584
2	66	30	4.0	413	452	541	583
	66	30.5	3.5	418	455	541	588
	66	30.5	3.5	421	457	547	594
3	66	31	3.0	421	459	592	607
	66	31.5	2.5	422	466	607	616
	65.5	31.5	3.0	421	466	605	612
4	63	30.0	7.0	412	445	460	471
	63	30	7.0	412	447	462	479
	63	30	7.0	412	447	471	482
	63	30	7.0	416	452	479	482

[a]See Table 10.

Additional points of interest regarding the cure system study
are the following: (1) with the possible exception of system
number four, there does not appear to be a large effect of cure
system on polymer decomposition in nitrogen. If this is gener-
ally true, it would be possible to ascribe variations in the poly-
mer decomposition region of extracted samples primarily to differ-
ences in polymer type. (As previously noted, resins could be an
interference here); (2) there is a significant change in decomposi-
tion characteristics of the different blacks for cure systems 1 and
2 [4]. For systems 3 and 4, three of the blacks have similar onset
temperatures, but larger differences in terminal temperatures are
evident.

Table 8.   Influence of cure system on butyl rubber -
FEF vulcanizate [1].

Cure System[a]	% Polymer	% Black	% Ash	Polymer decomposition (°C)		Carbon black decomposition	
				Temp. for 50% loss	Terminal temp.	Onset temp.	Terminal temp.
1	65.0	31	4.0	417	455	549	597
	65.0	31	4.0	413	447	550	592
	64.5	31.5	4.0	417	452	550	599
	65.0	32.0	3.0	417	454	551	595
2	65.0	31.0	4.0	414	449	569	610
	65.0	31.5	3.5	412	448	563	606
	65.5	31.5	3.0	416	453	569	611
	65.0	31.0	4.0	416	452	565	606
3	65.5	32.5	2.0	421	455	579	591
	64.5	32.5	3.0	416	452	610	624
	64.5	32.5	3.0	421	457	597	629
	64.5	32.5	3.0	421	457	600	624
4	63	30.0	7.0	416	457	466	497
	62.5	30.5	7.0	414	452	462	497
	62.5	30.5	7.0	412	450	464	502
	63.0	30.5	6.5	412	452	464	491

[a]See Table 10.

A new area of study is suggested by comparison of the shapes of
e.g., the FEF black decomposition regions for the different acceler-
ator systems.   The complex nature of some of these, Figure 6, sug-
gests that TGA monitoring of cure system uniformity is feasible; one
certainly detects the oxidative effect of the GMF system.   Its
uniqueness may enable detection in unknown vulcanizates.   It is also
interesting to note the strong two-step regions in some systems.
These have suggested to us additional studies to determine whether
each region relates to one accelerator component.

Table 9.   Influence of cure system on butyl rubber -
SRF vulcanizate [1].

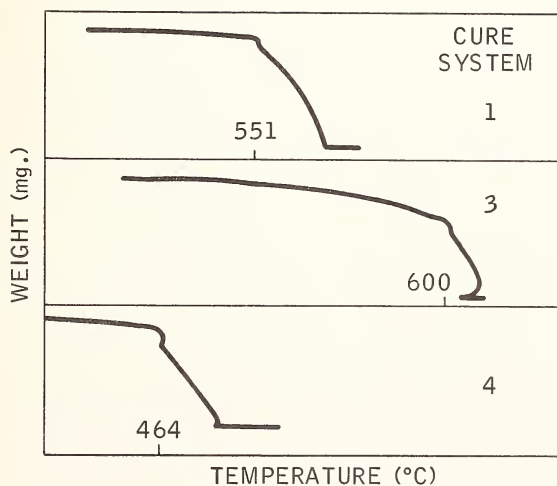| Cure System[a]	% Polymer	% Black	% Ash	Polymer decomposition (°C)		Carbon black decomposition	
				Temp. for 50% loss	Terminal temp.	Onset temp.	Terminal temp.
1	65	32	3.0	412	452	555	602
	64.5	31.5	4.0	413	452	546	607
	65	32	3.0	412	457	552	607
2	65	32	3.0	411	452	583	621
	65	32	3.0	411	452	579	621
	65	32	3.0	410	447	582	626
3	64	32.5	3.5	416	452	608	630
	64	33	3.0	417	452	593	630
	64	33	3.0	416	452	585	625
4	62	31	7.0	405	438	466	527
	63	30	7.0	408	447	459	537
	62	31	7.0	407	438	460	521
	63	31	6.0	407	443	460	532

[a]See Table 10.

Figure 6.   FEF oxidation in standard vulcanizate.

Table 10.   Effects of cure system and black type on decomposition
            of butyl rubber vulcanizates.

Cure System[a]	Average values			Polymer decomposition (°C)		Carbon black decomposition	
	% Polymer	% Black	% Ash	Temp. for 50% loss	Terminal temp.	Onset temp.	Terminal temp.
1	65.0	31.0	4.0	420	456	497	553
	65.2	30.8	4.0	418	455	529	582
	64.9	31.4	3.8	416	452	550	596
	64.8	31.8	3.3	412	454	551	605
2	65.0	32.0	3.3	418	453	513	558
	66.0	30.3	3.7	417	455	543	588
	65.1	31.3	3.6	415	451	567	608
	65.0	32.0	3.0	411	450	581	623
3	65.3	31.8	3.0	421	457	528	561
	65.8	31.3	2.8	421	464	601	612
	64.8	32.5	2.8	420	455	597	617
	64.0	33.0	3.3	416	452	595	628
4	63.3	30.0	6.7	417	464	427	461
	63.0	30.0	7.0	413	448	468	479
	62.8	30.4	6.9	414	453	464	497
	62.5	31.0	6.8	407	442	461	529

---

[a] Cure Systems (phr):

1. Altax (1.0), Tellurac (1.5), Sulfur -1.0, ZnO (5.0), Stearic Acid (2.0).
2. Sulfasan R (2.0), Tuads (2.0), ZnO (5.0), Stearic Acid (2.0).
3. SP-1055 (12.0), ZnO (5.0), Stearic Acid (2.0).
4. Altax (4.0), GMF (1.5), Red Lead (5.0), ZnO (5.0), Stearic Acid (2.0).

EXAMINATION OF CARBON BLACK BLENDS

Isothermal analysis of the carbon black residues obtained after
the nitrogen degradation step of the standard TGA procedure indi-
cated that the degradation characteristics of thermal blacks were
significantly different from those of the other blacks tested.
The magnitude of this difference indicated that at least semi-quan-
titative analyses of carbon black mixtures should be possible where
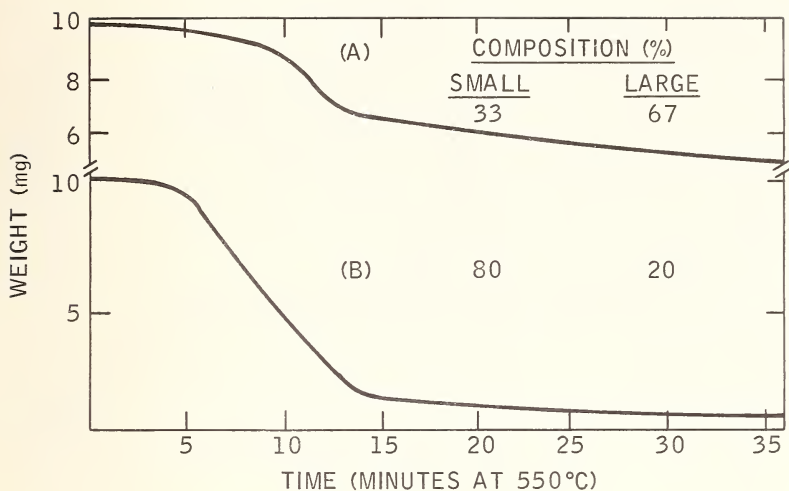
Figure 7.   Isothermal analysis of mixed blacks in TGA residue.

one component is a thermal black. A test of this idea is shown in
Figure 7 which clearly demonstrates the different characteristics
of the two formulations known to contain this type of carbon black
blend. Rough estimates of the composition were made based on the
weight loss at an arbitrary reference temperature [3]. For system
A, rather good agreement with the known content (25 small/75 large)
was obtained. This method obviously over-estimates the small black
content due to failure to correct for the initial weight loss due
to the large black. The other two, "unknown" development compounds
appear to differ significantly in carbon black blend composition.
More quantitative determinations may be possible for known systems
by means of a reference temperature technique similar to that used
in the estimation of oil content of known systems.

    Recent evidence has indicated that additional insight into vari-
ations in carbon black residues may be obtained even for systems
which do not contain thermal blacks. An example of this is shown in
Figures 8 and 9. Figure 8 shows the basic TGA thermogram for ex-
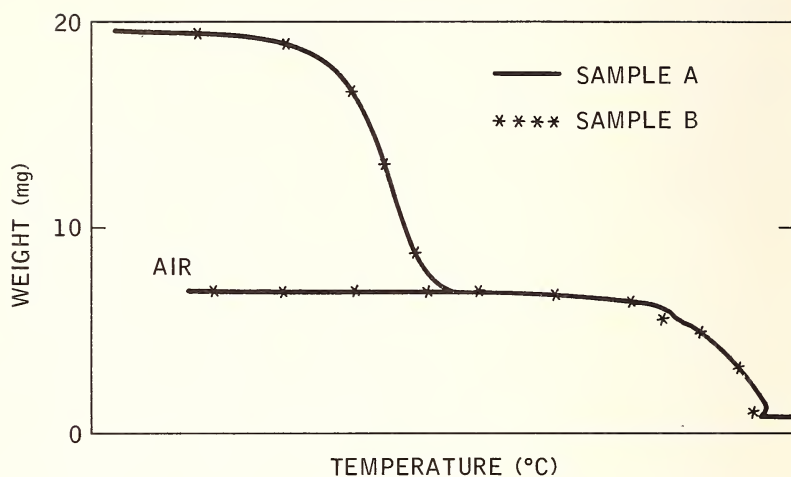tracted samples of commercial product produced in different loca-

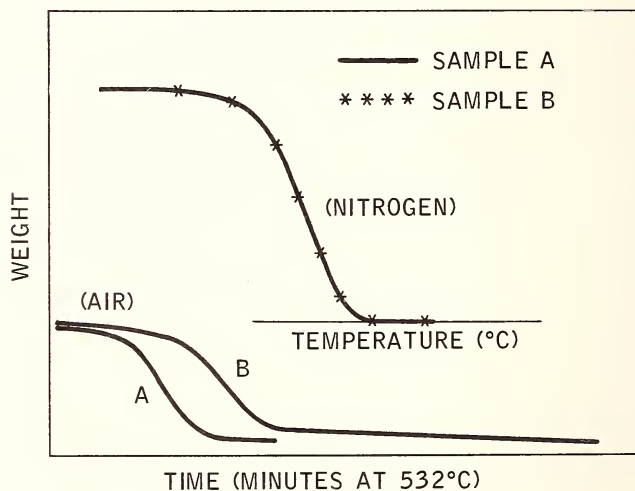Figure 8.   Comparison of vulcanizates by standard TGA conditions.

Figure 9.   Isothermal analysis of carbon black residue.

tions. This analysis indicates very similar basic compositions for the two materials; note especially the similar carbon black decomposition characteristics. However, when the analysis was repeated with the modification of decomposing the carbon black residues isothermally at 532 °C (Figure 9), a substantial difference in degradation characteristics is evident. Several suggestions can be made about the reasons for these differences; (a) different cure systems were used, (b) one of the samples (B) is a blend of carbon blacks and the other is not, (c) both are blends but the average particle size of the two components in one of them is too similar to be detected in this analysis. Our experience in this area to date leads us to favor interpretation (b). Additional experimental procedures to magnify further the oxidation rate differences of such blends are now under consideration in our laboratories.

REFERENCES

[1] ASTM Test D-297-67-T "1968 Book of ASTM Standards, Part 28, Rubber, Carbon, Carbon Black, Gaskets", p. 114.

[2] Maurer, J. J., Proceedings of the Second International Conference on Thermal Analysis, Worcester, Mass., 1968. Thermal Analysis, Schwenker, R. F. and Garn, P. D., Eds., Vol. 1, p. 373, Academic Press, New York, (1969).

[3] Maurer, J. J., Rubber Chemistry and Technology (Rubber Reviews), 42, 110, (1969).

[4] Maurer, J. J. Rubber Age, 102, 47 (1970).

Latest developments in the subject area of this publication, as well as

in other areas where the National Bureau of Standards is active, are

reported in the NBS Technical News Bulletin. See following page.

HOW TO KEEP ABREAST OF NBS ACTIVITIES

Your purchase of this publication indicates an interest in the research, development, technology, or service activities of the National Bureau of Standards.

The best source of current awareness in your specific area, as well as in other NBS programs of possible interest, is the TECHNICAL NEWS BULLETIN, a monthly magazine designed for engineers, chemists, physicists, research and product development managers, librarians, and company executives.

If you do not now receive the TECHNICAL NEWS BULLETIN and would like to subscribe, and/or to review some recent issues, please fill out and return the form below.

<div style="text-align: right">(cut here)</div>

Mail to: Office of Technical Information and Publications
           National Bureau of Standards
           Washington, D. C.   20234

Name _____

Affiliation _____

Address _____

City _____ State _____ Zip _____

☐ Please send complimentary past issues of the Technical News Bulletin.

☐ Please enter my 1–yr subscription. Enclosed is my check or money
  order for $3.00 (additional $1.00 for foreign mailing).
  Check is made payable to: SUPERINTENDENT OF DOCUMENTS.

SP 338